NATIONAL ENERGY TECHNOLOGY LABORATORY

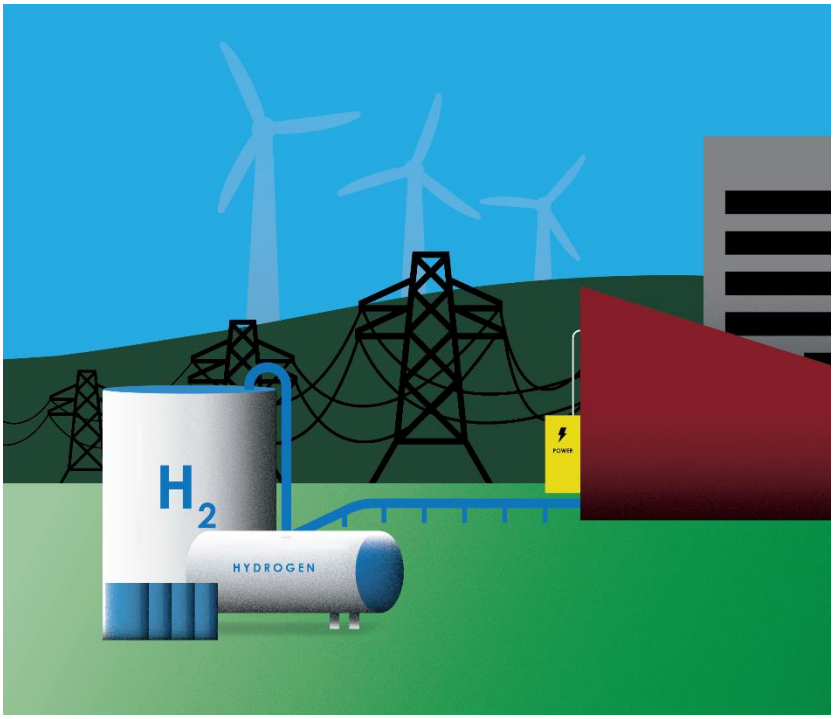

Hydrogen Safety Review for Gas Turbines, SOFC, and High Temperature Hydrogen Production

30 March 2023

U.S. DEPARTMENT OF ENERGY | NATIONAL ENERGY TECHNOLOGY LABORATORY

Office of Fossil Energy and Carbon Management

DOE/NETL-2022/3329

Disclaimer

Cover Illustration: Conceptual use of hydrogen in a power plant.

Suggested Citation: Rowan, S.; Kim, D.; Belarbi, Z.; Wells, A.; Hill, D.; Dutta, B.; Bayham, S.; Bergen, M.; Chorpening, B. *Hydrogen Safety Review for Gas Turbines, SOFC, and High Temperature Hydrogen Production*; DOE.NETL-2022.3329; NETL Technical Report Series; U.S. Department of Energy, National Energy Technology Laboratory: Morgantown, WV, 2023; p 132. 10.2172/1969531

An electronic version of this report can be found at:

https://netl.doe.gov/energy-analysis/search

Hydrogen Safety Review for Gas Turbines, SOFC, and High Temperature Hydrogen Production

Steven Rowan[1,2], Daejin Kim[3,4], Zineb Belarbi[5,6], Allan Wells[1,2], Daniel Hill[1,2], Biswanath Dutta[1,2], Samuel Bayham[1], Mike Bergen[1,2], Benjamin Chorpening[1]

[1]U.S. Department of Energy, National Energy Technology Laboratory, 3610 Collins Ferry Road, Morgantown WV 26505

[2]NETL Support Contractor, 3610 Collins Ferry Road, Morgantown WV 26505

[3]U.S. Department of Energy, National Energy Technology Laboratory, 626 Cochran Mill Road, Pittsburgh, PA 15236

[4]NETL Support Contractor, 626 Cochran Mill Road, Pittsburgh, PA 15236

[5]U.S. Department of Energy, National Energy Technology Laboratory, 1450 Queen Avenue SW, Albany, OR 97321

[6]NETL Support Contractor, 1450 Queen Avenue SW, Albany, OR 97321

DOE/NETL-2022/3329

30 March 2023

NETL Contacts:

Steven Rowan, Principal Investigator

Benjamin Chorpening, Technical Portfolio Lead

Bryan Morreale, Associate Laboratory Director for Research & Innovation, Research & Innovation Center

This page intentionally left blank.

Table of Contents

List of Figures

List of Figures (cont.)

List of Tables

Acronyms, Abbreviations, and Symbols

Term	Description
AHJ	Authority Having Jurisdiction
ALARP	As low as reasonably practicable
API	American Petroleum Institute
BLEVE	Boiling liquid expanding vapor explosion
CCGS	Combined cycle gasification system
CCGT	Combined cycle gas turbine
DAS	Detonation arresting system
DDT	Deflagration to detonation transition
DOE	U.S. Department of Energy
DSU	De-sulfurization unit
EIA	U.S. Energy Information Agency
FBG	Fiber Bragg grating sensors
Fr	Froude Number
GH_2	Gaseous hydrogen
GHG	Greenhouse gas
GR	General requirements
GT	Gas turbine
GWP	Global warming potential
HASCC	Hydrogen-assisted stress-corrosion cracking
HE	Hydrogen embrittlement
HEAC	Hydrogen environment assisted cracking
HIA	Hydrogen implementation agreement
HIC	Hydrogen induced cracking
HRSG	Heat recovery steam generators
HTHA	High-temperature hydrogen attack
HT-WGS	High-temperature water-gas shift
IDLH	Immediately dangerous to life or health value
IEA	International Energy Agency
IP	Industrial piping
LES	Large eddy simulation
LFL	Lower flammability limit

Acronyms, Abbreviations, Symbols (cont.)

Term	Description
LH_2	Cryogenic liquid hydrogen
LPFG	Long-period fiber grating sensor
LPG	Liquefied petroleum gas
LT-WGS	Low-temperature water-gas shift reactor
MAQ	Maximum allowable quantity
Mf	Materials performance factor
MHIDAS	Major Hazard Incident Database Service
MOS	Metal oxide semiconducting
MWCNT	Multi-walled carbon nanotubes
NDE	Non-destructive evaluation
NETL	National Energy Technology Laboratory
NFPA	National Fire Protection Association
OSHA	Occupational Safety and Health Administration
PANI	Polyaniline
PEL	Permissible exposure limit
PEM	Proton exchange membrane
PMMA	Poly (methyl methacrylate)
PNNL	Pacific Northwest National Laboratory
pOl	Olfactory power
PRU	Pre-reforming unit
PSA	Pressure-swing adsorption process
PWHT	Post weld heat treatment
QCM	Quartz crystal microbalance
R&D	Research and development
RFU	Reformer furnace unit
RHU	Residue hydrotreating unit
RT	Radiographic testing
SAW	Surface acoustic wave
SCC	Stress corrosion cracking
SCZY	$SrCe_{0.8}Zr_{0.1}Y_{0.1}O_{2.95}$
SMR	Steam methane reforming

Acronyms, Abbreviations, Symbols (cont.)

Term	Description
SOEC	Solid oxide electrolyzer cells
SOFC	Solid oxide fuel cell
SSC	Sulfide stress cracking
STEL	Short-term exposure limit
STP	Standard temperature and pressure
TIT	Turbine inlet temperature
TWA	Time weighted average
VCE	Vapor cloud explosion
WGS	Water-gas shift reactors
WPS	Welding procedure specifications

Acknowledgments

This work was performed in support of the U.S. Department of Energy's (DOE) Office of Fossil Energy and Carbon Management, under the Hydrogen with Carbon Management Program. The research was executed through the National Energy Technology Laboratory's (NETL) Research and Innovation Center's Hydrogen Safety Field Work Proposal.

The authors also wish to acknowledge support and helpful discussions with Sam Thomas, Bob Schrecengost, Jai-Woh Kim, and Eva Rodezno at the DOE Office of Fossil Energy and Carbon Management; Douglas Straub, Peter Strakey, Henry Long, Richard Dennis (Turbines Program Technology Manager), Shailesh Vora (SOFC Technology Manager), and Sydni Credle (Sensors and Controls Technology Manager).

Reproduced figures were authorized and approved for reproduction only as part of this report, with citations in the References.

EXECUTIVE SUMMARY

Hydrogen is a versatile molecule, useful as a clean energy carrier and chemical precursor. When combined with carbon capture and storage, natural gas reforming and gasification are well positioned to produce large quantities of hydrogen from a variety of feedstocks, including waste coal with biomass or municipal waste. New technologies such as solid oxide electrochemical cells (SOEC) are also being developed for hydrogen production. In addition, the form of hydrogen stored may have a significant impact on safety issues with the production and utilization technologies. This report was developed to address the unique safety challenges involved with the production, transportation, and storage of hydrogen as part of the National Energy Technology Laboratory's (NETL) Hydrogen Safety Field Work Proposal (FWP) to support the U.S. Department of Energy's (DOE) Office of Fossil Energy and Carbon Management's strategic vision for safe, widespread, and large-scale production and utilization of hydrogen as a carbon-free energy storage medium. This work documents the unique safety issues for solid oxide fuel cells (SOFCs) and gas turbines fueled from hydrogen, and production of hydrogen from fuel reforming, gasification, and SOEC. This report includes the approaches presently used to address hydrogen safety and identifies some potential technology advancements to improve the performance and reduce the cost for safety monitoring.

Hydrogen as a bulk energy storage medium poses safety challenges that differ from natural gas when used with SOFCs and gas turbines. Compared to natural gas, hydrogen has an increased flammability range and lower minimum ignition energy, which increases the likelihood of a fire starting from a hydrogen leak. The lower ignition energy makes smaller sparks a concern. Hydrogen flames are nearly invisible, making small fires difficult to notice and causing harm to unaware personnel. From a mechanical design standpoint, hydrogen also causes embrittlement in many steels and alloys, resulting in higher system costs than with natural gas. Hydrogen molecules are exceptionally small, which makes bulk hydrogen storage a challenge because it leaks more easily from pipe fittings and seals, and has greater diffusion through most materials than other gases. This can become hazardous if a small leak occurs in an enclosed space, resulting in a flammable mixture accumulating over time. However, proper material selection and greater material thickness can minimize diffusion, while tighter tolerances, careful selection of seal materials, and meticulous assembly will minimize seal leaks.

Hydrogen turbines have all of these concerns, along with several others. Flashback is a larger concern with hydrogen than natural gas due to the much higher flame speed of hydrogen. Flashback of the hydrogen flame from the combustor into the premixer or other inlet can rapidly burn away metal, with potentially dangerous consequences. The buoyancy of hydrogen can make it more difficult to purge the combustor and turbine, which is done prior to light-off to avoid accidental explosions.

High-temperature hydrogen attack (HTHA) on metal alloys can be a problem for gas turbines, SOFCs, steam methane reactors, and gasification systems. It results in pitting and cracking and can ultimately result in catastrophic failure of high-temperature piping and fittings which contain high-concentration hydrogen mixtures. These systems require careful material selection and design.

Aside from the risks of hydrogen delivery already covered above, SOFCs are at risk of internal stack failures. SOFCs use ceramic materials for the anode, electrolyte, and cathode. Hydrogen embrittlement (HE) is less a concern with these already brittle materials, especially given they

are designed to have near zero pressure difference across the stack. However, a crack in a cell could allow hydrogen to leak into the air side of the cell. With the high operating temperatures, reaction and additional heat generation is expected, which can accelerate mechanical failure to other cells across the stack. Quality control of the individual cells, which must be both thin and gas tight, is a special concern. The high-temperature seals on the system are also a challenge.

Like natural gas, hydrogen has no odor on its own. Methyl mercaptan is added to natural gas as an odorant, easily detected by smell at low concentrations. While this works well with domestic supplies and gas turbines, the odorant must be removed before the natural gas is supplied to a fuel cell to not poison the cell materials. This creates a question on the cost or benefit of adding an odorant to hydrogen, which is well suited for fuel cells.

While gasification systems have many of the above safety concerns, including HE, HTHA, and fire, the solids handling for gasifiers poses a special hazard. The entry point for solids into the gasifier can be subject to high pressures, high temperatures and hydrogen, along with erosive materials and sulfur compounds. Solid particulate fuel near the gasification systems can also provide an additional fire hazard.

Areas of technology development are needed to improve the safety surrounding hydrogen production and storage systems while reducing cost. Lower cost materials for hydrogen applications are needed in addition to current design options, which resist hydrogen embrittlement and hot hydrogen attack. Automated inspection technologies for welds, fuel cells, and systems with significant leak risk are needed to prevent hydrogen fires or explosions. For hydrogen-fired turbines, combustion systems which resist flashback are needed in addition to systems that can observe hydrogen flashback. Due to the buoyant nature of hydrogen which causes it to accumulate in unique ways, high-temperature hydrogen sensors are needed to monitor purge cycles in combustion systems. While many ambient environment hydrogen safety sensors are commercially available, there remains opportunity for additional development of low-cost, wide-area hydrogen leak detection technologies. These technologies should be able to continually sense hydrogen at multiple locations, to effectively provide leak detection throughout a large facility. Hydrogen concentration sensing in blended fuels is also needed, to allow hydrogen turbines, SOFCs, and industrial equipment to adjust their operation with variable hydrogen and natural gas blends. In addition, there are special concerns for liquid hydrogen and other hydrogen storage means, such as ammonia. Finally, while many of these risks have been known for many years, and these mitigation methods also employed, accidents resulting from hydrogen use still occur (see Section 1.2) pointing to a need for strong on-going maintenance and employee training programs wherever hydrogen is used. Over time, seals and containment materials degrade, and it should not be up to after-the-fact leak-sensors to detect these concerns.

1. INTRODUCTION

The vision of the U.S. Department of Energy's (DOE) Office of Fossil Energy and Carbon Management (FECM) is to enable a zero-carbon future for the United States (U.S.) through development of carbon management technologies and their integration with fossil energy technologies, as part of a larger portfolio to provide net-zero carbon power by 2035. Due to the intermittency of renewables, it is foreseen that a large amount of energy storage will be necessary to balance the supply and demand of energy in real time. Hydrogen is the leading candidate for large-scale energy storage and replacement fuel. A significant effort is underway to rapidly mature the hydrogen technologies necessary through the Hydrogen Energy Earthshot and other programs led by the Hydrogen Fuel Technology Office (HFTO). As part of this department-wide effort, shifting fossil energy technologies to production and use of hydrogen is an emphasis of the FECM Strategic Vision (DOE, 2022b).

Hydrogen is the most abundant element in nature, and it plays an important role in industrial energy. Hydrogen can be extracted from different sources such as fossil fuels, biomass, and water.

In the U.S., natural gas reforming technologies are currently the primary source of hydrogen production. This can be attributed to the reduced production cost and large-scale production rate. The U.S. Energy Information Agency (EIA) reported that 38% of natural gas consumed in 2020 was used for electrical power generation (EIA, 2021b) and approximately 60% of electricity was produced from burning fossil fuels (Figure 1) (EIA, 2022). However, electricity production from burning fossil fuels generates the second largest share of greenhouse gas (GHG) emissions (carbon dioxide, CO_2), which has a negative impact on climate. In addition, fugitive emissions from natural gas infrastructure (mostly methane) have also been identified as an important concern for climate change. Efforts are underway to locate sources of fugitive emissions, and minimize or eliminate them. Also part of efforts to end GHG emissions, clean hydrogen produced from natural gas with carbon capture can be used as a CO_2-free fuel for electricity generation by gas turbines and SOFCs (Nobel et al., 2021; Milani et al., 2021).

In recent years, hydrogen has emerged as one of the most attractive alternative fuel options. In the U.S., the infrastructure for hydrogen fuel (H_2) usage in gas turbines is still unavailable. Due to its physicochemical properties, implementation of H_2 infrastructure must overcome several safety requirements, such as its higher tendency to leak compared to natural gas. Hydrogen as a CO_2-free fuel source comes with special considerations that must be taken into account in relation to material selection and specification of critical system components.

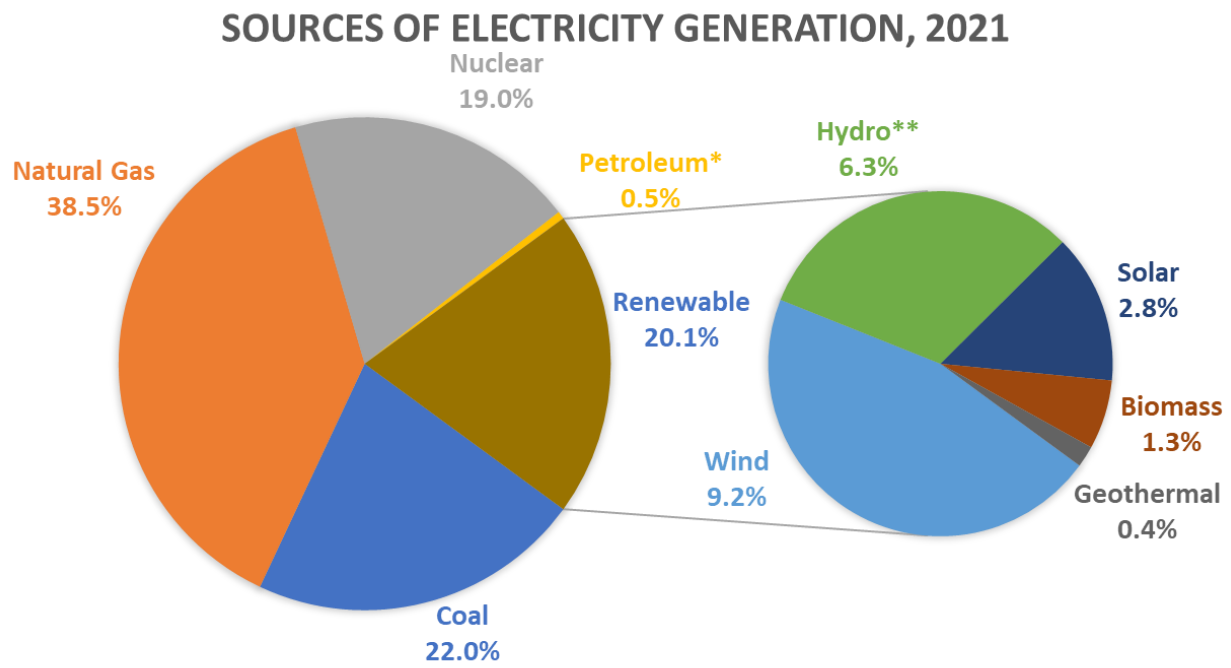

Figure 1: Source of U.S. electricity generation (EIA, 2022).

This report presents an introduction and summary on hydrogen safety issues, as they relate to hydrogen production, storage, and use in the energy sector, primarily as related to electricity generation via gas turbines, solid oxide fuel cell (SOFC) technologies, and combined cycle gasification systems (CCGS). The impetus behind this effort is the U.S. DOE goal for decarbonization of the energy sector by the year 2035, as in many cases, hydrogen is expected to replace natural gas as the primary fuel source to achieve this goal.

Large-scale energy storage for supporting a reliable and resilient grid, without the release of CO_2 characteristic of current carbon-based fossil fuels, will be required to achieve this decarbonization goal. Advanced technologies for large-scale energy production using hydrogen as a fuel source which can be deployed over the next 5–10 years will be required. However, to develop and mature these hydrogen-based technologies, it will be critical to identify the safety issues related to widespread use of hydrogen as a fuel source.

In support of this effort, this report presents a review of the existing knowledge base on the physical properties of hydrogen fuels, reported hydrogen safety incidents, examination of common hydrogen safety concerns (such as hydrogen embrittlement, fire, and explosion hazards as a result of hydrogen leaks), safety codes, as well as a structured high-level safety/hazard analysis for hydrogen use in gas turbines, gasification systems, and fuel cells (Appendix A). Additionally, comparisons between hydrogen and natural gas are presented where applicable. The topics of liquid hydrogen and ammonia, and the potential climate impact of hydrogen leaks are briefly discussed. This report concludes with a discussion of potential opportunities for

further technology research and development (R&D) activities identified during the course of this review.

1.1 HYDROGEN PROPERTIES AND GENERAL HAZARDS

Table 1 presents a comparison between hydrogen and natural gas for the physical properties of greatest importance from a safety standpoint (Yang et al., 2021; Appl, 1999; Verkamp et al., 1967; Hayakawa et al., 2015).

Table 1: Comparison of the Physical Properties of Hydrogen and Natural Gas at Standard Temperature and Pressure (Yang et al., 2021; Appl, 1999; Verkamp et al., 1967; Hayakawa et al., 2015)

Physical Property	Hydrogen	Natural Gas (with 85% CH_4)	Ammonia
Density (g/L)	0.089	0.717	0.7714
Minimum Ignition Energy in Air (mJ)	0.017	0.31	8
Flammability Limits in Air (%)	4–75	5–15	16–27
Energy Density at Lower Heating Value (MJ/kg)	119.96	50.07	18.577
Boiling Point (°C)	-253	-162	-33
Ignition Temperature (°C)	574	650	651
Laminar Flame velocity (m/s)	2.65–3.25	0.38	0.07

Hydrogen density is roughly 12.4% that of natural gas. When compared to the density of air at standard temperature and pressure, hydrogen is approximately 14.5 times more buoyant than air, compared to natural gas being approximately 1.8 times more buoyant than air. From a safety perspective, this means that when a hydrogen leak is not confined inside a structure, hydrogen will diffuse much more rapidly in air than natural gas.

While hydrogen possesses greater diffusivity in air thereby offering a way to become more quickly diluted than natural gas, it also has a much wider range of flammability in air compared to natural gas. Specifically, whereas natural gas has a flammability limit of 5–15% by volume, hydrogen-air mixtures are flammable over a range of 4–75% hydrogen by volume. Combining this with the fact that the minimum ignition energy of hydrogen is on the order of 5% that of natural gas, hydrogen-air mixtures pose a significantly greater fire hazard than natural gas-air mixtures. Once an ignition occurs, the initial laminar flame velocity of hydrogen is nearly an order of magnitude greater than that of natural gas. As a result, hydrogen fires tend to burn more intensely than natural gas fires, resulting in greater asphyxiation risks due to faster oxygen depletion, and faster flame acceleration and explosions (Yang et al., 2021; Astbury and Hawksworth, 2007; Weiner and Fassbender, 2012; Oran et al., 2020; Molkov, 2020).

Hydrogen has the smallest molecular volume and easily diffuses into steel and other materials in large quantities, which results in material strength reduction and embrittlement (Yang et al.,

2020). This also allows hydrogen to easily enter gaps in piping to form local stresses and cause leakage.

These factors combined have led to numerous hydrogen-related safety incidents, as addressed in the next section.

1.2 HYDROGEN SAFETY INCIDENTS

The Center for Hydrogen Safety at the Pacific Northwest National Laboratory (PNNL) launched an effort in 2006 to maintain the https://h2tools.org/ website for sharing lessons learned from hydrogen related safety events. This was then combined with the Hydrogen Safety Best Practices database in 2009, as well as formed a collaboration with the International Energy Agency (IEA) Hydrogen Implementation Agreement (HIA) to share hydrogen incident data from around the world (Weiner and Fassbender, 2012; Weiner, 2014; Yang et al., 2021). The h2tools.org website now contains information of more than 200 hydrogen related incidents self-reported from industry, research, and academia.

Separately, OSHA (29 CFR 1904.39) has reporting requirements for incidents involving injuries/fatalities. These requirements are applicable to all industrial operations, including hydrogen/natural gas-based incidents.

In Figure 2, Weiner and Fassbender (2012) categorized the hydrogen incidents reported to the h2tools.org website by location type and found that the greatest number of reported hydrogen incidents occurred in laboratory settings, followed distantly by incidents located at hydrogen refueling stations, commercial facilities, power plants, and hydrogen delivery vehicles (discounting the first “misc” category). Figures 3–6 below were compiled for this report using the 10 most commonly reported incidents for categories including damages and injuries (Figure 3), equipment involved in reported incidents (Figure 4), reported probable cause for incidents (Figure 5), and reported contributing factors (Figure 6).

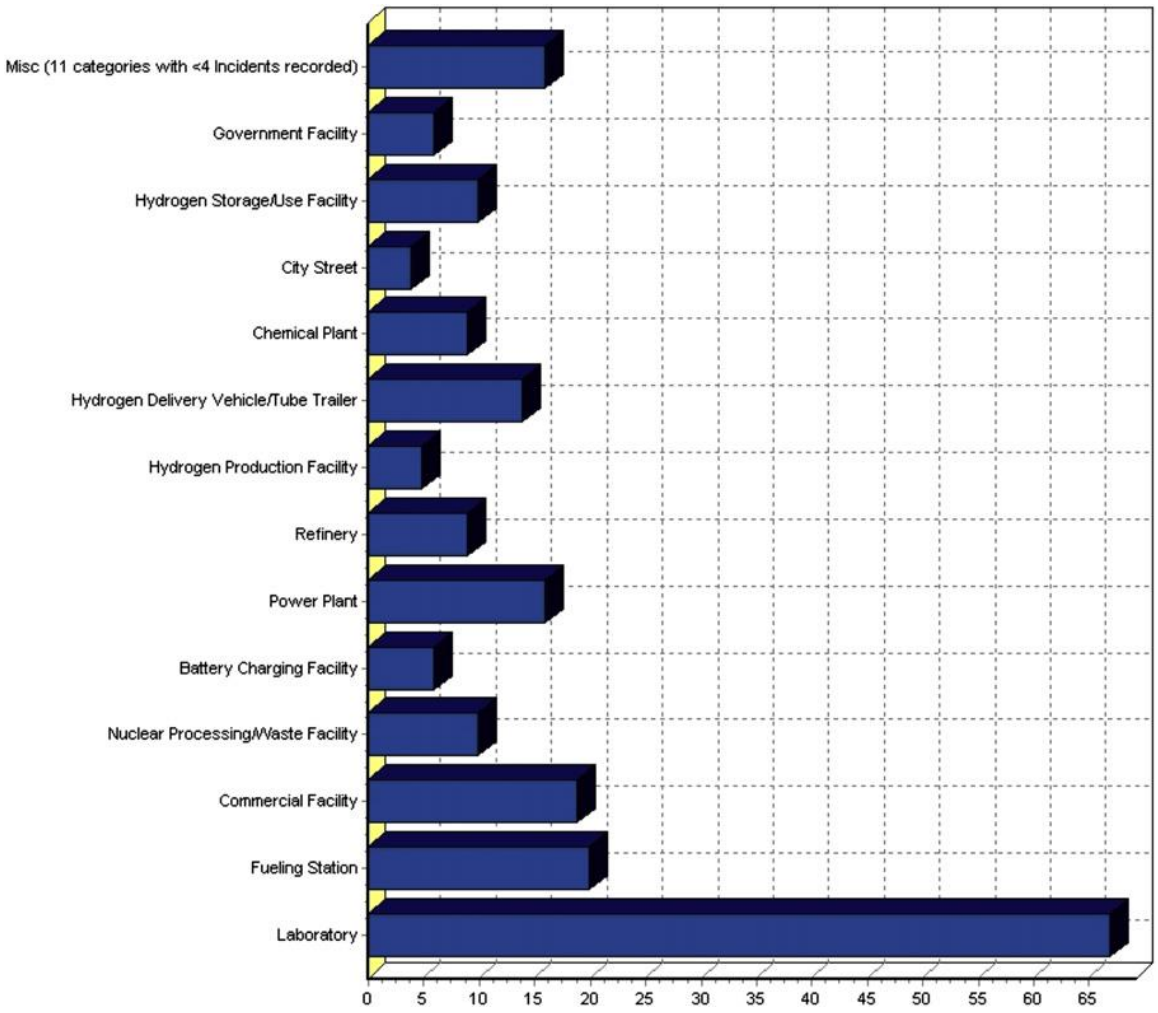

Figure 2: Bar graph showing settings of all incidents in the h2tools.org database as of 2012 (Weiner and Fassbender, 2012).

As seen in Figure 3, most reported hydrogen incidents have resulted in property damage and facility closures, with approximately 17% of incidents reporting minor or lost time injuries, as well as fatalities in 5% of reported incidents. Furthermore, Figure 4 shows that roughly half of reported incidents have involved pressure vessels, piping, and valve systems, and to a lesser extent compressed gas canisters, electrical issues, and measurement sensor failures. Figures 5 and 6 show that, for the reported incidents, equipment failure and human error (including situational awareness, training, improper maintenance, failure to follow established procedures, etc.) were either the probable cause or a contributing factor to the incident.

In addition to the information provided by PNNL's hydrogen incident database, Astbury and Hawksworth (2007) reviewed hydrogen incident data compiled in the Major Hazard Incident Database Service (MHIDAS) maintained by the government of the U.K., which contained information on hydrogen related incidents dating back to the 1920s. In review of several early incidents that were initially reported as having unknown causes, Astbury and Hawksworth concluded that many of these incidents could be contributed to factors such as: diffusion ignition, electrical discharge, or presence of charged rust particles in storage or piping systems.

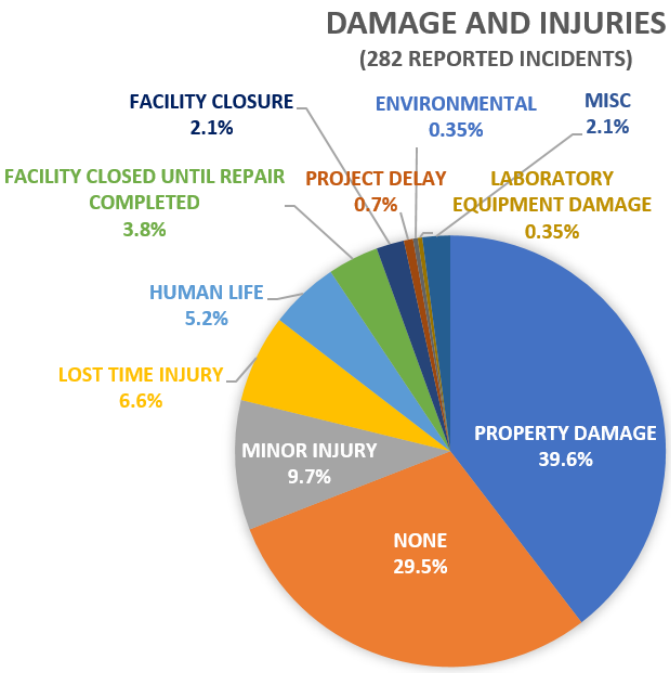

Figure 3: Reported damage and injury categories resulting from hydrogen related incidents reported to h2tools.org.

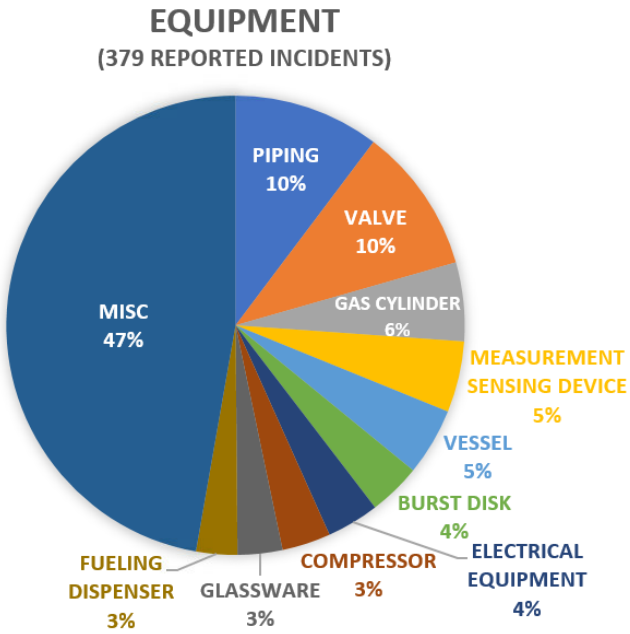

Figure 4: Reported categories for equipment involved in hydrogen incidents reported to h2tools.org. (The primary causes for the equipment-related incidents include component failure, operation error, installation/maintenance, etc.).

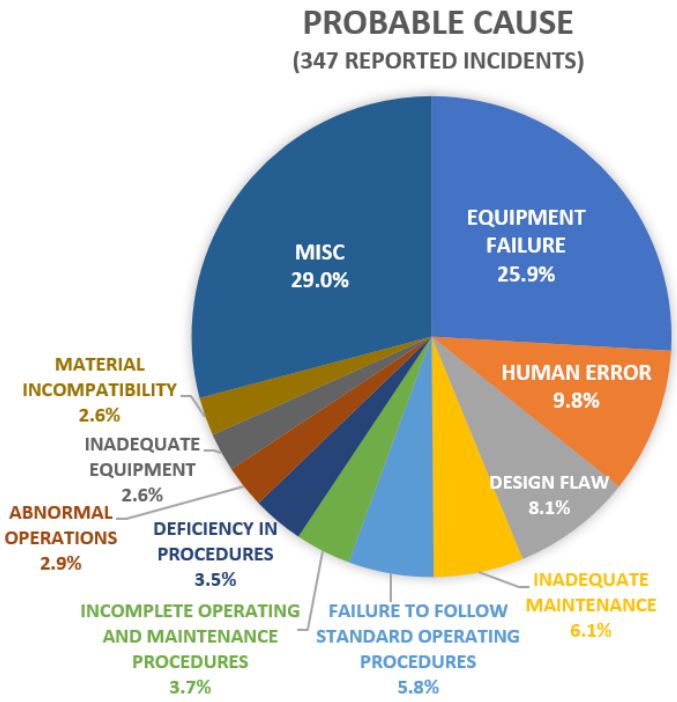

Figure 5: Probable cause categories for hydrogen incidents reported to h2tools.org.

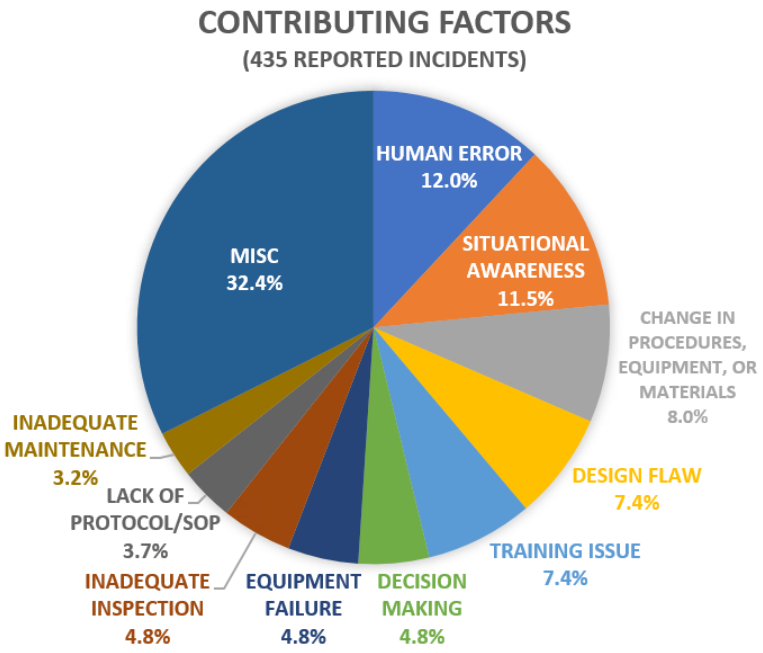

Figure 6: Contributing factors categories for hydrogen incidents reported to h2tools.org.

2. HYDROGEN HAZARDS

2.1 FIRES AND EXPLOSIONS

The most damaging risks associated with accidental release of compressed and/or liquified flammable gases, such as hydrogen or natural gas, are fires and explosions. This section presents a brief overview of the different types of fires and explosions that commonly result from the accidental release and ignition of compressed or liquified flammable gases, discussion of the underlying concepts of how a combustible mixture may undergo self-ignition in the absence of an external ignition source, propagation of a sub-sonic deflagration, as well as deflagration to detonation transitions (DDT), including deflagrations and detonations of combustible gases in high-pressure storage and piping systems. Finally, a brief overview of common deflagration and detonation mitigation methods will be presented.

In a review of hydrogen safety issues related to hydrogen diffusion and detonation processes (Yang et al., 2021), the likely results from gaseous hydrogen leaks included harmless diffusion, jet fires, fireballs, ignition kernels, and explosions; depending on whether the leak occurred in an open or a confined space, as well as the occurrence of rapid ignition, delayed ignition, or no ignition, and the presence of an instantaneous or continuous leak, as shown in Figure 7.

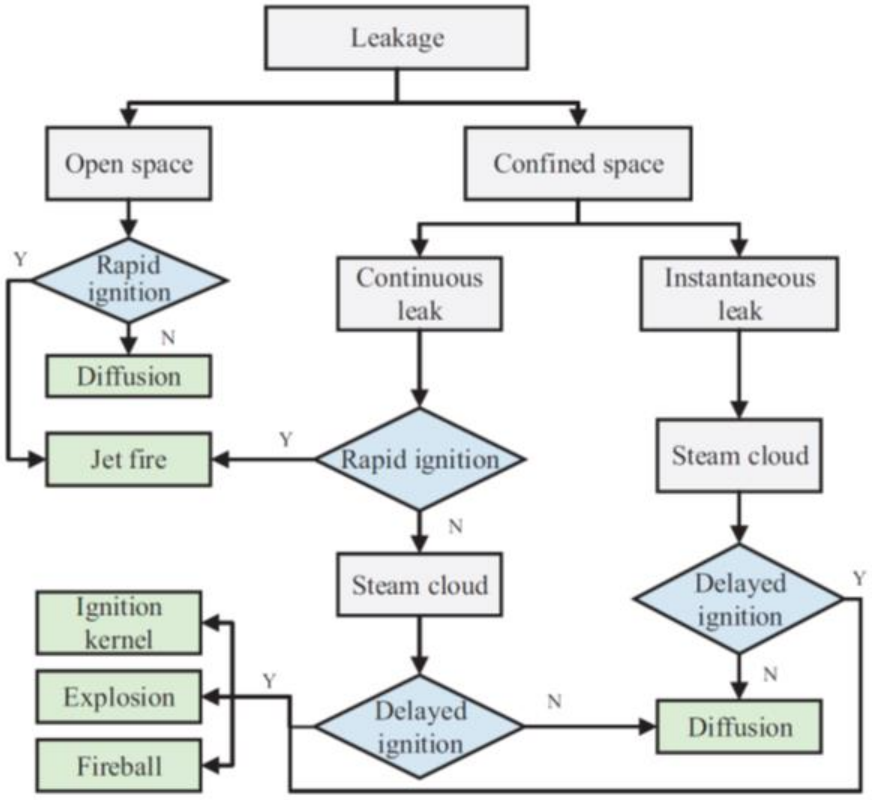

Figure 7: Flow chart hazard occurrence due to hydrogen leak (Yang et al., 2021).

Furthermore, the ignition and/or explosion of a cloud of flammable gases can take the form of either a vapor cloud fire (or flash fire) or a vapor cloud explosion (VCE) depending on whether

or not the flame front propagating through the flammable cloud accelerates enough to undergo DDT and produce an over pressure, or blast wave (Oran et al., 2020).

To discuss these different types of fires and explosions, it is important to establish a common lexicon. The following definitions from the Industrial Health and Safety Review Fire and Explosion Hazards website (isrmag.com/fire-and-explosion) and the UK's Health and Safety Executive Offshore Guidance on Jet Fires (hse.gov.uk/offshore/strategy/jet.htm) website will be used.

Jet Fire

A jet fire (or spray fire) is defined as a turbulent diffusion flame resulting from the combustion of a fuel continuously released with some significant momentum in a particular direction. The high heat fluxes to impinged or engulfed objects can lead to structural failure of storage vessel and piping systems, leading to potential incident escalation.

Vapor Cloud Fire

A vapor cloud fire, or flash fire, occurs when a flammable mixture of air and vapor ignites and the resulting flame passes through the mixture at less than sonic velocity, such that negligible over pressure is generated. In a flash fire, the gas burns, but does not explode. The resulting heat radiation and flames may cause severe burn injuries and sudden oxygen depletion.

Vapor Cloud Explosion

Unlike a vapor cloud fire, a VCE occurs when a flammable mixture of air and vapor ignites and the resulting flame propagates through the mixture at sonic velocities, resulting in a blast wave (i.e., over pressure) that can cause major damage at a long distance from the initial incident location.

Ignition Kernel

An ignition kernel (or flame kernel) is the initial shape of a freshly ignited air/fuel mixture during the first few milliseconds of combustion. In an internal combustion engine, this would correspond to the early stage of flame initiation due to spark ignition or local ignition in a compression ignition engine.

Fireball

A fireball is a spherical cloud of flammable vapor, the bulk of which is too fuel rich to combust, allowing only the outer envelope to burn. Upon ignition, the fireball tends to rise vertically due to the buoyancy of the hot combustion gases, resulting in the ubiquitous "mushroom cloud" shape. Fireball flame temperatures are typically around 1400ºC and generate high amounts of radiant heat. Typically, there are two types of events which give rise to a fireball. The first is sudden and catastrophic release of a liquified gas, the other is an eruption in hot oil resulting in the release of burning vapor.

In addition to the forms of fires and explosions discussed by Yang et al. (2021), there are additional fire and explosion hazards related to liquefied flammable gases, such as compressed hydrogen and natural gas (isrmag.com/fire-and-explosion/; Ustolin and Paltrinieri, 2020).

Boiling Liquid Expanding Vapor Explosion

A boiling liquid expanding vapor explosion (BLEVE) occurs when a vessel containing pressurized flammable liquid above its atmospheric pressure boiling point suffers a catastrophic failure. The sudden depressurization during release leads to near instantaneous vaporization of the remaining liquid, as well as generation of a shock wave. This also results in immediate ignition of the expanding fuel-air mixture, leading to intense combustion and the formation of a fireball.

Pool Fire

A pool fire happens when a flammable liquid spills onto the ground and is ignited. It is defined as a pool of liquid burning with a stationary diffusion flame or the combustion of material evaporating from a layer of liquid at the base of a fire.

Running Liquid Fire

A running liquid fire is a flame associated with a flowing flammable liquid.

2.1.1 Ignition Sources

Each of the forms of fire and explosions discussed in the previous section are predicated on the presence of availability of an ignition source to ignite the fuel/gas mixture. These ignition sources can either be an external ignition source or a form of self-ignition. External sources can be as simple as an external flame or the result of intentional "energy focusing," or rapidly directing high levels of energy into a small area via igniting a condensed or gas phase explosive, or focusing a high-energy laser directly into the flammable mixture, etc. (Oran et al., 2020). As most hydrogen-related fires and explosions are not the result of intentional ignition as seen with energy focusing, the emphasis here will be on discussion of the mechanisms by which hydrogen leaks are believed to undergo self-ignition.

Astbury and Hawksworth (2007) and Yang et al. (2021) postulated and examined potential self-ignition sources that have been identified in earlier literature. The four identified modes for self-ignition of hydrogen leaks are presented in Figure 8: (1) the reverse Joule-Thomson effect, (2) electrostatic ignition, (3) diffusion ignition, and (4) hot surface ignition. Each of these modes of self-ignition are discussed below.

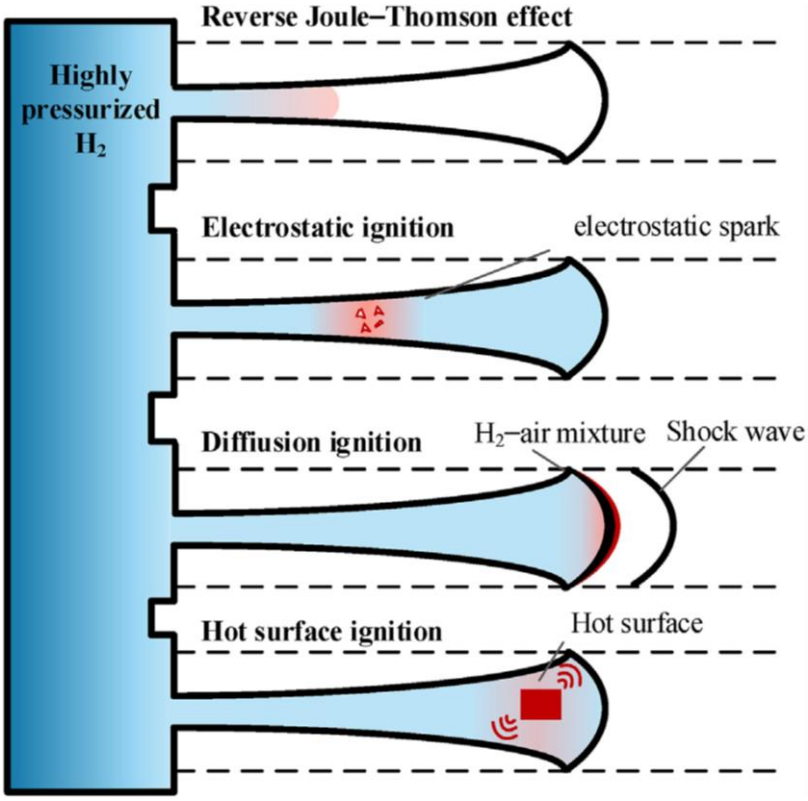

Figure 8: Commonly accepted modes of self-ignition of gaseous hydrogen leaks (Yang et al., 2021).

Reverse Joule-Thomson Effect

When a compressed gas is vented to atmosphere through a nozzle or passes through a throttling element such as a pressure-reducing valve, porous plug, blockage, or orifice, a pressure drop occurs, and the temperature changes accordingly. When the compressed gas temperature is below the Joule-Thompson inversion temperature associated with the lower expanded pressure (which is the case for nearly all gases at atmospheric pressure except for hydrogen and helium) the gas will cool as it expands. This is known as the Joule-Thomson effect (Yang et al., 2021; Astbury and Hawksworth, 2007). For hydrogen, the Joule-Thompson inversion temperature at atmospheric pressure is 193 K (-80 ºC), thus hydrogen will undergo heating upon expansion to atmospheric conditions. The resulting increase in temperature is a function of both the magnitude of the change in pressure and the value of the Joule-Thompson coefficient. According to Astbury, the worst-case value of the Joule-Thompson coefficient for hydrogen is 0.53 K/MPa, thus hydrogen stored at 25 ºC and 250 MPa that is vented to atmosphere would undergo a temperature increase of 132.5 K to a maximum temperature of 157.5 ºC when expanded to standard atmospheric conditions (Astbury and Hawksworth, 2007). Astbury goes on to state that while this is still well below hydrogen's autoignition temperature of 574 ºC and will not in and of itself lead to self-ignition, it may prove to be a contributing factor when combined with other factors.

Electrostatic Ignition

The minimum ignition energies of stochiometric mixtures of natural gas and air and hydrogen and air are 0.31 and 0.017 mJ, respectively. To put this in perspective, the minimum sensible static shock detectible by the human body is approximately 1 mJ, or approximately 3 times the minimum ignition energy of natural gas and 60 times that of hydrogen (Astbury and Hawksworth, 2007).

Hydrogen has a low-minimum ignition energy. The hydrogen incident database maintained by PNNL at h2tools.org (Weiner and Fassbender, 2012; Weiner, 2014; Yang et al., 2021) and Astbury et al. (2007) have identified numerous hydrogen related incidents whose cause can be attributed to hydrogen ignition via static discharge. The nature of these discharges includes, but are not limited to, faulty or improperly grounded electrical equipment, improperly grounded piping, the presence of charged particles in the gas flow (including those derived from oxide layers on the inner surfaces of piping), coronal discharges between pipe flange pairs through which hydrogen is leaking, and static discharges from plant personnel.

Diffusion Ignition

Diffusion ignition of a gaseous fuel-air mixture can occur when shock waves form and propagate through the mixture. The shock wave has a heating effect upon the gas located just in front of the shock wave. If the shock wave is strong enough, either by itself or in combination with reflected shock waves, the temperature of the gaseous mixture ahead of the shock can exceed the auto-ignition temperature of the mixture and ignite. This effect can be seen in the DDT that can occur in piping systems, as well as lead to VCEs, and will be discussed in more detail in those sections.

Hot Surface Ignition

Hot surface ignition occurs because of partial heating of a flammable gas mixture, such as a hydrogen-oxygen mixture, by a high-temperature hot surface. When a hot surface acts as an ignition source, the required hot surface temperature is typically higher than the self-ignition temperature of flammable gas mixture hydrogen. As the heat transfer between the gas and the hot surface is predominantly driven by convection, hot surface ignition is affected by factors such as the shape and area of the hot surface (Yang et al., 2021).

2.1.2 Jet Fires

The initial manifestation of a hydrogen safety incident is usually that of a leak of high-pressure hydrogen into the atmosphere in the form of a hydrogen jet. As previously stated, a jet fire is defined as a turbulent diffusion flame resulting from the combustion of a fuel continuously released with some significant momentum in a particular direction. To understand some of the basics of jet fires, it is important to consider the nature of jets.

Depending upon the ratio of pressure between the high-pressure gas and the atmosphere into which it is leaking, the resulting jet can be classified into one of the three following categories: a subsonic jet where the gas is fully expanded at the leak location (i.e., outlet or nozzle), a critical-state jet where the gas velocity at the outlet reaches the local sonic velocity, or an under-expanded jet where the leaking gas continues to expand and accelerate into the surrounding atmosphere. For hydrogen gas, the critical pressure corresponding to the formation of a critical-state jet venting to atmosphere is 0.2 MPa. Since most hydrogen storage and piping systems are

at pressures greater than 0.2 MPa, hydrogen jets will typically fall within the under-expanded jet category (Yang et al., 2021)

In general, fully expanded subsonic jets (subsonic free jets) can be either buoyancy-driven or momentum-driven, while under-expanded jets tend to be momentum driven. As will be discussed later in this report, this has a significant effect on factors such as the dispersion nature of the jet, the length over which the fuel concentration within the jet falls within the flammability limits for the fuel, as well as the flame length of the resulting jet fire, which must be considered from a safety aspect.

For fully expanded subsonic free jets, the ratio of momentum forces to buoyancy forces is quantified by the Froude Number, *Fr*, given by (Yang et al., 2021) as:

$$Fr = \frac{U_{exit}}{\sqrt{g d_{noz} (\rho_{\infty} - \rho_{exit}) / \rho_{exit}}} \quad (1)$$

Where U_{exit} is the gas velocity at the exit, g is the gravitational acceleration, d_{noz} is the bore diameter of the leak or nozzle, ρ_{∞} is the ambient air density, and ρ_{exit} is the exit density of the gas.

As shown in Figure 9, when the *Fr* is less than 10 the jet behavior will be dominated by the buoyancy forces; when the *Fr* is greater than 1,000 the jet behavior will be dominated by the momentum forces; when the *Fr* is greater than 10 but less than 1,000, there will be regions of the jet that are dominated by momentum, as well as regions that are dominated by buoyancy.

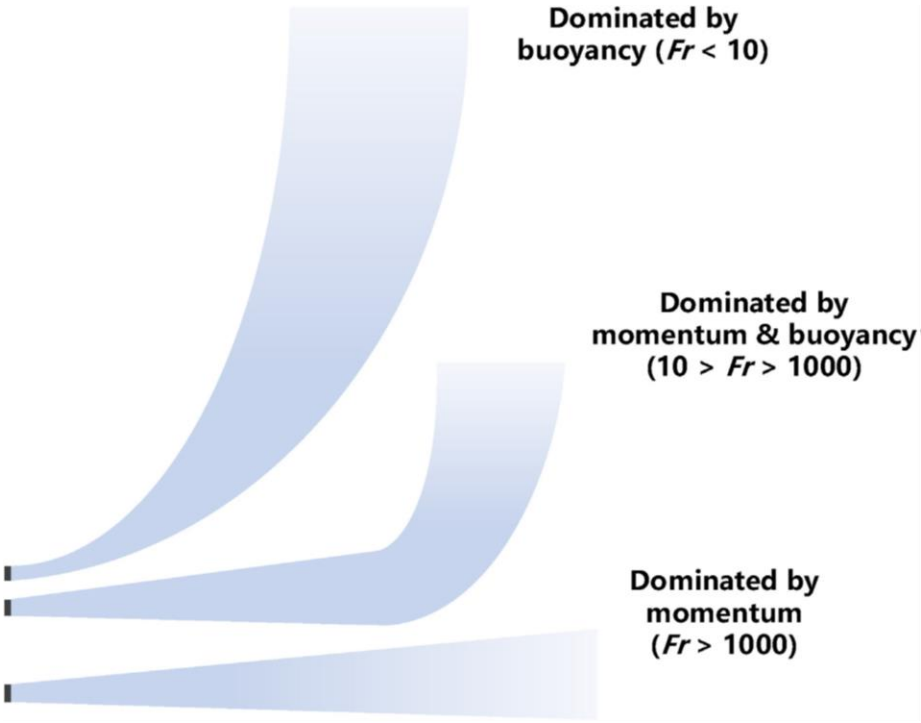

Figure 9: Schematic diagram of hydrogen jets dominated by different mechanisms (Yang et al., 2021).

Molkov (2020) presented Figure 10 which depicts the logarithmic relationship between x/D and U^2/gD for fully expanded horizontal jets with different volumetric concentrations of hydrogen (with air), along with a downward facing jet where the x/D represents the point at which the jet turns from downwards to upwards flow. The intersection between the 5 horizontal jet lines and the downward jet represents the points at which the horizontal jets transition from momentum driven to buoyancy driven regimes. In Figure 10, U and D are the exit velocity and diameter of the fully expanded jet, respectively. Molkov states that Figure 10 is also accurate to within 20% for under-expanded jets when U and D are taken as the notional exit velocity and diameter as calculated by the under-expanded jet theory presented in Section 4.2 of Molkov (2020).

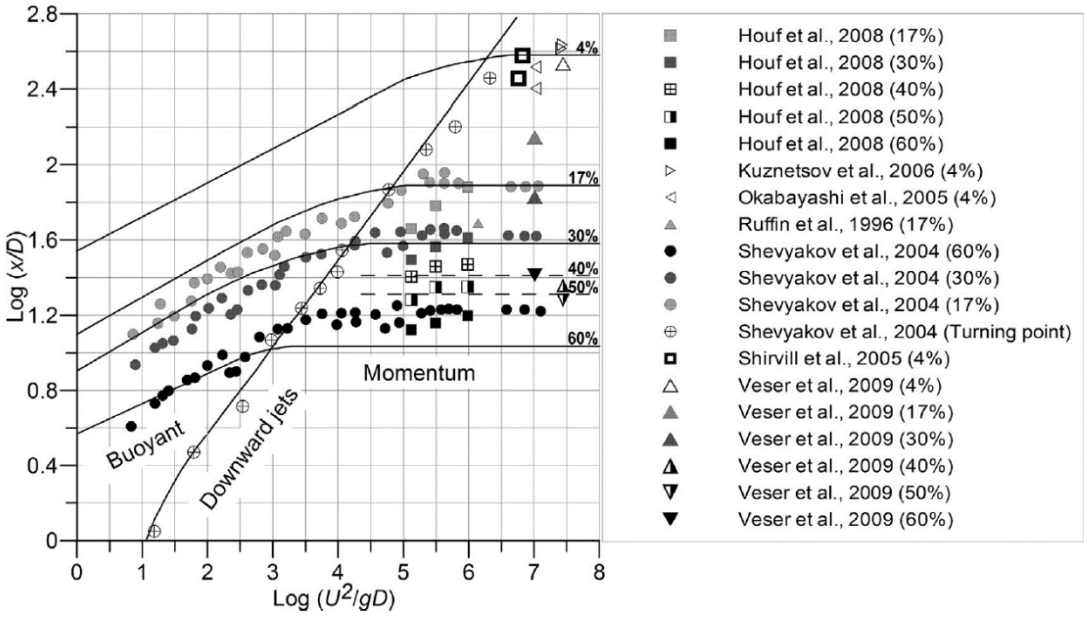

Figure 10: The dependence of distance to nozzle diameter (notional nozzle exit diameter for an under-expanded jet) ratio *x/D* on the *Fr* (Shevyakov et al., 1980; Molkov, 2020).

When a jet forms due to a leak in a high-pressure vessel of a given flammable gas, the concentration of that gas within the jet will decrease the further the distance along the jet away from the source as the turbulence of the jet leads to dissipation and mixing with the surroundings. Thus, it is important to know at what length along the jet is the jet subject to ignition hazards. The distance over which a momentum driven jet is at risk of ignition corresponds to the distance at which the fuel concentration within the jet equals or exceeds the lower flammability limit (LFL) (Molkov, 2020).

In Figure 11, Molkov compiles previously published experimental data for hydrogen jet mass fractions at different dimensionless jet lengths to develop his similarity law for predicting the mass fraction of hydrogen as a function of jet length. If the density of the surrounding air is assumed to be at standard atmospheric conditions (i.e., ρ_S=1.204 kg/m^3), Figure 11 can be condensed down into the following equation for predicting the jet length at which the concentration of hydrogen within a hydrogen jet equals the LFL of 4%:

$$x_{4\%} = 1574D\sqrt{\rho_N} \tag{2}$$

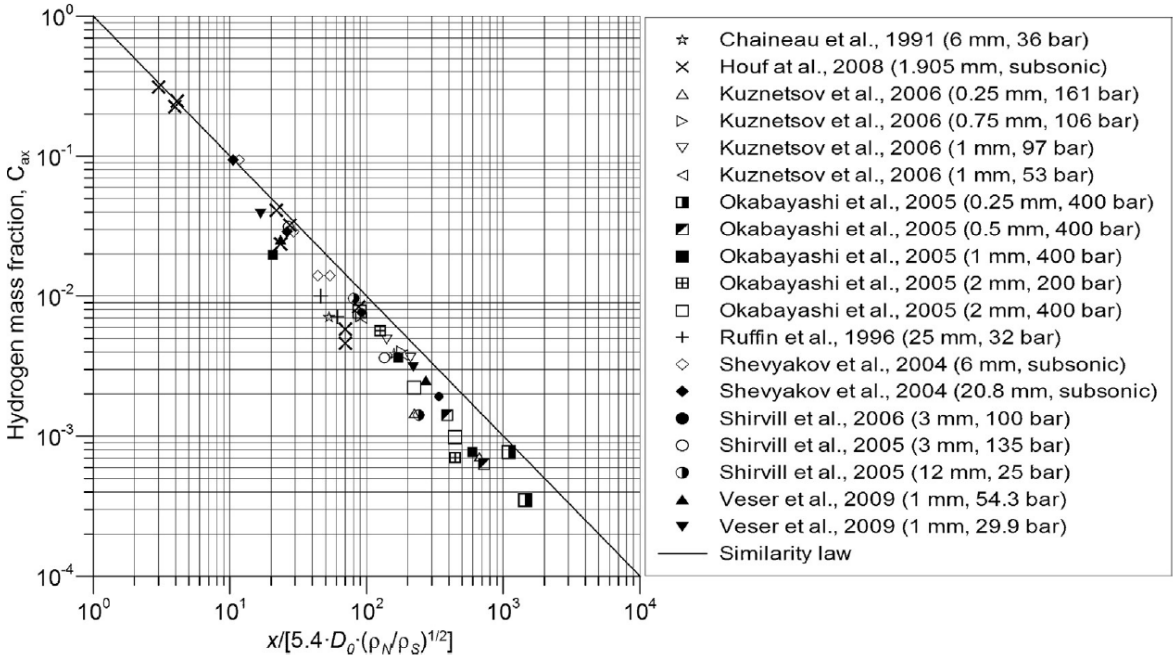

Figure 11: The similarity law (line) for hydrogen concentration decay in expanded and under-expanded momentum-controlled hydrogen jets and experimental data (*x*—distance from the nozzle, m; D_0—actual nozzle diameter, m) (Molkov, 2020).

Similarly, Saffers and Molkov (2013) also examined the dimensionless flame length, L_F, by compiling previously published literature on hydrogen flame length experimental values for buoyancy- and momentum-driven fully expanded and under-expanded jets into Figure 12, where C_N, is the speed of sound in hydrogen under the thermodynamic conditions at the nozzle or leak location.

Furthermore, Molkov (2020) simplifies Figure 12 into the following empirical correlation for the hydrogen flame length:

$$L_F = 76\left(\dot{m}D\right)^{0.347} \tag{3}$$

Where the mass flow rate of hydrogen, $\dot{m}$, is determined from Molkov's under-expanded jet theory (Molkov, 2020).

From a hydrogen safety perspective, the data provided in Figure 11 can be used to estimate the distance over which the hydrogen concentration in a jet resulting from a hydrogen leak into surrounding air will fall within the flammability limits for hydrogen (further simplified by Equation 2). Similarly, Figure 12, and the simplified Equation 3 allows for easy estimation of the length of the resulting flame jet if the momentum-driven jet ignites. These distances can then be compared to the distance from the source at which a momentum-driven jet will transition to a buoyancy-driven one, thus potentially reducing safe separation distances for nearby structures, etc. The data presented in Figure 12 is segmented into three sections by the vertical dashed lines.

The regions, from left to right, correspond to data for buoyancy-driven fully expanded, momentum-driven fully expanded, and under-expanded jets, respectively.

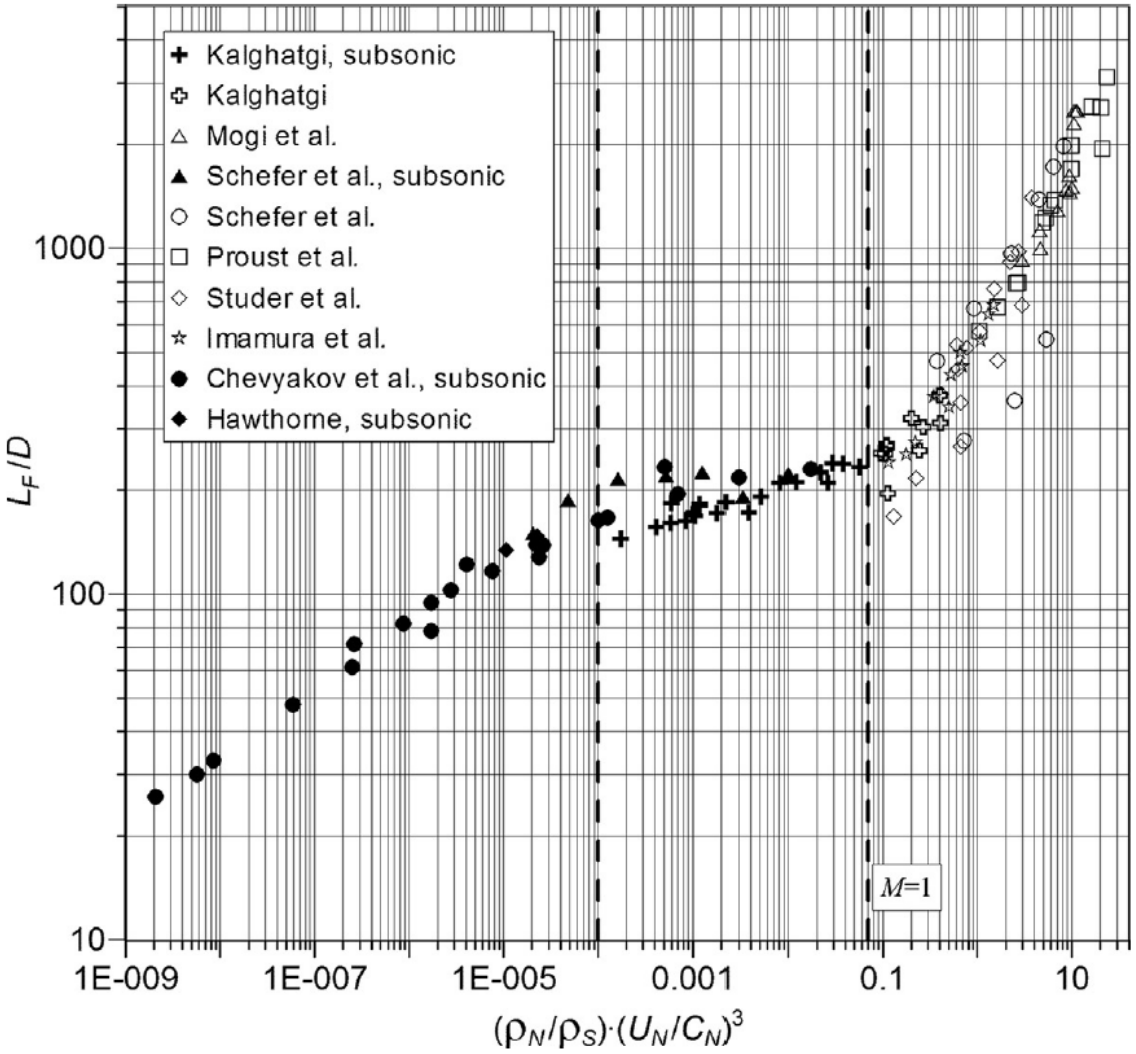

Figure 12: The dimensionless hydrogen jet flame length correlation (Molkov and Saffers, 2011).

2.1.3 Deflagration and Detonation

Vapor cloud fires, vapor cloud explosions, as well as internal pipe fires and detonations are similar in that they all undergo a process known as *deflagration* and potentially *detonation*.

When a gaseous mixture of fuel and oxidizer (i.e., air) ignites, the initial flame kernel will grow as the turbulent flame front travels out from the initial ignition location through the mixture. This traveling turbulent flame front behavior is known as *deflagration* when its propagation speed is subsonic, or as *detonation* once it reaches sonic velocities and generates a blast wave.

Oran et al. (2020) identified five intermediate stages for the deflagration to detonation/DDT process, as shown in Figure 13.

In the first stage, or *slow deflagration*, the propagation speed of the flame front begins to accelerate as the surface area of the flame begins to increase due to production of combustion gases, background turbulence, and interactions with confinement and congestion such as obstacles, walls, etc. The flame velocities at the very early stages of slow deflagration are in the range of 10–30 m/s. Large scale deflagrations at this stage of development are often referred to as cloud fires, or vapor cloud fires. In a slow deflagration, the flame speed can accelerate too close to sonic velocities, up to ~350 m/s in hydrocarbon-air mixtures.

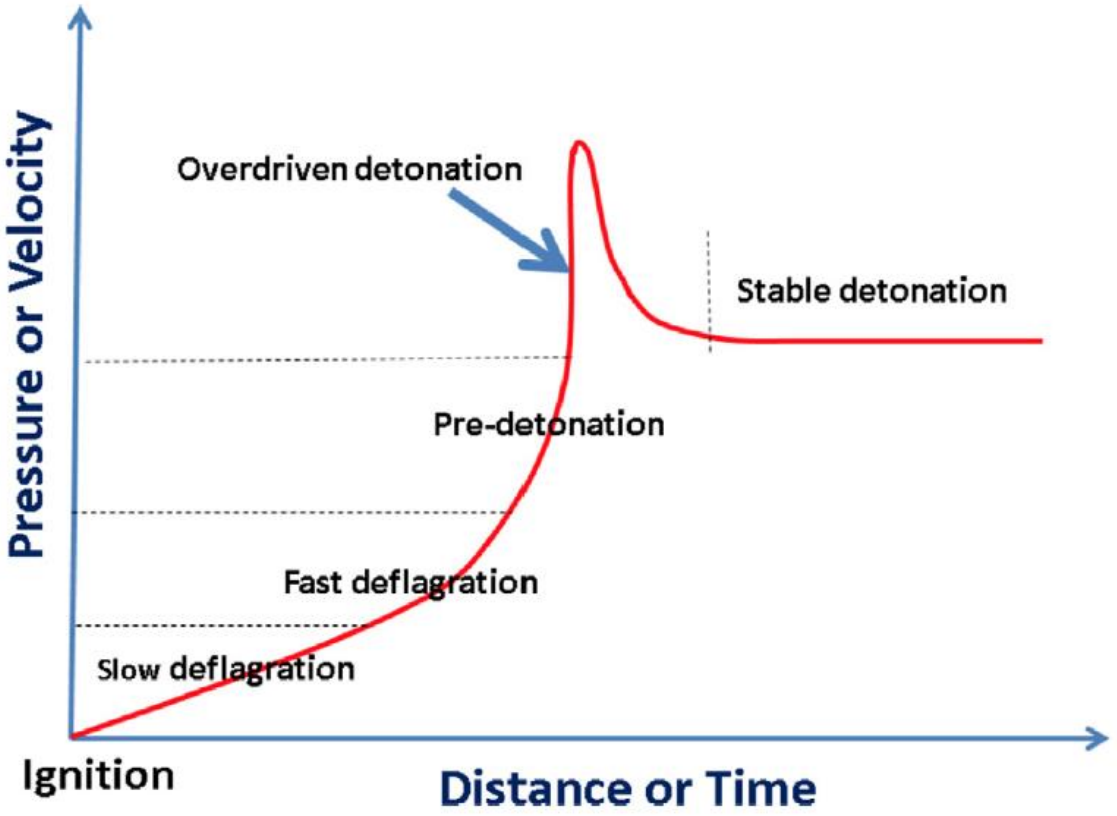

Figure 13: Schematic showing the phases in the evolution of a combustion system from a deflagration to a detonation (Oran et al., 2020).

In the second stage, known as *fast deflagration*, the accelerating turbulent flame begins to generate pressure waves that eventually form a strong leading shock downstream from the flame. This shock compresses the gases ahead of the deflagration flame, reducing the reaction time of the combustion process. This reduced reaction time, combined with the interactions between the turbulent flame, as well as interactions between the turbulent flame and any interacting shock waves behind the leading shock leads to rapid growth of the flame surface area. The result is that the turbulent deflagration flame accelerates even more, potentially up to as high as half the Chapman-Jouguet detonation velocity, $D_{jc,}$ of the flammable mixture. Where D_{jc} corresponds to the flame propagation speed (along with the corresponding Chapman-Jouguet pressure) that allows for stable, continuous detonation where the combustion products are at sonic conditions once localized combustion is complete (Oran et al., 2020).

In the third stage, the *pre-detonation* stage, the deflagration flame has accelerated to the point where it nearly overtakes and couples with the leading shock, causing the rapid formation of numerous "hot spots", or sharp gradients in the reaction time, within the flow and expansion of the flame area.

In the fourth stage, or *overdriven detonation*, the conditions behind the leading shock reach a critical state and the system transitions to detonation. Immediately after this transition, the local transient pressures are very high (up to twice the stable Chapman-Jouguet detonation pressure) and the detonation is said to be overdriven.

The final stage of the *deflagration to detonation transition/*DDT is *stable detonation propagation*. In this stage, the detonation wave is steady and continues to propagate through the mixture at the Chapman-Jouguet velocity and pressure (which are functions of the flammable gas mix and are provided for methane and hydrogen in Table 2) until the flammable gas mixture is consumed.

Table 2: Chapman-Jouguet Detonation Pressures and Velocity for Hydrogen and Methane Gases (NFPA 67, 2019)

Chapman-Jouguet Property	Hydrogen	Methane
Detonation Pressure (bar)	15.8	17.4
Detonation Velocity (m/s)	1,968	1,802

2.1.3.1 Vapor Cloud Fires and Vapor Cloud Explosions

Vapor cloud fires (i.e., slow deflagration) and vapor cloud explosions (i.e., detonation) can occur both inside structures (laboratories, garages, factories, etc.) and in external open-air environments such as storage tank areas/farms when a leak occurs, and ignition is delayed long enough for the flammable gas to mix with air to form a vapor cloud. Once ignited, the slow deflagration of a vapor cloud fire may or may not accelerate and transition into a vapor cloud explosion through the DDT process detailed above. The likelihood of a vapor cloud explosion depends greatly on several factors including atmospheric conditions, turbulence intensity of the deflagration flame, the presence or absence of congestion or confinement within the area of the fuel-air mix (the presence of which can lead to increased flame turbulence as well as the production of numerous interacting reflected shock waves that accelerate flame propagation as well as initiate additional ignition points) (Oran et al., 2020). While slow deflagrations such as cloud fires tend to cause primarily heat damage and localized oxygen depletion within the original confines of the vapor cloud, the lack of a pressure-driven blast wave normally leads to very little pressure-induced damages, the detonation associated with a vapor cloud explosion can cause widespread pressure related damages to people, structures, and vehicles well outside of the confines of the vapor cloud (Oran et al., 2020).

2.1.3.2 Deflagration and Detonation in Piping Systems

Deflagrations and detonations can occur within piping systems which contain a combustible gas mixture (containing both fuel and oxidant). This may be a normal operating condition, or abnormal such as the case of fuel gas mixing with air in a pressure relief vent line. After ignition,

the flame accelerates and generates a leading pressure wave. This starts the growth of the flame front, development of flow turbulence, and increasing compression of the burnt and unburnt gas, which can lead to the formation of shock waves (NFPA 67, 2019; Yang et al., 2020; Wang et al., 2018; Heidari and Wen, 2014). With increasing compression, the location at which self-ignition can occur due to the heating of the unburnt gas moves ahead of the flame front, meaning that the gas reacts before encountering the flame. This leads to an increase in the intensity of the shock wave, as well as the creation of a retonation wave, or a pressure wave traveling in the opposite direction of the original shock wave generated by the deflagration flame front.

Pipe bends and obstacles (orifices, blind expansions, and reductions of pipe diameter with sharp corners, etc.) can have a drastic effect on the speed at which a pipe deflagration accelerates and transitions into a detonation (NFPA 67, 2019; Yang et al., 2020; Wang et al., 2018; Heidari and Wen, 2014). In the case of pipe bends, the flow along the outer radius of the bend will accelerate compared to that along the inner radius. This has the effect of increasing the net flow turbulence, which will "stretch" the flame, thus increasing the flame area and turbulence. In addition, any oblique shocks reflected from the walls of the pipe bend will increase the intensity of the shock-related compression and pre-heating of the flow. Similarly, flow obstructions within the pipe system will enhance flow and flame turbulence, as well as generation of multiple oblique shock waves whose interactions increase the intensity of the compression and heating of the flow ahead of the flame front, potentially leading to the creation of additional hot spots and ignition kernels. A significant amount of experimental and modeling research has been conducted into the effects of pipe bends and obstacles on DDT in pipes and channels and can be found in Yang et al. (2020), Xiao and Oran (2020), Wang et al. (2018), and Heidari and Wen (2014), as well as other literature.

2.2 EFFECTS OF HYDROGEN ON METALS

To use the existing infrastructure or design new systems where hydrogen is used as fuel, careful consideration must be made in the design and materials selection of fuel system components. Compatibility of the materials with hydrogen is a major concern due to a phenomenon known as hydrogen embrittlement (HE). Hydrogen can cause embrittlement of metals, and deterioration of plastic and rubber seals which can lead to significant safety and environmental risks. HE of metallic alloy is of big concern in hydrogen production and storage systems, where failure can have catastrophic consequences. For this reason, handling and the safety issues for hydrogen are different from methane or natural gas.

The causes of hydrogen leaks can be divided into four categories, regardless of location:

- Permeation leaks due to the very small size of the hydrogen molecules, which facilitates gas migration through the materials.
- Leaks due to progressive wear of materials (corrosion and mechanical fatigue).
- Leaks due to leaks in the component's connection or instrumentation (flange, joint, valve).
- Leaks resulting from a rupture of the walls of equipment due to an external and sudden mechanical attack, chemical or thermal, or to overpressure.

2.2.1 Hydrogen Embrittlement

The ingress of atomic hydrogen from a gaseous environment, or during corrosion from an environment containing moisture, can severely reduce the mechanical strength and fracture resistance of high-performance metallic materials by HE, leading to hydrogen environment assisted cracking (HEAC) and its various subfamilies: hydrogen-assisted stress-corrosion cracking (HASCC), hydrogen induced cracking (HIC), sulfide stress cracking (SSC), stress corrosion cracking (SCC), debonding, etc. (Lynch, 2011). The ingress of atomic hydrogen causes metals to become brittle and fracture easily, especially when they are exposed to hydrogen over long periods, particularly with hydrogen in high concentrations and at high pressures.

HE takes place either at low or high temperature. At low temperature, if the operation temperature is below the ductile-brittle transition temperature, embrittlement of metals can take place. This type of embrittlement called “cold embrittlement” can occur when the hydrogen is stored or transported in liquid form (HySafe, 2007; Tashie-Lewis and Nnabuife, 2021). Cryogenic temperature embrittlement for austenitic stainless steels may occur during the transition from room temperature to cryogenic temperature (lower than 77K) (Wang et al., 2021). This is due to the decrease of toughness of structural materials as ferritic steels (Ogata, 2008). Therefore, during design and the selection of the materials for cryogenic vessels or piping systems, cold embrittlement must be taken into account to avoid large thermal stresses.

At higher temperatures and pressures, hydrogen permeates and diffuses through mild steels, causing decarburization and embrittlement. Therefore, during the materials selection involving storage, transfer, and use of hydrogen gas under pressure, HE should be taken into account. In bulk, metal stresses may cause cracking, and the absorption of hydrogen causes metal embrittlement.

HE results from the diffusion of hydrogen atoms through the lattice structure of the metals and affecting their mechanical and physical properties (Barrera et al., 2016). High hydrogen concentrations are known to occur at grain boundaries, slip bands/dislocations, and around second-phase particles and other interfaces (Figure 14) (Lynch, 2011). Austenitic stainless steels, aluminum (including alloys), and copper (including alloys) are generally applicable for most hydrogen service applications. However, high-strength (above 100 ksi) and low-alloy steels, nickel and titanium alloys are more susceptible to hydrogen embrittlement (Gillette and Kolpa, 2007). Additional questions such as loss of material strength, fracture toughness, enhanced fatigue crack growth rates, low cycle fatigue, subcritical and sustained load cracking, susceptibility to stress corrosion cracking, and hydrogen-induced cracking must also be answered. Exposures to hydrogen can reduce fracture toughness, crack propagation resistance, ductility (as measured by reduction in area), and increase the fatigue crack growth rates. In addition, during the selection of material, protection from internal, external, and atmospheric corrosion need to be considered.

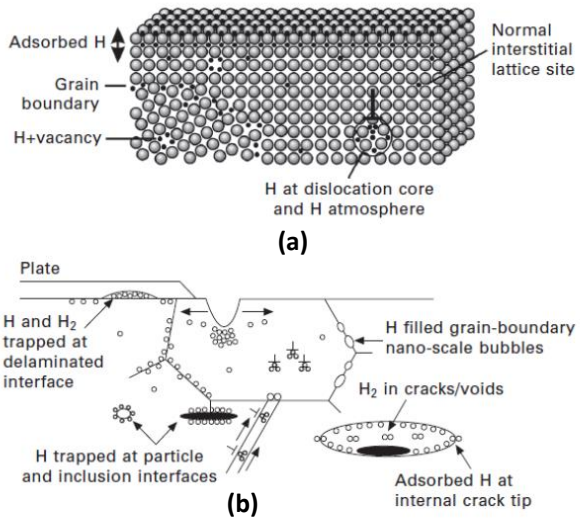

Figure 14: Sites and traps for hydrogen in materials at (a) atomic and (b) microscopic scale (Lynch, 2011).

2.2.1.1 Hydrogen Embrittlement in Gas Phase

HE in gas phase initially requires adsorption of hydrogen gas and formation of atomic hydrogen on the metal surface, which allows hydrogen diffusion into the surface (Figure 15). Once hydrogen atoms diffuse into the material, they can form hydrogen molecules too large to diffuse through the alloys. This results in pressure builds at crystallographic defects, such as dislocations or voids, that cause microscopic internal cracks to form. These cracks will reduce the alloys' ductility and load bearing capacity (Marchi, 2013). The resulting stress, which is lower than the yield stress of the alloy, can cause catastrophic failure of embrittled alloys. Hydrogen diffusion throughout the metals depend on the hydrogen gas pressure, dissociation reaction rates, concentration, and stress field in the metals near the crack tip (Nanninga et al., 2010). In addition to the susceptible materials and an environment conducive to this attack, internal or external stress is also required to initiate HE. To quantify HE, the interactions among material mechanical properties, external stress, and the environmental conditions need to be investigated.

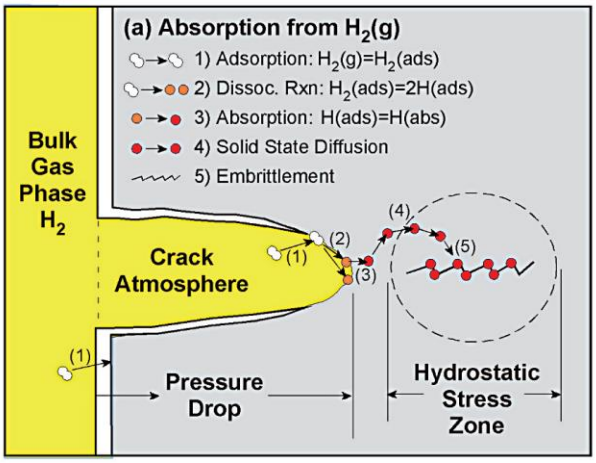

Figure 15: Model methods for hydrogen adsorption into a metal surface exposed to hydrogen gas (Herring, 2020).

2.2.1.2 Corrosion and Hydrogen Embrittlement in Aqueous Phase

Hydrogen production is expected to increase to balance the impact of intermittent generation from renewable power sources, in this case, hydrogen gas production coming from the electrolysis. Hydrogen from this source is relatively pure with the possibility of very small concentrations of water and oxygen as an impurity. In the scenario of large-scale hydrogen production, the hydrogen gas will be stored and dispatched later for use. The small amount of water and oxygen may accumulate leading to the corrosion of the metal and possibly result in further hydrogen charging and embrittlement of the metal (Figure 16).

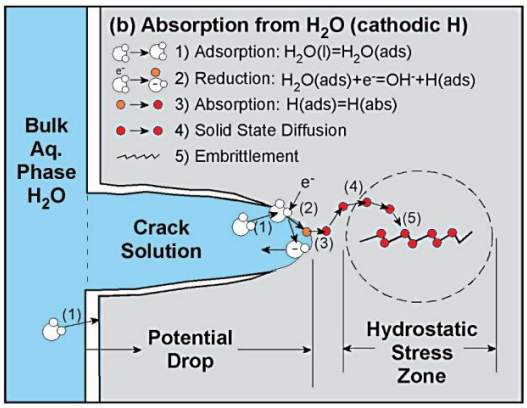

Figure 16: Model methods for hydrogen adsorption into a metal surface exposed to aqueous phase (Herring, 2010).

2.2.2 High-Temperature Hydrogen Attack

Temperature, hydrogen pressure, service exposure time, and stress play a critical role in high-temperature hydrogen attack (HTHA; API, 2016). American Petroleum Institute (API) published a report on steel alloys susceptible to HTHA (API, 2016). At high temperature (typically above 220 °C) and hydrogen-rich atmospheres with hydrogen pressure above 100 psi (~ 6.9 bar), alloy steels are susceptible to HTHA, also called hot hydrogen attack or methane reaction. This phenomenon occurs in high-pressure steam boilers, catalytic reformers, hydrogen producing units, hydrogen clean up units such as pressure swing adsorption (PSA), gas blade turbine, and boiler tubes. At elevated temperatures, hydrogen molecules dissociate into atomic form, which diffuse into the steel and react with non-metallic phases (carbides Fe_3C) forming voids (methane) in the metals (HySafe, 2007; Khoshnaw and Gubner, 2021). Methane cannot diffuse through steel due to its molecular size. Therefore, the increase in methane pressure inside the steel may lead to embrittlement. At temperatures above 540 ^{o}C, hydrogen can cause decarbonization of the steel alloy surface instead of blistering or cracking in the metal. The decarbonization happens only if the bare steel surface is directly in contact with steam containing hydrogen.

Microscopically, HTHA appears as small intergranular cracks parallel to the surface. In addition, hydrogen can react with intermetallic elements (Ti, Zr,V, Nb) from the host metal to form brittle hydrides, leading to embrittlement of metals.

Figure 17 shows the hydrogen partial pressures and temperatures below which various materials are not expected to exhibit susceptibility to HTHA. Carbon steels with low amounts of Cr and Mo are most susceptible to HTHA. However, Cr-rich and Mo-rich carbides are more stable than iron carbides and resist decarbonization (methane formation) at higher temperatures and hydrogen pressures. The curves (Nelson curves) shown in Figure 18 can be used in selection of the materials for high-temperature hydrogen application. However, the Nelson curves do not take into account parameters such as grain size, type of weld, stress, and time of operation.

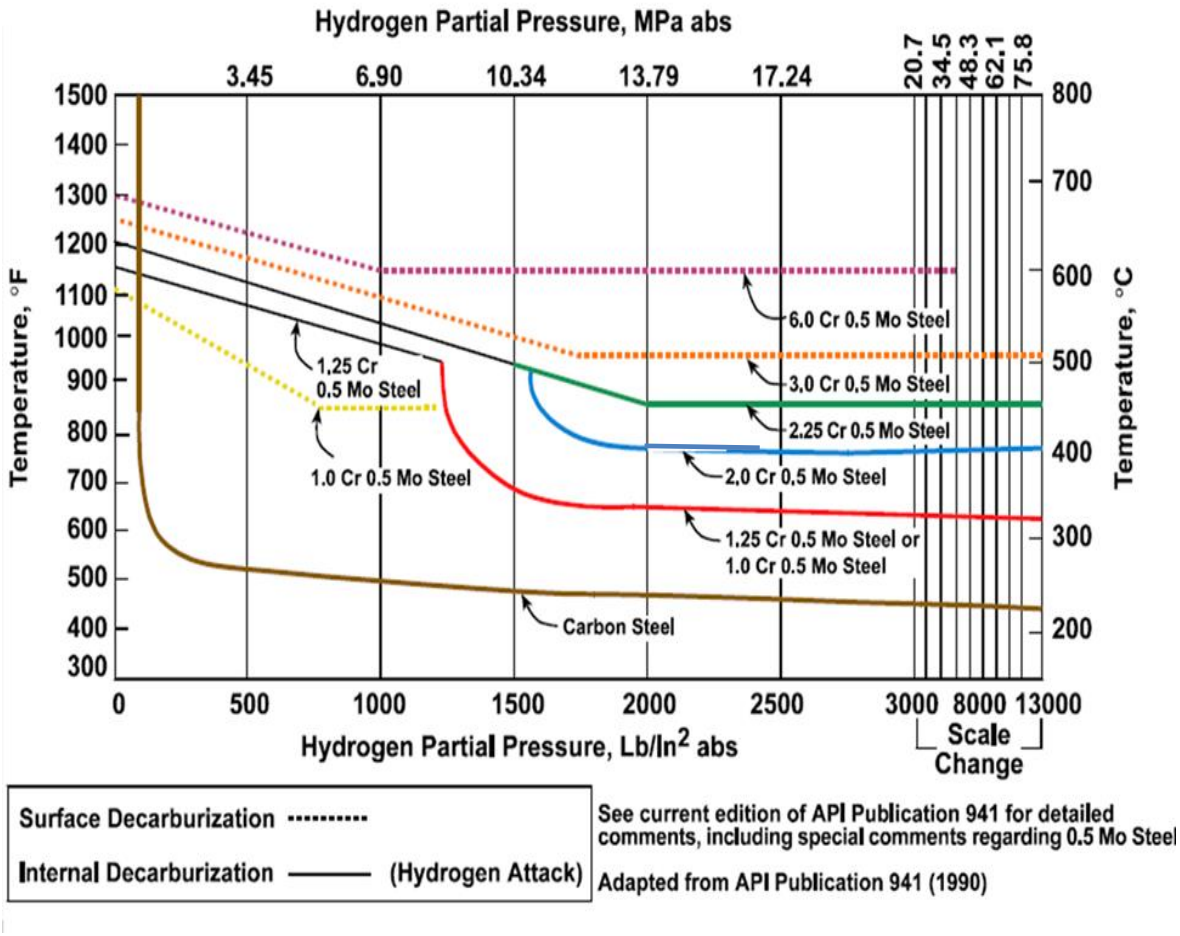

Figure 17: Steel in high-temperature hydrogen service showing effect of Mo and trace alloying elements (API, 2016). Hydrogen attack occurs at conditions above the curves.

In 2005, the BP Texas City refinery experienced a devastating incident and a major fire in the resid hydrotreater unit (RHU) that caused $30 million in property damage. The cause of the incident was a leakage of the hydrogen gas from the ruptured carbon steel elbow which was due to the HTHA (U.S. Chemical Saferty and Hazard Investigation Board, 2005). The hydrogen was pressurized up to 3,000 psi (~207 bar) and preheated in the RHU heat exchanger up to 316 ^{o}C before it passed through the furnace (Figure 18). The carbon steel elbow shown in Figure 18 experienced HTHA after operating for only 3 months, due to the reaction of hydrogen atoms with the dissolved carbons or carbides (Fe_3C) to form methane gas, which causes the decarbonization of the steel and degradation in mechanical properties of steel. The combination of the three factors summarized in the Venn diagram (Figure 19) led to HE of the carbon steel elbow.

The industry standard for components in hydrogen service is grade 316 stainless steel due to the high content of chromium and molybdenum, which increases carbide stability thereby minimizing methane formation. Cupro-nickel is also suitable for hydrogen service and copper can be used for low-pressure application.

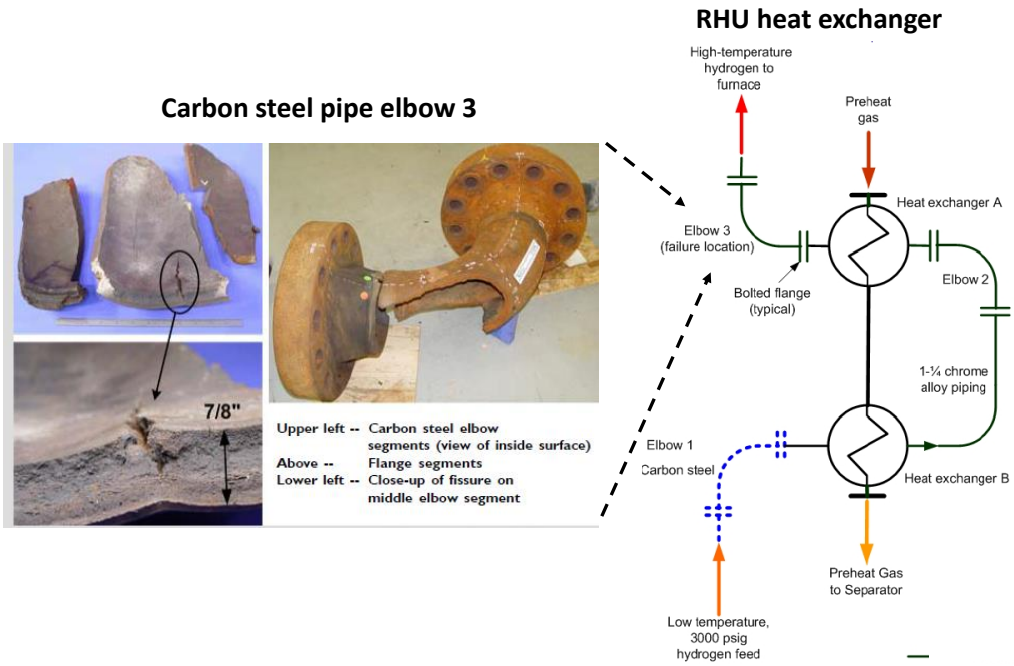

Figure 18: Rupture of carbon steel pipe elbow exposed to HTHA environment (3,000 psi H_2 and 316°C) at RHU heat exchanger (U.S. Chemical Saferty and Hazard Investigation Board, 2006).

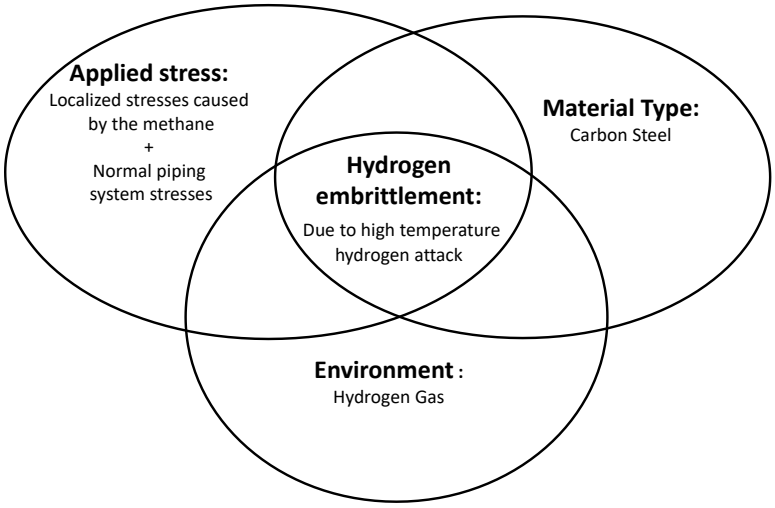

Figure 19: Three influencing factors associated with HE.

2.2.3 Effect of Temperature and Impurities on HE

2.2.3.1 Effect of Impurities

The presence of impurities in hydrogen depends on the source of the feedstock, the process technology, and the purification steps used in hydrogen production plants. Therefore, the purity of hydrogen output from the different production systems will vary. Table 3 shows a summary of

commercial hydrogen production technologies. The purity requirement for hydrogen depends on the industrial application where the produced hydrogen will be used. An increase in purity requirement necessitates incorporation of additional purification processes which increases the capital and operating costs. In addition, a high degree of purity of the hydrogen favors embrittlement which could be influenced by adding gaseous promoters (e.g., H_2S), or inhibitors (e.g., O_2 and CO), or inert gases (Ar, N_2) depending on the specific operating conditions.

In the presence of moisture, H_2S dramatically accelerates hydrogen entry to most alloys resulting in sulfide stress cracking. In addition, some contaminants such as CO and H_2S can reduce the efficiency of hydrogen production which can result in catalyst poisoning and premature system failure. Table 4 shows the impurity levels for hydrogen produced by a reformer with carbon capture. The International Organization for Standardization (ISO14687-3) (Smith, 2004) and Compressed Gas Association (CGA G-5.3) (Smith, 2004) provided purity requirements and estimated range concentration of impurities in hydrogen (Table 5). Impurities in hydrogen may also be introduced through the transmission and distribution through the pipeline network.

Table 3: Possible Impurities in Hydrogen Production Technologies (Kalamaras, 2013; DNV GL, 2019)

Technology	Feedstock	Efficiency	Possible Impurities in Produced H_2
Steam reforming	Hydrocarbon	70–85%	CO, CO_2, CH_4, N_2, Ar, H_2O, O_2, H_2S
Partial oxidation	Hydrocarbon	60–75%	CO, CO_2, CH_4, N_2, Ar, H_2O, O_2, H_2S
Biomass gasification	Biomass	35–50%	CO, CO_2, CH_4, N_2
Electrolysis	H_2O + Electricity	50–70%	H_2O, O_2

Table 4: Impurity Levels for Hydrogen Produced by a Reformer with Carbon Capture (DNV GL, 2019)

Impurities	Steam Methane Reforming (SMR) (dry mol %)	Oxygen- Fed Autothermal Reforming (ATR) (dry mol %)	Air- Fed Autothermal Reforming (ATR) (dry mol %)
CO	0.1-4	0.3–2	0.6–0.7
CO_2	0.35–0.7	0.7–1.7	0.4
CH_4	3.5–8	0.3–3	0.08– 4
N_2	0-0.3	0.7	23–46
Ar	0	0.6	0.5–0.6
H_2O	< 0.03–0.4	<0.03–0.4	<0.03–0.4
O_2	0	0	0
H_2S	$<50 * 10^{-4}$	$<50 * 10^{-4}$	$<50 * 10^{-4}$

Table 5: Directory of Limiting Characteristics (maximum allowable limits of contaminants) (Smith, 2004)

			ISO 14687-3
Contaminants	Type I (Gaseous Hydrogen) B* (ppm_v)	Type II (Liquid Hydrogen) A* (ppm_v)	Type I (Gaseous Hydrogen) Grade E, Cat. 1** (μ mol/mol)
CO	10	1	10
CO_2	10	1	Included in total non-hydrogen gases (max 0.5 mol %)
CH_4	10	9	10
N_2	400	-	400,000
Ar	-	1	400,000
H_2O	34		Non-condensing at ambient temperature
O_2	10	1	200
H_2S	-	-	0.004

*General industrial application.

**Gaseous hydrogen fuel for proton exchange membrane (PEM) fuel cell application for stationary.

2.2.3.2 Effect of Temperature

Adsorption and diffusion of hydrogen is a function of temperature. Because the solubility of hydrogen increases at higher temperatures, raising the temperature can increase the diffusion of hydrogen through the metal which increases hydrogen attack (decarbonization, hydrogen hybrids) of steels alloys, leading to embrittlement of metals (Khoshnaw and Gubner, 2021). Generally, near-room temperature is where alloys are most susceptible to HE. Hydrogen diffusion can occur even at lower temperatures when the HE is mass transport controlled.

Carbon and low-alloy steels exhibit less HE as temperature increases. However, at elevated temperature (above 220 ^oC) steel alloys are susceptible to HTHA. At low temperature, if the operation temperature is below the ductile-brittle transition temperature, cold embrittlement of metals can take place (HySafe, 2007; Tashie-Lewis and Nnabuife, 2021).

Cryogenic temperature embrittlement may occur during the transition from room temperature to cryogenic temperature (lower than -196 ^oC (77 K)) (Wang et al., 2021), as many steels exhibit ductile to brittle transition. In general, steel alloys have a decreasing tendency to embrittle with increasing temperature, and the maximum susceptibility to HE is around 25 °C.

2.2.4 System Specific Challenges Due to Hydrogen Embrittlement

2.2.4.1 Material Challenges Issue Related to Hydrogen in a Gas Turbine System

Today, gas turbines are among the most widely used in power generation stations. Gas turbines fueled with hydrogen have led to considerable reduction in CO_2 emissions. In the Netherlands, blended natural gas with hydrogen (<20 vol.-%) are used to fuel conventional gas turbines (Quarton and Samsatli, 2018). The challenges of burning hydrogen-rich fuels in gas turbines are

encountered mainly in the combustor. This is due to the combustion characteristic and higher reactivity of hydrogen in comparison with natural gas, which effect the durability of gas turbine components (Griebel, 2016). High-temperature oxidation and hot corrosion of hot path materials and turbo machinery components is a big issue in gas turbine fueled with hydrogen. This is due to the higher moisture content in the exhaust gas compared to natural gas combustion, causing a higher heat transfer to the combustor walls and turbine blade material in the hot section. At high temperature, the microstructure of the materials is not stable, causing the materials to be exposed to creep load and oxidation. In addition, the presence of impurities in air intake and ingested fuel (hydrogen), such as sulfur and water vapor, can cause hot corrosion due to formation of low melting compounds (Oskarsson, 2007; Wright and Gibbons, 2007). High-nickel superalloys such as Hastelloy X and Haynes 230 are frequently selected as materials for the combustion chamber, due to their corrosion and heat resistance (Oskarsson, 2007). Figure 20 shows main parts of an Alstom gas turbine, exposure conditions, and materials used in different sections. Hastelloy X and Haynes 230 possess good resistance to carburizing and nitriding environment in high-temperature environment containing hydrogen, nitrogen, and ammonia, due to their high nickel content. Therefore, high-nickel superalloys are less susceptible to HTHA. However, the Haynes 230 alloy, when operated with thermal cycling undergoes creep and fatigue which also makes it more susceptible to hydrogen attack (Barrett et al., 2016). High-temperature oxidation and hydrogen attack can be prevented by a proper selection of alloys and coatings. Annealing at temperatures lower than the solution heat-treating temperatures (1,177 to 1,246 °C) will produce some carbide precipitation in the Haynes 230 alloy, which cause the loss of alloy integrity and marginally affect the alloy's strength and ductility. The loss of alloy integrity results from chromium depletion in the vicinity of carbides precipitated at grain boundaries, which causes the alloy to become susceptible to HE, intergranular corrosion, or intergranular SCC.

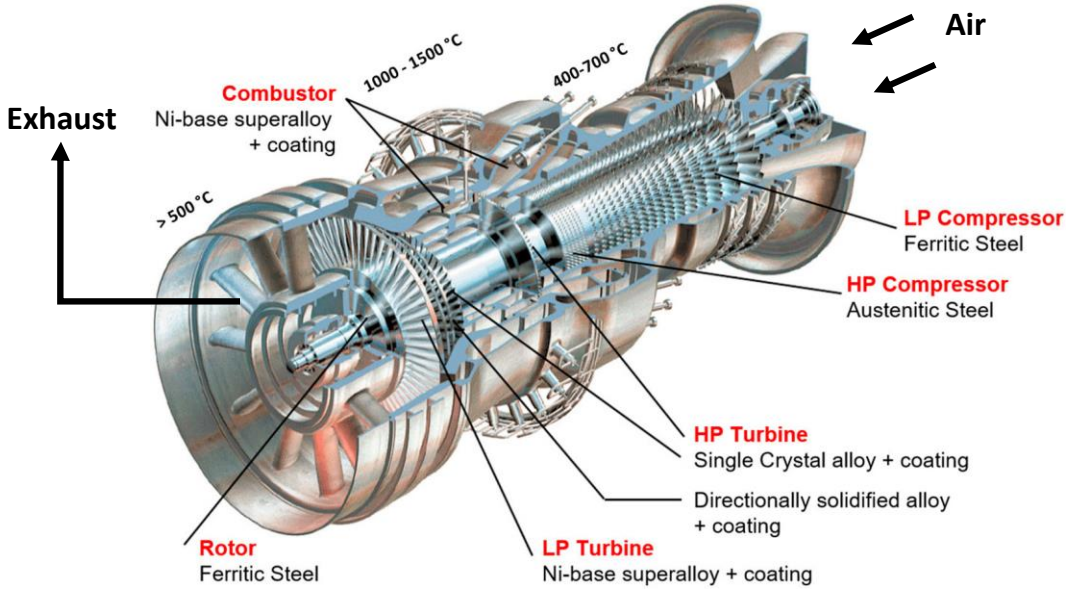

Figure 20: Main parts of an Alstom gas turbine, exposure conditions, and materials used in different sections (Shaikh, 2018).

2.2.4.2 Hydrogen Embrittlement in Fuel Cell Systems

Fuel cell systems are an alternative way to produce electricity, using hydrogen produced by the reforming of hydrocarbon fuels. SOFCs are most suitable for stationary power generation due to their fuel flexibility, high efficiency and low CO_2 emission. Metallic components in the SOFCs are a concern for hydrogen embrittlement and other high-temperature issues.

2.2.4.3 Hydrogen Pipelines

Storage and transport of hydrogen are other challenges facing hydrogen production plants. For example, this challenge could be addressed by producing hydrogen in the proximity of chemical plants where it can be used as a feedstock to produce electricity. Unfortunately, the existing network of pipelines (mostly natural gas) is made mainly of carbon and low alloy steels that are susceptible to HE (Gillette and Kolpa, 2007; Folga, 2007). HE of the lines is a risk factor with both the base steel and the welds. The welds are a largely unexplored area on older pipes that constitute a significant portion of the existing lines. Breakthrough material technologies are necessary to overcome material issue caused by HE. Hydrogen metals interaction studies need to be expanded to include further alloys of interest and fundamental research is still needed to understand the role of parameters effecting HE.

2.3 CLIMATE IMPACT OF HYDROGEN

Hydrogen is spotlighted and regarded as a future fuel and energy carrier that could replace fossil fuels currently being used in most industries. Hydrogen gas is generally regarded as cleaner and more environmentally friendly compared to other GHG. However, this perception on hydrogen needs to be revisited and carefully assessed prior to being extensively used as an alternative fuel in the near future.

The first viewpoint of how hydrogen impacts the environment is to evaluate how environmentally clean hydrogen can be produced. In the U.S., 95% of the hydrogen commercially produced is from steam reforming of natural gas (DOE, 2022a). This process generates CO_2 as a by-product which is a main GHG. The emission of CO_2 from hydrogen production is similar to the extent of direct combustion of fossil fuels (Nowotny et al., 2011). Although hydrogen can also be produced from water by electrolysis without generating any GHG, the electricity required for electrolysis is mostly from combustion of fossil fuels that cannot be free from carbon emission. The only route that enables hydrogen not to have a negative impact on the environment is to produce hydrogen from renewable energy sources such as wind, solar, water, geothermal energy, etc.

Figure 21 shows the comparison of carbon emission from fossil fuels and hydrogen, which is produced by either natural gas or renewable energy (Nowotny et al., 2011). When hydrogen produced from natural gas is used in the fuel cells, the carbon emission from that route can decrease by approximately 20%; a zero-emission level can be reached when hydrogen produced from renewable energy source is utilized for combustion. Hydrogen can be claimed as an environmentally clean fuel only when the technologies associated with hydrogen production are also environmentally clean.

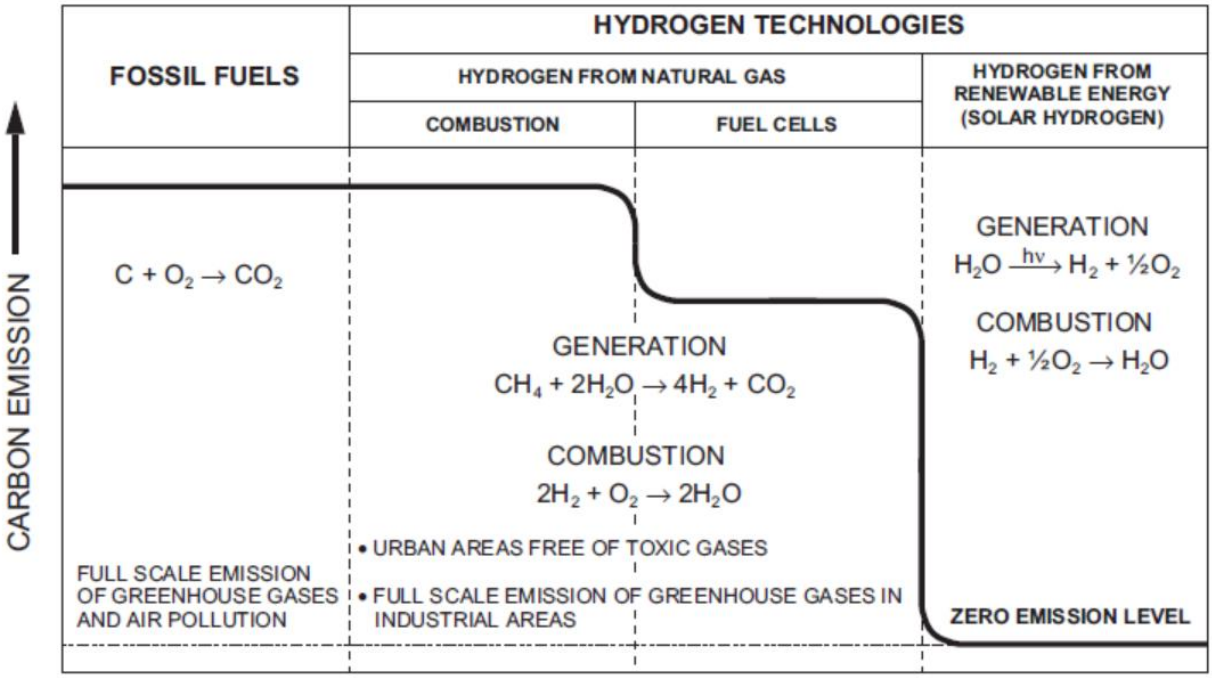

Figure 21: The effect of hydrogen generation and combustion on carbon emission (Nowotny et al., 2011).

The other perspective on the environmental impact of hydrogen is to look at the behavior of hydrogen in the atmosphere. Hydrogen reacts with hydroxyl radicals in the troposphere (Novelli et al., 1999; Derwent et al., 2006):

$H_2 + \cdot OH \rightarrow H_2O + \cdot H$

This hydroxyl radical is produced by the photolysis of the ozone in the atmosphere as described below (Novelli et al., 1999; Derwent et al., 2006):

$O_3 + h\nu \rightarrow O^1D + O_2$ (O^1D: excited oxygen atoms)

$O^1D + H_2O \rightarrow \cdot OH + \cdot OH$

The hydroxyl radicals, the powerful oxidants in the troposphere, react with methane and reduce its concentration in the atmosphere through the methane oxidation cycle (Novelli et al., 1999; Derwent et al., 2006):

$OH + CH_4 \rightarrow CH_3 + H_2O$

$CH_3\cdot + O_2 + M \rightarrow CH_3O_2\cdot + M$ (M: a random molecule that facilitates energy transfer)

$CH_3O_2\cdot + NO \rightarrow CH_3O\cdot + NO_2$

$CH_3O\cdot + O_2 \rightarrow HO_2\cdot + HCHO$

$$HCHO + h\nu \rightarrow H_2 + CO$$

Hydroxyl radicals play a critical role as a cleaning agent in the atmosphere to remove the GHG, methane. However, if more hydrogen reacts with hydroxyl radicals in the atmosphere, the hydroxyl radicals available for methane oxidation would decrease, leading to an increase in the concentration of methane in the atmosphere.

The tropospheric ozone is the third most dominant GHG after CO_2 and methane (Solomon et al., 2007). Hydrogen is one of the ozone precursor species that include methane, nitrogen oxides, carbon monoxide, and organic compounds (Leighton, 1961). Thus, the growth of hydrogen emission to the atmosphere not only builds up the methane concentration, but also augments formation of ozone, perturbing the distributions of methane and ozone in the atmosphere.

Derwent et al. (2006) defined the global warming potential (GWP) of GHG over a 100-year time period (GWP-100) as follows:

$$\text{GWP} = \frac{heat\ trapped\ by\ one\ unit\ mass\ of\ GHG}{heat\ trapped\ by\ one\ unit\ mass\ of\ CO2}$$

The GWP of hydrogen is the sum of GWPs of both methane and ozone, which are originated from hydrogen emission as explained earlier:

$$GWP^{H2} = GWP^{CH4\sim H2} + GWP^{O3\sim H2}$$

According to their calculation, the $GWP^{CH4\sim H2}$ and $GWP^{O3\sim H2}$ were 3.4 and 2.4, respectively over 100 years. Therefore, the overall GWP of hydrogen caused by the changes in the global distributions of methane and the ozone is 5.8 over a 100-year time horizon. Considering the GWP of methane itself which is 23 (Watson et al., 2001), hydrogen may increase global warming by approximately 25% that of methane.

Recent modeling studies on atmospheric hydrogen also reported that hydrogen has a global warming potential of 5 ± 1 over 100 years, asserting that the increased hydrogen in the atmosphere could cause man-made global warming (Derwent et al., 2020). Their suggestions to reduce global warming caused by hydrogen is to carefully control the leakage from any hydrogen-related system such as hydrogen production, storage, transmission, and distribution systems.

If the entire fossil fuel-based energy systems were replaced with hydrogen-based systems, the required hydrogen production would be 2,500 Tg H_2 per year. If there was a hydrogen leakage of 1% (25 Tg H_2), then the equivalent emission of CO_2 would be 145 Tg CO_2 per year. The total estimated GHG from fossil fuels systems would correspond to 23,000 Tg of CO_2 per year; the 1% hydrogen leak rate would have approximately 6% of the climate impact for the entire fossil fuel system (Derwent et al., 2006).

According to Ocko et al. (2022), the GWP introduced by Derwent (2006, 2020) was assessed through just one time pulse of hydrogen emission at time=0, which cannot be an accurate representation of actual hydrogen deployment over time. Instead, Ocko (2022) considered continuous hydrogen emissions to better understand the climate effects of hydrogen over the entire 100-year timeframe. As shown in Figure 22, the GWP of hydrogen below a 10-year time horizon can be more than 10 times higher than what GWP-100 shows, indicating that the traditional GWP-100 calculation does not convey the near- and medium-term climate effects. In

addition, the radiative forcing of H_2 relative to CO_2 caused by the continuous H_2 emissions is approximately double that of the GWP-100 approach over the entire time horizon.

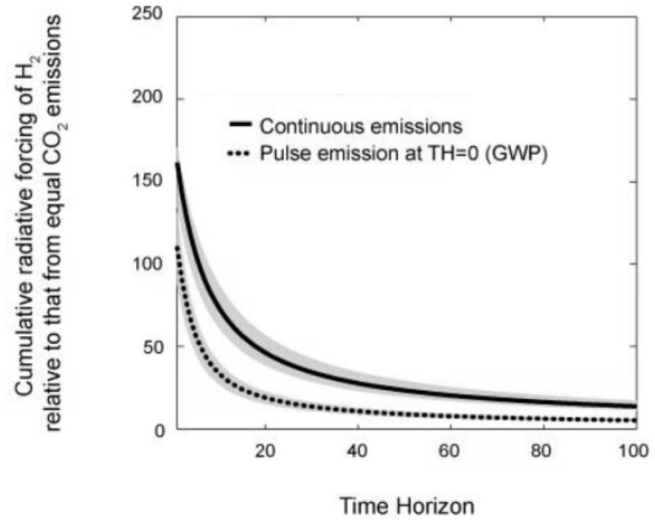

Figure 22: Cumulative radiative forcing of H_2 relative to CO_2 for equal emissions (Ocko et al., 2022).

Figure 23 shows relative climate impact over time from continuous emissions by replacing fossil fuel technologies with green or blue hydrogen (Ocko et al. 2022). In this graph, if there was no replacement of fossil fuel with hydrogen, the result would be 0%. If the climate pollutant emissions generated from hydrogen applications result in more (or less) warming than fossil fuels, the result would be a positive (or negative) percent change in cumulative radiative forcing. As shown in Figure 23, as fossil fuels are replaced with green hydrogen produced via renewable electricity and water at 1% leak rate per unit H_2 deployed, the warming impact could be a negative 84% in the first 5 years. However, if the leak rate is 10% with green hydrogen, the warming could result in a 74% increase over the first 5 years, indicating that green hydrogen is not inherently climate neutral.

If blue hydrogen produced from natural gas with carbon capture, usage, and storage could replace fossil fuels, the warming effects relative to that from the fossil fuels at 10% and 1% leak rates would be a 133% increase and 67% decrease in the first 5 years, respectively. Overall, the blue hydrogen replacement generates higher warming impacts than the replacement with green hydrogen, and it takes more than a decade and 25 years to see climate benefits by adopting green hydrogen and blue hydrogen applications, respectively, at the worst case leak rates. Therefore, short-term climate impacts caused by hydrogen applications should not be overlooked when hydrogen leakage is expected.

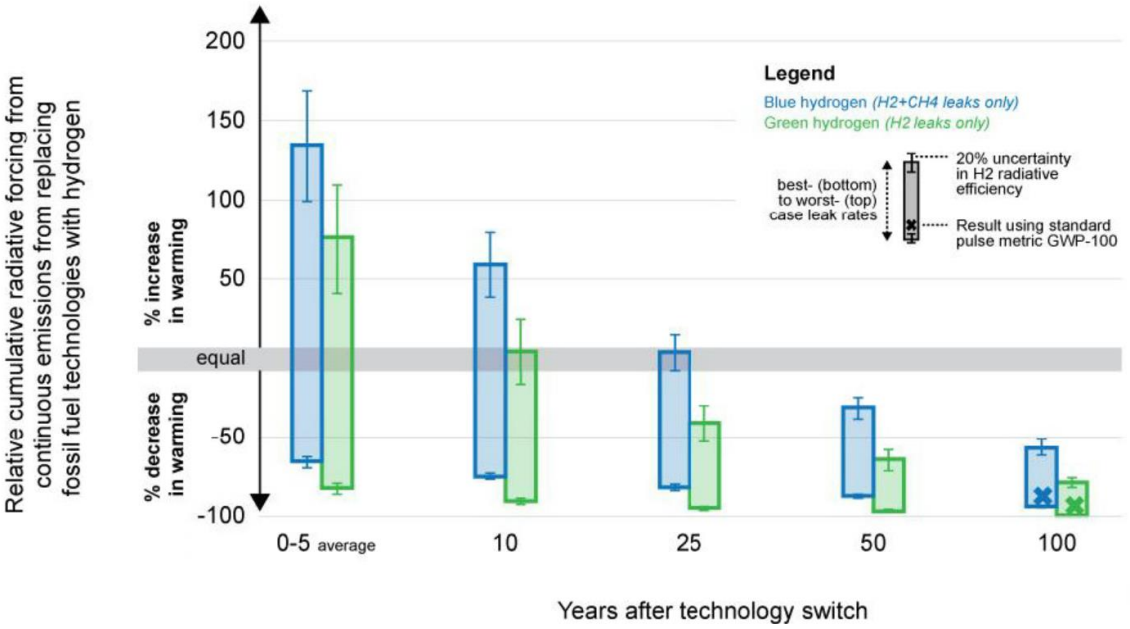

Figure 23: Relative climate impact over time from replacing fossil fuel systems with green or blue hydrogen (Ocko et al., 2022).

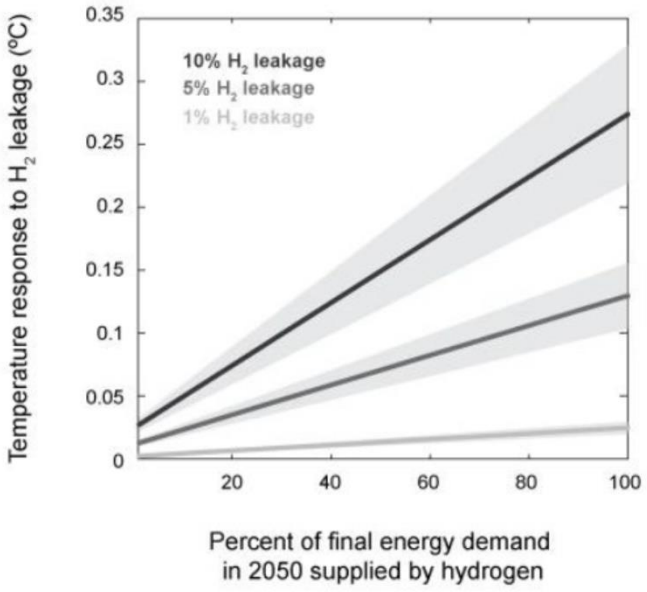

Figure 24: Temperature responses in 2050 depending on hydrogen leak rate and level of hydrogen deployment (Ocko et al., 2022)

Figure 24 shows the anticipated temperature increase in 2050 depending on hydrogen leakage rate and level of hydrogen deployment. If the hydrogen deployment accounts for 50% of final energy demand in 2050, 10% hydrogen leakage could bring about at least 0.1 ºC of warming in 2050. If the final energy demand is completely (100%) supplied by hydrogen in 2050, the 5% hydrogen leakage could contribute to the warming of around 0.1 ºC. However, this warming potential could be minimal if the total leakage reduces to 1%. According to Schultz et al. (2003),

if today's fossil fuel combustion were completely replaced with hydrogen systems, the global hydrogen emission would increase by a factor of 1.35 to 2, based on the assumption of a 3% loss rate of hydrogen. This change would cause a decrease in the tropospheric OH burden of 6.2%, which is primarily driven by the reduction in the emission of nitrogen oxides, an ozone precursor. The reduction in the tropospheric OH burden would, in turn, increase the lifetime of methane by up to 26%.

Based on the publications reviewed in this section, it appears that hydrogen is an indirect and secondary GHG that causes global warming to some extent. Hydrogen would not be completely free from climate impact if hydrogen leakage could not be prevented from the entire hydrogen-based energy systems. Additional research to check these findings is expected.

2.4 LIQUID HYDROGEN

2.4.1 Properties of Liquid Hydrogen

Liquid hydrogen possesses properties that result in several safety-related concerns that must be factored into any use of liquid hydrogen as a fuel source (H2tools.org). Among these are the fact that it is colorless and odorless, making optical or olfactory detection of its presence difficult. At atmospheric pressure, the boiling point of 20ºK (-253 ºC) is the second lowest of all gases (with only helium having a lower boiling point), and all other gases except for helium solidify at that temperature. In fact, when poorly insulated or exposed to the atmosphere, liquid hydrogen can liquify, or even solidify, the surrounding air. This can result in plugging or damaging valves or flow orifices in liquid hydrogen transfer equipment. Liquid hydrogen has a low heat of vaporization and will evaporate quickly when exposed to the atmosphere, resulting in a violent evolution of gas (approximately 850 liters of hydrogen gas for every liter of liquid hydrogen) and potential splashing of liquid hydrogen. This "boil off" gas that evolves from liquid hydrogen can produce severe burns; cause carbon steel, plastic, and rubber materials to become brittle and fracture under stress; accumulate in ground level pits and trenches for short periods of time depending on temperatures and relative density differences between the hydrogen and surrounding atmosphere (hydrogen gas density ranges from 1.34 kg/m^3 at cryogenic conditions to 0.083 kg/m^3 at standard temperature and pressure, the corresponding air density at STP is 1.2 kg/m^3, so for a very brief time following a liquid hydrogen leak the density of the evaporated hydrogen gas will actually be higher than the surrounding air at standard temperature and pressure) (Nesser, 2022); and it can condense atmospheric moisture, creating highly visible fog.

The gaseous hydrogen that is released during these "boil off" events can lead to the formation of gaseous fuel-air mixtures that can lead to vapor cloud fires or vapor cloud explosions if ignited. Liu et al. (2021) and Tang et al. (2020) have conducted independent numerical simulation studies examining the formation and spread of hydrogen vapor clouds arising from liquid hydrogen leaks, factoring in leak rates and atmospheric conditions. Hall et al. (2014) also conducted experiments to study the behavior of fires arising from liquid hydrogen leaks, and concluded that fires that do not result in a BLEVE or vapor cloud explosion typically involve first a deflagration of gaseous hydrogen that propagates back to the leak location (such as a failed burst disk or pressure relief device), at which point the fire transitions into a jet fire sustained by the continuous release of gaseous hydrogen/boil-off. In addition, as previously mentioned in the discussion related to fire and explosions, a sudden, catastrophic failure of a liquid hydrogen storage tank can lead to a BLEVE.

The hydrogen molecule is composed of two types of hydrogen atoms: ortho-hydrogen and para-hydrogen, with the ortho-hydrogen atom having a higher energy level than para-hydrogen. As the temperature of the hydrogen decreases, the ortho-hydrogen will spontaneously change to para-hydrogen to reach equilibrium. This reaction releases approximately 670 kJ/kg of heat, which is significantly greater than the latent heat of vaporization of hydrogen (452 kJ/kg). Consequently, the conversion of ortho-hydrogen to para-hydrogen leads to large quantities of hydrogen evaporation, potentially as high as 50% over a period of 10 days (Sun et al., 2022). As a result, it is necessary for the hydrogen to be converted from ortho- to para- during the liquefaction process, prior to cooling it below the temperature at which it happens naturally, to avoid conversion and boil-off related over-pressurization during storage and transportation.

2.4.2 Incident Statistics for Liquid Hydrogen

Lowesmith et al. (2014) conducted a review of liquid hydrogen accident statistics available through both NASA and the H2Tools.org database. Of the 57 incidents examined, 18 of the incidents occurred during transport and the remaining 39 were associated with liquefaction and storage (Lowesmith et al., 2014). From these, seven causes and five consequences were identified. The seven incident causes that were identified were:

- Design and/or construction failures (likely due to inadequate hazard assessments)
- Equipment failure (excluding incorrect equipment or materials)
- Incorrect operation or inadequate maintenance
- Impact or road traffic accidents
- Contamination
- Escalation (where an incident begins elsewhere and propagates to an liquid hydrogen system)
- Natural causes (extreme weather) or terrorism.

The five general consequences of these events were:

- Fires
- Explosions
- BLEVE
- Accumulation/dispersion
- No release of hydrogen.

Of the 18 road transportation incidents examined, 5 occurred during transit and 13 occurred during loading/offloading of the liquid hydrogen. Of the 5 incidents that occurred during transit, 2 were the result of vehicle accidents and the remaining 3 were attributed to unexpected failure of burst disks. Out of the 13 loading/unloading incidents, 5 of these incidents were caused by equipment failures such as unexpected burst disk failure, loss of vacuum, or loose connections. The 8 transportation incidents that were attributed to incorrect operation occurred during offloading or transfer operations, and included over-pressurization of the head space, deviating from established procedures related to transfer hoses, operating valves incorrectly or too quickly.

The consequences of these transportation incidents were 1 explosion, 4 fires, 12 accumulation/dispersion of hydrogen, and 2 with no release of hydrogen. Three injuries were reported, including 2 cold burns.

Of the 39 reported incidents related to liquefaction and storage systems, 2 occurred in the liquefier or purifier, 11 occurred in vent systems or piping, 6 occurred in valves or fittings, 14 in storage vessels (including their valves and pressure reliefs), 6 occurred in pumps, compressors or vaporizers, and the remaining 5 occurred in transfer lines or pipelines. Of the 6 major incidents reported involving storage vessels, 3 occurred during the commissioning or decommissioning stage. Several of the incidents related to venting systems involved the unexpected ignition of hydrogen resulting in fires or explosions in the vent system pipework or in the vicinity of the vent stack outlet.

The attributed causes for these 39 incidents included: 12 design/construction failures, 8 equipment failures, 18 incorrect operation or inadequate maintenance, 1 contamination, 2 escalation events, and 5 natural case/terrorism events. It should also be noted that some incidents were attributed to multiple causes. The consequence of these incidents were 5 incidents with no liquid hydrogen release, 14 with accumulation or dispersion of liquid hydrogen, 9 fires, 13 explosions, and 1 BLEVE. Injuries occurred in 3 of the incidents, and non-trivial damage occurred in 23 cases.

3. MITIGATION OF HYDROGEN HAZARDS

3.1 MITIGATION OF DEFLAGRATIONS AND DETONATIONS

This section provides a brief introduction to common methods for mitigating the risks of deflagrations and detonations. For a more detailed discussion reference the appropriate National Fire Protection Association (NFPA) codes: NFPA 67 (2019): Guide on Explosion Protection for Gaseous Mixtures in Pipe Systems; NFPA 68 (2018): Standard on Explosion Protection by Deflagration Venting; and NFPA 69 (2019): Standard on Explosion Prevention Systems.

3.1.1 Buildings, Structures, and Enclosures

General methods for mitigation of deflagrations and detonations for buildings, structures, and enclosures (excluding piping systems) can be classified into passive systems and active systems. Passive systems typically take the form of ventilation and explosion diverters; either to allow a flammable gas (such as hydrogen) to escape the confines of the building or enclosure via buoyancy and dissipation to prevent the gas concentration from reaching the lower flammability limit and pose a fire or explosion hazard, or to vent a deflagration or detonation post-ignition away from the structure in a safe manner to avoid damage or injuries to surrounding personnel or structures. Active mitigation methods typically involve the combination of a system of sensors to detect the presence of a flammable gas with activation of ventilation fans and/or activation of spray systems to prevent ignition of the flammable gas through dilution of the mixture below the flammability limits, or inertization.

3.1.2 Piping and High-Pressure Storage Systems

Fire safety systems for high-pressure storage and piping systems can be categorized as either passive systems or active systems. Passive systems can include deflagration and pressure venting, deflagration (or flame) arrestors, and explosion diverters. However, in many instances involving detonations, these passive systems may not be sufficient (per NPFA 67, 2019; Oran et al., 2020), as just venting or arresting the flames does not address the likelihood of reignition of compressed hot flammable gas downstream of the flame arresting system. In the case of detonations within piping systems, both the flame and the shock must be mitigated. To accomplish this, NFPA 67 (2019) recommends use of active detonation arresting systems (DAS), which incorporate both pressure sensors to detect the shock wave and optical flame sensors to detect the appropriate wavelength of the flame produced by flammable gas to determine the location and velocity of the flame front. In addition to these sensors, the DAS also incorporate an extinguishing system that targets the flame with either a water spray or flame retardant spray, as well as a fast-actuating gate valve that closes ahead of the shock wave to prevent the shock from propagating further downstream.

3.2 ODORANTS FOR HYDROGEN DETECTION

An odorant is a chemical with perceptible odor which can be added to odorless gas to be detected for safety purposes. Odorants enable detection of a gas leak without any equipment that requires consistent maintenance and replacement to prevent its malfunction and failures. Odorants can also be ubiquitous without limitation in locations and space where gas detectors cannot be applicable.

Natural gas and liquefied petroleum gas (LPG) are currently odorized with mercaptan that has the unpleasant rotten-egg odor, so that the leaked gas can readily be detectable and recognized. According to NFPA 58 (Liquefied Petroleum Gas Code, 2020), gas should be detectable by the odorant at the concentration of less than one-fifth of the lower limit of flammability. In case of natural gas, which has the lower flammability limit of 5.3%, the concentration of natural gas at 1.06% in air should be detectable by the odorant. Likewise, the LPG should be detected at ~0.4% with the odorant (Kopasz, 2007).

Hydrogen is an odorless and colorless gas, which is extremely flammable and ignites over a wide range of concentration in air. However, hydrogen is not being odorized in any energy-related application including automobiles, turbines, stationary fuel cells, etc. The odorants most commonly used for natural gas and LPG contain sulfur are known to poison the catalyst on the fuel cell electrodes. Catalyst poisoning reduces available reaction sites for hydrogen. This interference from sulfur compounds results in decreased cell performance. Even at levels as low as 0.05 ppm a detrimental impact on the PEM cell performance was reported with sulfur compounds (Zamel et al., 2011). A 1.2 ppm hydrogen sulfide could cause a PEM cell voltage drop of approximately 300 mV within 25 hours (Cheng et al., 2007). Kushi (2017) reported that the internal resistance losses increase during the SOEC and SOFC operations for 5,000 hours with 0.74 ppb of sulfur in the oxidizing gas were 48 mV and 74 mV, respectively, which are due to sulfur deposition on lanthanum strontium cobalt oxide electrode. Wang et al. (2020) reported that the oxygen surface exchange coefficient of the SOFC cathode decreased by a factor of 400 after sulfur poisoning (2 ppm SO_2), which is mainly attributed to the decrease of effective area of active perovskite surface caused by the coverage of the secondary reaction products such as $La_2O_2SO_4$ and $SrSO_4$. Therefore, the odorants containing sulfur compounds are not suitable for hydrogen supplied to fuel cells.

Other potential odorants for hydrogen gas application are nitrogen-containing odorants, such as ammonia and amines. However, those compounds have also shown degradation in fuel cell performance due to the reduction in proton conductivity through the electrolyte membrane and the ionomer in the catalyst layer (Uribe et al., 2002). Fatty acids such as acetic acid or butyric acid have also been suggested to be added to hydrogen gas as odorants (Hibino et al., 2003). However, organic acids tend to have adverse effect on cell performance by decreasing cell voltage at the ppm level of concentration (Kopasz, 2007).

Flynn et al. (2013) provided a method for selecting proper odorants for hydrogen. According to their criteria, the suitable hydrogen odorants should be in a vapor phase at detectable concentration under hydrogen storage conditions at 6,000 psi and also be in the same phase and well blended with hydrogen. The odorants should also be non-toxic to both human beings and the environment at the required concentration. In addition, the odorants for hydrogen should have: 1) a low solubility in water; 2) a vapor pressure of >0.5 psi at standard conditions; 3) a low odor threshold in the gas phase; 4) a smell detectable at <1 ppm by a human nose; 5) good oxidative stability; and 6) sufficient olfactory power or diffusivity.

The olfactory power (pOl) is given as the negative log of odorant concentration (-log[odorant]), indicating the minimum concentration at which a chemical compound is detectable by the average person (Flynn et al., 2013). Based on the definition of pOl, a compound with a greater pOl would be detected at lower concentration levels. Table 6 shows the pOls of several compounds at different types of functional groups. The amines can be detected at sub-ppm levels and the thiol groups can be detected at around ppb levels. The selenium groups have very similar

or higher pOls than thiol groups used for natural gas, and especially ethyl selenol has 67 times higher detectability than ethyl mercaptan. As shown in Table 7, the required loading of ethyl selenol is the lowest among other key odorants. Thus, ethyl selenol is a potent candidate as an odorant for hydrogen.

Table 6: Functionality and Olfactory Power of Chemical Compounds (Flynn et al., 2013)

Functionality	Compound	Olfactory Power (pOl)
Hydrocarbons	ethane	2.00
	propane	2.57
Alcohols	methanol	3.85
	ethanol	4.54
Ketones	acetone	4.84
Aldehydes	formaldehyde	6.06
Amines	methylamine	7.73
	dimethylamine	7.09
	ethylamine	6.49
	propylamine	7.96
Thiols (mercaptans)	methyl mercaptan	8.98
	ethyl mercaptan	8.97
	t-butyl mercaptan	9.48
Sulfides	diethylsulfide	8.41
Selenides	diethylselenide	9.13
Selenols	ethylselenol	10.74

Table 7: Sample Odorant Loading Requirements for Hydrogen (Flynn et al., 2013)

Odorant	Olfactory Power (pOl)	Odorant Threshold (ppm)	Required Odorant Loading in Hydrogen (ppm)	Standard Odorant Loading [6,000 psi H_2] (ppm)
Ethyl mercaptan	8.97	0.001072	30	1,705
Ethyl selenol	10.74	0.000018	0.5	833
Propyl amine	7.96	0.010965	307	999
Methyl amine	7.73	0.018621	521	8,543

Braun et al. (2013) proposed a nitrogen-free, sulfur-free, and selenium-free odorant for hydrogen, which contains at least one acrylic acid C1-C6-alkyl ester and acetophenone. Braun et al. (2013) argued that those odorants have superior properties to other odorants with regard to their warning odor, stability over an extended period of time, and compatibility with noble metal catalysts.

The National Physical Laboratory (NPL) in the UK identified five candidate compounds for hydrogen odorants, as listed in Table 8. According to their report, the odorant-bearing hydrogen should contain less than 4 nmol/mol of total sulfur for a fuel cell system. They have used a single PEM cell for fuel cell degradation testing, and all tubing and fittings were treated with Sulfinert coating. As shown in Figure 25, the odorants containing sulfur such as NB, NB Dilute, and THT (defined in Table 8) led to substantial loss of fuel cell voltage, which are incompatible with PEM fuel cell operation. In contrast, the non-sulfur odorants, Acrylates and Norbornene, have shown the insignificant voltage loss of the PEM fuel cell. However, they mentioned that it is required to have much longer test duration to determine that there is no detrimental effect of those non-sulfur-containing odorants on PEM fuel cell performance.

Table 8: Five Odorants Selected by NPL and SGN (Becker et al., 2019)

Odorant Name	Compound
NB	78% 2-methyl-propanethiol, 22% dimethyl Sulphide
NB Dilute	34% Odorant NB, 64% Hexane
THT	100% tetrahydrothiophene
Acrylates	37.4% ethyl acrylate, 60.1% methyl acrylate, 2.5% 2-ethyl-3methylpyrazine
Norbornene	5-ethylidene-2-norbornene

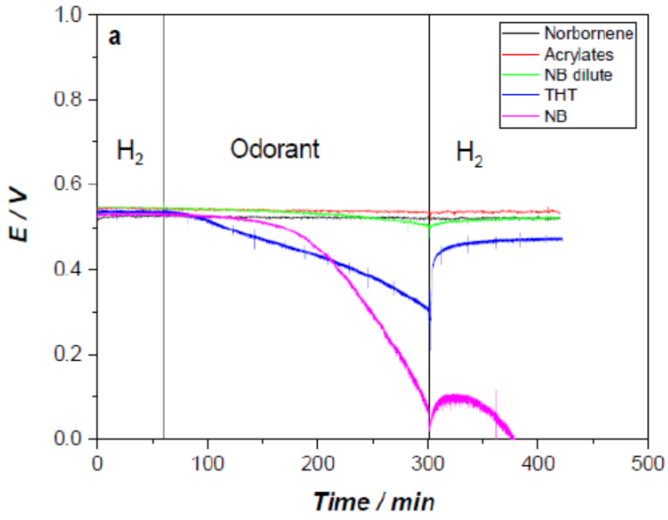

Identifier	Cell voltage loss after 4 h (mV)
Norbornene	5 ± 2
Acrylates	10 ± 2
NB dilute	40 ± 2
THT	225 ± 2
NB	460 ± 2

Figure 25: The voltage loss of PEM fuel cell with odorants in hydrogen (Becker et al., 2019).

If odorants are utilized in the hydrogen energy system, it is necessary for the odorant added in the hydrogen supply lines to be removed before being fed into the fuel cells to prevent the catalytic poisoning issue and to avoid any false leak warning in the exhaust gas stream. The U.S. patent (Flynn et al., 2013) provided two different routes in the fuel cell system designed to remove the odorant from hydrogen. The odorant adsorber can be installed prior to an on-board, onsite high-pressure hydrogen storage unit, or prior to the fuel cell stack, as shown in Figure 26. The odorant may be removed through an adsorber unit (a fixed bed adsorption column), which contains commercial activated carbon.

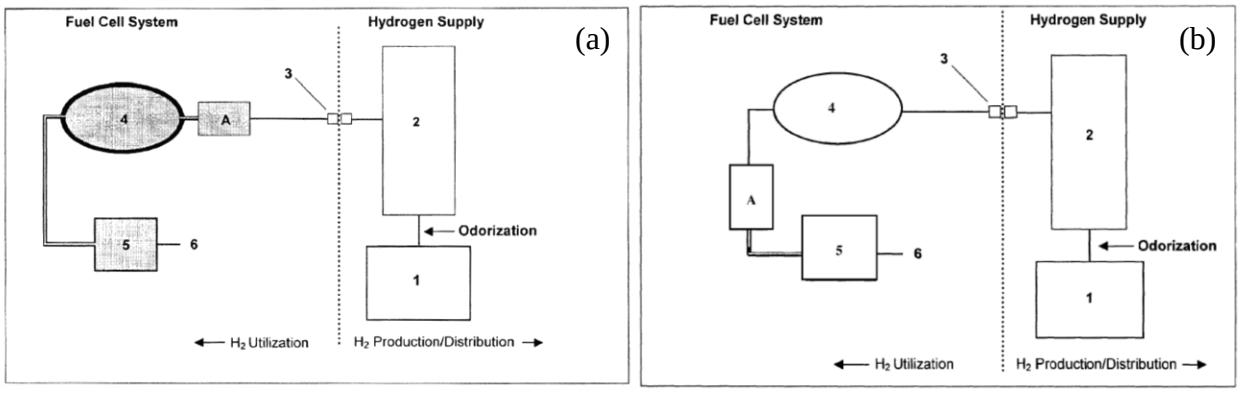

Figure 26: A schematic of a system design with odorant adsorbers arranged prior to (a) a solid storage unit and (b) a fuel cell stack; 1: hydrogen production, 2: supplier hydrogen storage (compressed gas), 3: mobile system or stationary system connector, 4: on-board, onsite high-pressure hydrogen storage, 5: fuel cell stack, 6: odorant "free" exhaust, A: odorant adsorbers) (Flynn et al., 2013).

3.3 HYDROGEN SENSORS

As hydrogen economy emerges, the detection of hydrogen becomes more inevitable to prevent any potential explosion risk throughout the entire lifespan of hydrogen from generation to utilization. As mentioned in the previous section, it is also essential to detect any hydrogen leakage throughout the hydrogen-involved systems to avert the undesired environmental impact. Hydrogen sensors are to be used for monitoring hydrogen leakage from hydrogen production plants, pipelines, storage tanks, refueling stations, and automobiles (Hübert et al., 2011). For hydrogen sensors to be applicable in the various hydrogen platforms, they require fast response, high sensitivity and selectivity, low interference, small size, easy to install and use, low cost, low maintenance, long lifetime, etc. The detailed requirements for hydrogen sensors are listed in Table 9.

Table 9: Requirements for Hydrogen Leak Sensors (Boon-Brett et al., 2010)

Parameter	Stationary System	Automotive System
Measuring range	0-4% H_2 in air; survivability at 100%	
Detection limit	<100 ppm or <0.1%	<0.1% or <0.2%
Operating temperature	-40 to 50°C	-40 to 125°C
Operating pressure	80 to 110 kPa	62 to 107 kPa
Humidity	20–80% RH	0–95% RH
Response time	<30 s	<1 s or <3 s
Accuracy	25%	5%
Lifetime	3-5 years	15 years
Power consumption	n/a	<650 mW

Hydrogen sensors measure a certain change in the specific property of sensing materials in the presence of hydrogen, and then transduce it into electrical signals to be analyzed. The materials used for hydrogen sensing require large surface area, fast adsorption/desorption rate, high diffusivity, and significant change in material property to be monitored in presence of hydrogen molecules (Chauhan et al., 2019). These hydrogen sensing materials can be categorized into four different groups: 1) metals, 2) metal oxide semiconducting (MOS) materials, 3) carbon-based materials, and 4) polymers.

Palladium (Pd) is the most commonly used metal for hydrogen sensing due to its unique property of fast and high adsorption of hydrogen. When palladium is exposed to hydrogen gas, hydrogen molecules are dissociated into hydrogen atoms which diffuse through palladium and remain inside the crystalline lattice. This behavior converts palladium metal into palladium hydride (PdH_x), leading to swelling of the Pd shell (Silva et al., 2012). The physical change in palladium upon the hydrogen exposure can be translated into electrical signal changes to be measurable and quantifiable for hydrogen detection. Palladium can also be alloyed with other metals to improve stability and reversibility of hydrogen sensors. Nickle (Hughes et al., 1995; Hughes and Schubert 1992), magnesium (Sanger et al., 2015), gold (Zhao et al., 2006, Luna-Moreno et al., 2007), and

silver (Cui et al., 2009) have shown better stability and faster response to hydrogen when alloyed with palladium.

The MOS materials utilized for hydrogen sensor are CeO_2-SnO_2 (Motaung et al., 2018), Pd/ZnO (Kim et al., 2018), and PdO-In_2O_3 (Inyawilert et al., 2019). These materials have shown an increase in electrical conductivity and the improved adsorption of oxygen, resulting in significant reduction in resistance. Carbon-based materials provide high mechanical strength, large surface area, and high charge transfer rate which can enhance hydrogen sensing response. The stacked multi-walled carbon nanotubes (MWCNTs) with a thin palladium layer (3 nm) have shown high hydrogen sensing response at 4% H_2 concentration (Yan et al., 2018). The Pt-decorated functionalized graphene sheets (Pt/*f*-G) have demonstrated a similar response time to that of Pt/CNT, but with a twofold increase in sensitivity at room temperature detection of hydrogen (Kaniyoor et al., 2009). These sensors were stable over repeated cycles of hydrogenation and dehydrogenation.

Polymers were also utilized as hydrogen sensing materials in the sensor applications. The polyaniline (PANI) was applied into the fabrication of SnO_2/PANI composite nanofibers, which have shown high sensitivity to 1,000–5,000 ppm of hydrogen (Sharma et al., 2017). Molecular hydrogen dissociates and bonds with N atoms of imine group of PANI, resulting in an increase of hopping conductivity and a decrease of resistance. Poly (methyl methacrylate) (PMMA) has also shown high selectivity for hydrogen in the presence of interfering gases such as methane, carbon monoxide, and nitrogen dioxide gas (Figure 27; Hong et al., 2015). The PMMA/Pd nanoparticle/graphene hybrid sensor has exhibited reliable and repeatable sensing response when exposed to different concentration of hydrogen from 0.025 to 2% (Hong et al., 2015).

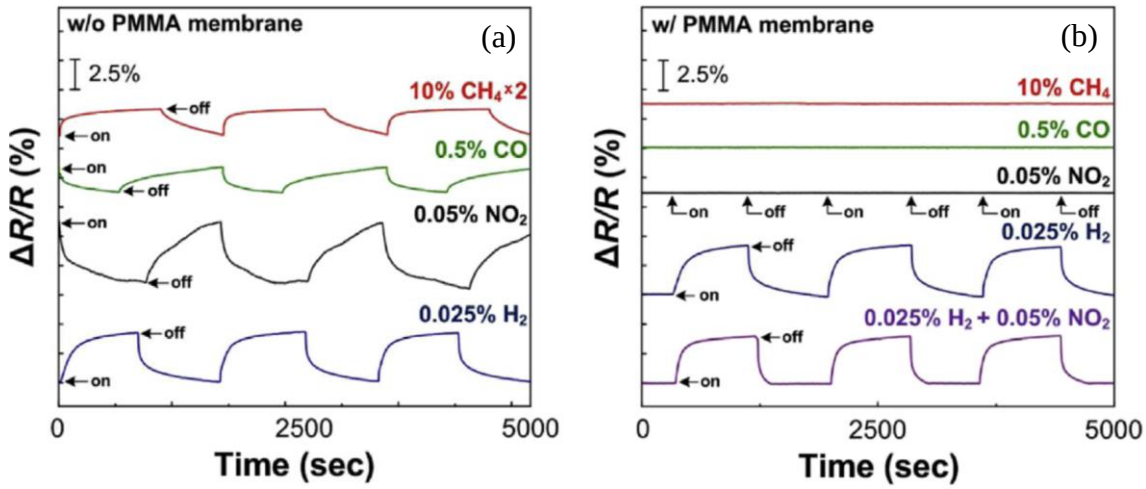

Figure 27: Sensing response with the Pd nanoparticle/graphene hybrid sensor (a) without PMMA and (b) with PMMA filtration layer (Hong et al., 2015).

Hydrogen sensors using different types of sensing materials can be classified into various sensing methods: 1) acoustic, 2) catalytic, 3) electrochemical, 4) mechanical, 5) optical, 6) resistive, 7) thermal, and 8) work function. The acoustic sensors are based on the detection of hydrogen in the form of surface acoustic waves on a piezoelectric device, and the catalytic

sensors detect heat released from the oxidation of hydrogen at a catalyst surface. The electrochemical sensors are based on the changes in charge transfer due to electrochemical reactions occurring at a sensing electrode, and the mechanical hydrogen sensors operate with a micro cantilever coated with a hydrogen-sensitive metal which shows expansion properties (deflection or bending) in the presence of hydrogen gas. The optical sensors detect a change of optical properties (transmission, reflectance, wavelength, phase shift) of sensing materials when exposed to hydrogen, and the resistive sensors measure the variation of electrical resistance when a metallic sensing layer is exposed to hydrogen. In the thermal sensors, hydrogen detection is based on thermal conductivity measurements due to heat loss of a body to the surrounding gas. The work function-based sensors measure voltage changes in work function of the metal through which hydrogen atoms diffuse and get adsorbed at the interlayer of metal and oxide. The detailed operating principle, physical chances, and advantages and disadvantages of each different type of hydrogen sensors are summarized in Table 10.

These hydrogen sensors have been already well developed and commercially available for years. However, there is still much room for improvement in terms of repeatability for large number of cycles and long-term stability under harsh environments to meet the demand of emerging hydrogen economy in near future.

Table 10: Characteristics of Ambient to Moderate (150 °C) Temperature Hydrogen Sensor Types (Hübert et al., 2011; Chauhan et al., 2019)

Sensor Type	Operating Principle	Physical Change	Advantage	Disadvantage
Acoustic	Quartz crystal microbalance (QCM) Surface acoustic wave (SAW) Sound velocity measurement	Frequency Time Wave velocity	High sensitivity Room temperature operation Operate in the absence of O_2 Low power consumption Wide range of detection Rapid response Long-term stability	Sensitive to interfering sound and waves and vibrations Unstable at high temperature Interference from other gases and humidity and temperature
Catalytic	Pellistor Thermoelectric	Temperature Resistance Thermoelectric voltage	Wider operating temperature range Robust and stable Long lifetime	Low sensitivity High power consumption Requires 5–10% O_2 to operate Poisoning - P, S, Si Long response time Sensitive to temperature fluctuations

Table 10: Characteristics of Hydrogen Sensor Types (cont.)

Sensor Type	Operating Principle	Physical Change	Advantage	Disadvantage
Electro-chemical	Amperometric Potentiometric	Electrical current Electromotive force Voltage	Sensitive down to 100 ppm Low power consumption Resistant to poisoning Operation at high ambient temperature Heating element is not required	Costly Low lifetime Cross sensitivity with CO Specific electrolyte requirement Aging Requires regular calibration
Mechanical	Cantilever	Bending Curvature Length	Operate in explosive environments Small size Micromachinable Does not require O_2 to operate	Interference from other gases Slow response time Aging
Optical	Optrodes Interferometric	Reflectance Transmission Wavelength Color Polarization Phase shift Surface plasmon resonance	No source of ignition Fast response Wide area monitoring Operate in the absence of O_2 Unaffected by electromagnetic interference	Cross-sensitivity with interfering gases Interference from ambient light Drift due to aging effects Poisoning - SO_2, H_2S
Resistive	Semiconducting metal oxide Metallic resistor	Resistance	High sensitivity Wide operating temperature range Low cost Easy fabrication Rapid response Low power consumption Long term stability Operate in the absence of O_2 (metallic resistor)	Interference from other gases, humidity, and temperature Poor selectivity High operating temperature Contamination Requires O_2 to operate (metal oxide) Affected by total gas pressure Poisoning - SO_2, H_2S Aging and costly

Table 10: Characteristics of Hydrogen Sensor Types (cont.)

Sensor Type	Operating Principle	Physical Change	Advantage	Disadvantage
Thermal	Calorimetric	Thermal conductivity Resistance Temperature Voltage	Low cost Rapid response Operate in the absence of O_2 Long term stability Wide measuring range Easy construction Resistant to poisoning	Cross sensitivity with He Heating element reacts with gas Lower detection limit is high
Work Function	Schottky diode MOS field effect transistor MIS capacitor	Voltage Capacitance Current	High sensitivity and selectivity Easy fabrication Wide range of operating temp. Rapid response Low cost and power consumption High accuracy Small size	Hysteresis Baseline drift Saturation at modest concentrations

Table 11 shows the applications and limitations of different types of commercially available hydrogen sensors. Table 12 lists performance specifications of hydrogen sensors, such as high and low detection limits, response time, accuracy, power consumption, etc.

Table 11: Common Hydrogen Sensor Elements (Buttner et al., 2017)

Sensor Types	Catalytic	Electrochemical	Thermal Conductivity	Resistive
Applications	Petroleum industry; Infrastructure	Potable monitors; Low level detection	Vehicles; Controlled environment	General deployment; Containers
Limitations	Cross-sensitivity; Require O_2 to operate	Poisoning; Aging; Low lifetime	Non-selective	Instability; Humidity and temperature effect

Table 12: Performance Specifications of Commercially Available Hydrogen Sensors (Hübert et al., 2011)

Sensor Type	Catalytic	Thermal	Electro-chemical	Resistive		Work Function		Optical
Principle/Device	pellistor	calorimetric	amperometric	Semiconducting metal-oxide	metallic resistor	capacitor	MOS field effect transistor	optrode
Accuracy (% of indication)	<±5	±0.2	≤±4	±10–30	≤±5	≤±7	≤±7	±0.1
Response Time, t90 (s)	<30	<10	<90	<20	<15	<60	<2	<60
Power Consumption (mW)	1,000	<500	2~700	<800	>25	4,000	700	1,000
Gas Environment	-20~70 °C, 5–95% RH, 70~130 kPa	0-50 °C, 0~95% RH, 80–120 kPa	20~55 °C, 5~95 RH, 80–110 kPa	-20~70 °C, 10~95% RH, 80–120 kPa	0~45 °C, 0~95% RH, up to 700 kPa	-20~ 40 °C, 0~95% RH 80~120 kPa	-40~110 °C, 5–95% RH, 70~130 kPa	-15~50 °C, 0~95% RH, 75~175 kPa
Lifetime (Year)	5	5	2	>2	<10	10	10	>2
High Detection Limit (Vol%)	4	100	4	2	100	5	4.4	100
Low Detection Limit	2,000 ppm*	200 ppm*	10 ppm*	10 ppb*	500 ppm*	1,000 ppm*	100 ppm*	500 ppm*
***Reference**	Henriquez et al. (2021)	Park et al. (2014)	Korotcenkov et al. (2009)	Hu et al. (2018)	Kondalkar et al. (2021)	Sahoo and Kale (2021)	Sahoo and Kale (2021)	Liu and Li (2019)

Note: “Low detection limit” is estimated from the research papers referenced, not from commercially available specifications.

3.3.1 H_2 Sensors for Harsh Environments

Detection of hydrogen at harsh environments such as high temperature, high pressure, high frequency, high power, intense vibrations, and chemically corrosive conditions are of great attention in automotive, aerospace, turbomachinery, SOFCs, etc. Among several types of hydrogen sensors, SiC-based MOS capacitor sensors have demonstrated sensitivity towards hydrogen up to a maximum temperature of 1000 ^oC (Spetz et al., 1993). The high diffusion rate of hydrogen at high temperature can be attributed to the reversible occupation and vacation of surface states at the insulator SiC interface above 427 ^oC (Soo et al., 2010). Table 13 shows various MOS capacitor SiC-based H_2 sensors with different metal electrodes and dielectric layers investigated in the past.

Table 13: Various MOS Capacitor SiC-Based H_2 Sensors (Soo et al., 2010)

MOS Structure	Thickness	Highest Operating Temperature	Response Time	Reference
Pt/$TaSi_2$/Pt/oxide/SiC	Pt(top): 50 nm $TaSi_2$: 50 nm Pt(middle): 100 nm Oxide: 135 nm	650 ^oC	-	Baranzahi et al. (1995)
Pt/$TaSi_xO_y$/SiO_2/SiC	$TaSi_xO_y$: 10-50 nm SiO_2: 100-150 nm Pt: 100-150 nm	650 ^oC	<100 ms	Baranzahi et al. (1997)
Pd/SnO_2/SiC	SnO_2: 5 nm, Pd: 40 nm	350 ^oC	26.7 s	Hunter et al. (2000)
Pt/SiO_2/SiC	SiO_2: 50 nm Pt: 100 nm	527 ^oC	171 s	Ghosh et al. (2003)
Pt/Ga_2O_3/SiC	Ga_2O_3: 90 nm Pt: 70 nm	610 ^oC	120 s	Trinchi and Wlodarski (2004)
Pt/Cr_3C_2/SiC	Cr_3C_2: 60 nm Pt: 30 nm	580 ^oC	38.6 s	Hunter et al. (2004)
Pt/SiO_2/SiC	SiO_2: 45 nm Pt: 100 nm	800 ^oC	-	Ghosh and Tobias (2005)
Pt/WO_3/SiC	WO3: 100 nm	700 ^oC	-	Kandasamy et al. (2005)
Pt/Ti/SiO_2/SiC	Ti: 2 nm SiO_2: 46 nm Pt: 100 nm	427 ^oC	92.3 s	Lundstrom et al. (2007)
Pt/SnO_2 nanowires/SiC	Pt: 100 nm	620 ^oC	66 s	Shafiei et al. (2008)
Pt/nanostructured ZnO/SiC	Pt: 100 nm	620 ^oC	72 s	Shafiei et al. (2010)

Another type of hydrogen sensors that can be employed in harsh environments is fiber Bragg grating (FBG) sensors. The FBGs are optical filtering devices that reflect light of a specific wavelength within the core of an optical fiber waveguide. The grating structure allows all wavelengths of light to pass that are not in resonance with it and reflects wavelengths that satisfy the Bragg condition of the core index modulation, acting as a band-rejection optical filter (Mihailov, 2012). The high-temperature stable gratings are suitable for harsh combustion environments such as jet engines, coal gasification reactors, and natural gas turbines. Figure 28 shows the wavelength shift of an FBG side-hole sensor when exposed to 1,000 psi of hydrogen at room temperature. The resonant Bragg wavelength was negatively shifted at the beginning due to the applied high pressure. After that, the wavelength shift slowly increased while hydrogen was introduced to the FBG by the hydrogen diffusion into the fiber core.

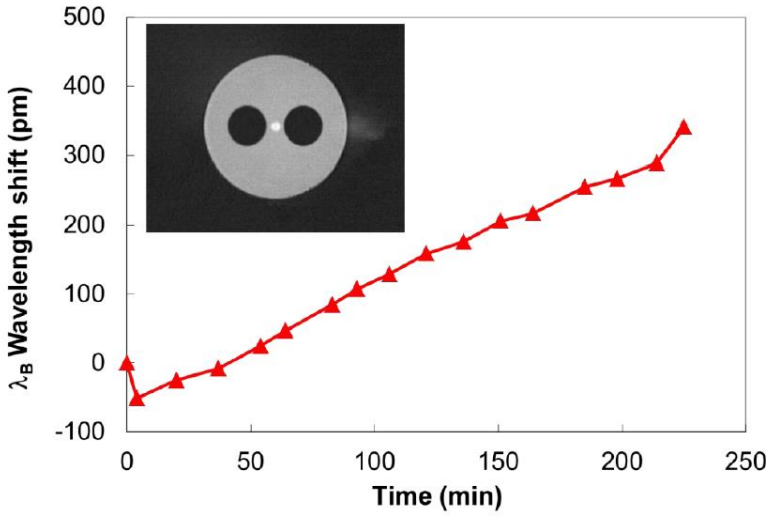

Figure 28: Wavelength shift with FBG side-hole fiber when exposed to 1,000 psi of H_2 (Mihailov, 2012).

Figure 29 shows an SEM image of a long-period fiber grating (LPFG) sensor coated a proton conducting $SrCe_{0.8}Zr_{0.1}Y_{0.1}O_{2.95}$ (SCZY) nanocrystalline thin film and the transmission spectrum shift of the sensor at different concentrations of hydrogen at 500 ^oC. The SCZY-LPFG sensors have shown good hydrogen sensitivity and selectivity over coexisting gas streams from coal gasification such as CO_2, H_2O, CO, CH_4, and H_2S (Tang et al., 2009). As shown in Figure 30 (b), the wavelength shift increased as hydrogen concentration increased, which results from an increase in hydrogen sorption in the SCZY phase due to the increased hydrogen partial pressure, leading to change in SCZY refractive index.

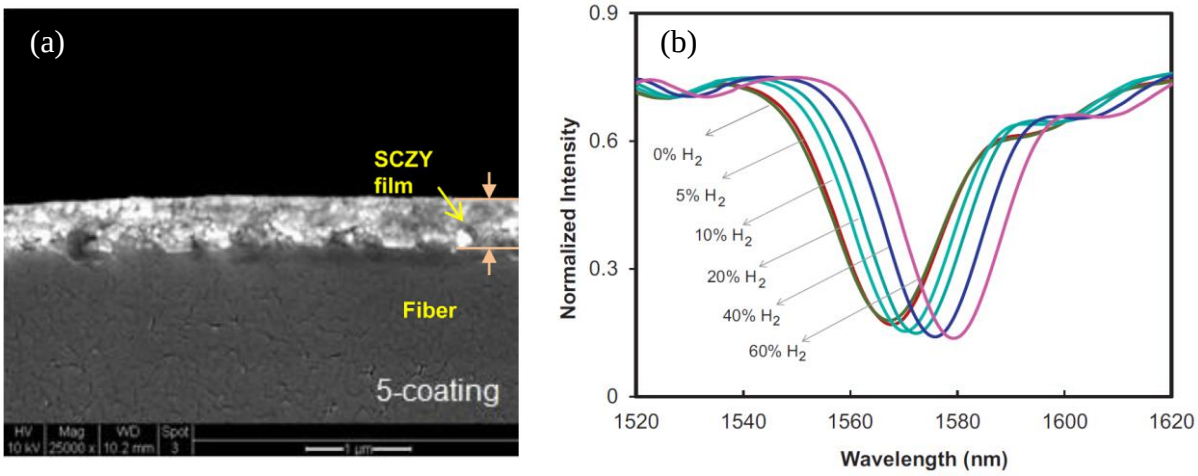

Figure 29: (a) SEM image of the cross-section of optical fiber with 5-coating SCZY films, and (b) transmission spectrum shift as a function of H_2 concentration at 500 ºC for the 5-coating SCZY-LPFG sensor (Jiang et al., 2013).

A crystal sapphire fiber has superior mechanical and chemical stability at high temperature and in corrosive environments with a very high melting point above 2000 ºC. This type of fiber can be a good platform for hydrogen sensors applicable in harsh environments. Figure 30 shows the example of usage of sapphire fiber for hydrogen sensing application. Figure 31(a) shows TEM image of the Pd-TiO_2 film coated on sapphire fiber, and its sensing response at different hydrogen concentration tested at 800 ºC is shown in Figure 30(b). The Pd-TiO_2 coated-sapphire fiber demonstrated clear hydrogen sensing measurement at different concentration of hydrogen at high temperature of 800 ºC.

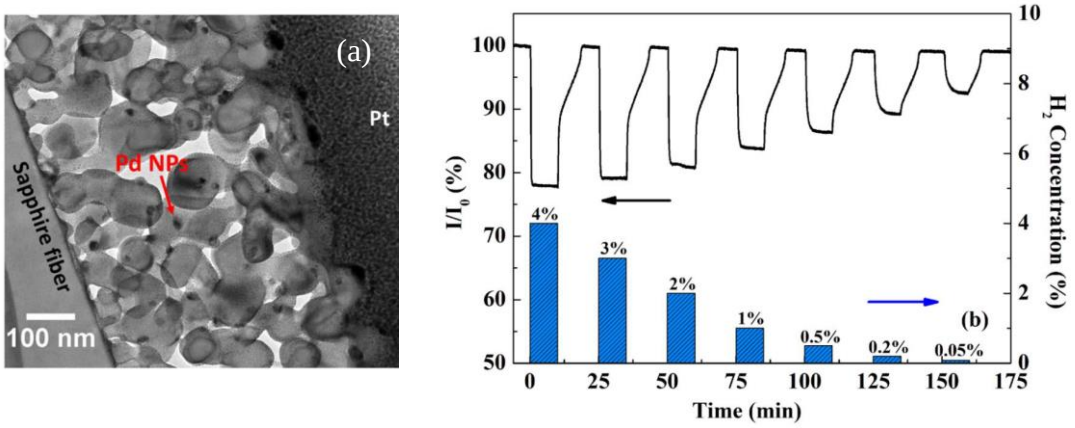

Figure 30: (a) TEM image of the Pd-TiO_2 film coated on sapphire fiber, and (b) its sensing response at different concentrations of hydrogen at 800 ºC (Yan, 2017).

3.4 SUMMARY OF HYDROGEN FOCUSED SAFETY CODES

The safety codes relevant to hydrogen are listed below. Refer to Appendix B for additional information.

Hydrogen Piping and Pipelines, ASME B31.12

This code sets forth engineering requirements deemed necessary for safe design, construction, installation, inspection, testing, operation, maintenance, and quality system program of piping and pipeline systems in hydrogen service.

Hydrogen, CGA G-5

This standard provides general physical and general information about hydrogen and some basic descriptions of safe use practices and hazard mitigations.

Hydrogen Vent Systems, CGA G-5.5

This standard provides an overview of the properties of hydrogen, including its flammability, temperature impact, diffusion and leakage characteristics, asphyxiation hazard, characteristics of liquid hydrogen, and hydrogen embrittlement. System considerations for the design and operation of a hydrogen vent system are included.

Hydrogen Technologies Code, NFPA 2

This standard addresses a variety of items including fire prevention control area, occupancy, piping systems (grounding, construction/materials/pressure relief), ventilation, electrical equipment, fire alarms, explosion control, fire protection, gas detection, gas cabinets, cleaning/purging of gas lines, etc.). Installation, location, storage and use of hydrogen are covered in detail.

Compressed Gases and Cryogenic Fluids Code, NFPA 55

This code applies to the installation, storage, use, and handling of compressed gases and cryogenic fluids in portable and stationary cylinders, containers, equipment, and tanks in all occupancies. This standard applies to all gases, not just hydrogen; however, chapters on gas hydrogen systems and bulk liquified hydrogen systems, specifically cover hydrogen. Methane is not covered by these chapters. NFPA 2 has incorporated nearly all of the requirements from these chapters.

Hydrogen, OSHA 29 CFR 1910.103

This code covers stationary or moveable hydrogen containers, pressure regulators, safety relief devices, manifolds, and piping. This code is a legally enforceable OSHA standard that covers much of the same ground as NFPA 2, although in much less detail.

Storage and Handling of Anhydrous Ammonia, OSHA 29 CFR 1910.111

This code is a legally enforceable OSHA standard. It covers the design, construction, location, installation, and operation of anhydrous ammonia systems.

Anhydrous Ammonia, CGA G-2

This code covers chemical/physical information on anhydrous ammonia. Design/safety information is provided on numerous aspects of anhydrous ammonia usage, including containers, piping, transportation equipment, and general usage/storage.

4. SYSTEM HAZARDS FOR TURBINES, SOFC, AND BULK HYDROGEN PRODUCTION

4.1 HYDROGEN GAS TURBINES

In addition to being able to respond quickly to fluctuations in power grid demands, natural gas- and syngas-fired combined cycle gas turbines (CCGT) are currently considered to be one of the cleanest forms of thermal power generation, producing roughly 50% lower CO_2 emissions than coal-fired power plants (ETN Global, 2020; Tashie-Lewis and Nnabuife, 2021; Oberg et al., 2020). This reduced carbon footprint can be further reduced through the mixing of renewable gases (e.g., green hydrogen biogas, syngas from biofuel sources with CCS, etc.), or through use of 100% hydrogen-fueled gas turbines.

The lower heating value (LHV) per mole of hydrogen is approximately 30% that of methane, so a hydrogen volumetric fuel flow rate that is nearly 3 times that of methane is required to achieve the same energy release at a fixed pressure. Oberg et al. (2020) asserts that a minimum hydrogen concentration (mixed with natural gas) of 51% is required for a CCGT to operate at the carbon neutral level as mandated by the Paris Climate Accords. Furthermore, Palacios and Bradley (2021) state that the overall heat release rate of a hydrogen gas turbine exceeds that of methane when the hydrogen concentration in the fuel exceeds 80%.

ETN Global's (2020) report on hydrogen gas turbines states that the current state of the art in hydrogen gas turbines are combustion systems with diffusion flames incorporating nitrogen or steam dilution that are capable of being fired with 100% hydrogen. They also report that there are several disadvantages to these units. Among these disadvantages are:

- A steep thermal efficiency penalty compared to combustion systems that do not use dilution
- Higher NOx emission levels compared to newer lean-premixed technologies (up to 3 times higher NOx emissions according per Cappelleti and Martelli (2017))
- Requirements for greater capital and operational costs due to higher plant complexity arising from the need for air separation units (if nitrogen dilution is used), post-combustion NOx removal, addition of steam source (if steam dilution is used), etc.
- Typically require "safer" fuels such as natural gas or diesel for start-up and shutdown operations despite ability to use different fuels
- Requirements for extensive modifications in auxiliary systems to handle the required increased flow rates of hydrogen fuel

On the topic of dilution, there are a number of published studies that find a potential efficiency gain from steam dilution of the fuel as part of a more complex cycle. This is due to the increased mass flow through the turbine provided (Bouam, 2008). However, these approaches do add complexity to the system, requiring steam generation to be provided into the fuel stream. Heat recovery steam generators (HRSG) are commercially combined with gas turbines to provide overall increased cycle efficiency in many installations. However, extracting part of the steam from the HRSG for blending into the fuel stream remains a research topic. More exotic cycles, such as partial oxidation gas turbines with a Rankine bottoming cycle, have also been proposed for efficiency gains (Heyen, 1999; Zhang 2015).

The ETN Global's (2020) report then goes on to state that newer lean-premixed systems have a higher potential for meeting the requirements for a transition to a hydrogen-based energy infrastructure, but the technology as it relates to hydrogen combustion is currently less mature and not able to handle pure or high concentration hydrogen fuel mixtures. It is stated in the report that the current limitations for hydrogen fuel concentrations is 30–50% for heavy duty turbines, 50–70% for smaller turbines due to different firing temperatures, and that there are currently no commercially available fuel-flexible premixed turbine systems capable of using pure hydrogen fuels. Therefore, further research and development is required to deploy such a fuel flexible gas turbine system, including combustor design, that can utilize a wide range of fuel mixtures, including those with high hydrogen concentrations.

The challenge that must be addressed by future research and development include developing technical solutions for the following:

- Auto-ignition risks posed by the lower ignition delay time for hydrogen fuels
- Flashback risks due to the higher flame speeds of hydrogen fuels
- Differences in the thermo-acoustic amplitude and frequencies associated with hydrogen fuels
- Increased NO_x emissions
- Reduced component lifetime
- Need for more cooling of the hot gas path components due to increased heat transfer
- Effects of hydrogen's lower Wobbe index compared to natural gas

Auto-Ignition

The low minimum ignition energy and ignition temperature of hydrogen compared to natural gas results in pure and high hydrogen content fuels being much more reactive and prone to pre-mature ignition in the fuel/air pre-mixing sections of turbine systems with high air inlet temperatures, such as those utilizing heat recuperators to pre-heat inlet air (ETN Global, 2020). Consequently, better methods for detecting and/or preventing auto-ignition events that lead to flame stabilization in undesired locations are needed.

Flashback

Burning hydrogen-rich fuels with 25% or more hydrogen increases the fuel flame speed, which in turn increases the risk of flame instabilities that lead to flashback, or flame propagation into the fuel/air premixing chambers (Oberg et al., 2020; Capelletti and Martelli, 2017; ETN Global, 2020). Flashback in lean premixed combustion systems is commonly countered by higher fuel flow rates to prevent unwanted flame stabilization prior to the combustor; however, the higher fuel flow rates required for hydrogen fuels to prevent flashback can result in adverse flame stability and thermo-acoustic effects on the combustor (Capalletti and Martelli, 2017). In order to protect burners and other components from being overheated or damaged by flashback-initiated flames, new methods of detection and prevention are needed, such as the combustion control and diagnostics sensor (CCADS) developed by NETL and Woodward Industrial Controls, which has been shown to be capable of detecting both flashback and lean blow-off in gas turbines operating with hydrogen and natural gas fuels containing up to 80% hydrogen (Thornton et al., 2004, 2007).

Thermo-Acoustics

Due to the higher flame speeds, shorter ignition delay times, and differences in flame shapes/position/reactivities for hydrogen as compared to natural gas, hydrogen flames exhibit significantly different thermo-acoustic behavior than natural gas flames. Unlike natural gas flames, turbulent hydrogen flame speed is pressure dependent, which increases the risk of self-sustained combustion oscillations at or near the acoustic resonant frequencies of the combustion chamber. Due to the different combustion properties, different resonant frequencies can be excited in hydrogen-fueled combustors, as a result a combustor that is stable for natural gas can be unstable for hydrogen or hydrogen-blends. Thermoacoustic instabilities can lead to other combustion issues such as auto-ignition, flashback, and lean flame extinction (Oberg et al., 2020; ETN Global, 2020). These risks are even greater during transient operations such as start-up, shutdown, power ramping, and rapid fuel blend changes.

In one numerical study, Nam et al. (2019) used large eddy (LES) simulations of a partially premixed combustor to show that the flame structure is altered with variations of syngas composition. The simulations show that increased hydrogen concentrations in the fuel lead to shorter flame structures that minimized the effect on the flow field and pressure oscillations in the combustor for hydrogen concentrations below 50%; however, for concentrations above 50%, the simulations predicted flame attachment to the combustor wall and amplified pressure oscillations that could result in damage to turbine components.

NOx Emissions

The higher adiabatic flame temperature of hydrogen (as shown in Figure 31) can lead to increased NO_x emissions, as compared to natural gas, requiring additional measures to meet NO_x emissions requirements. This can be achieved by reducing the flame temperature by steam dilution (Oberg et al., 2020). However, Oberg suggests that NO_x emissions comparable to those of natural gas fuels can be obtained with a 50/50 mix of hydrogen and natural gas, and lean premixed turbine power output is not derated. Application of post-combustion de-NO_x technologies such as selective catalytic reduction is possible, but combustor NO_x reduction is preferred due to the difficulties and costs associated with post-combustion NO_x reduction (ETN Global, 2020).

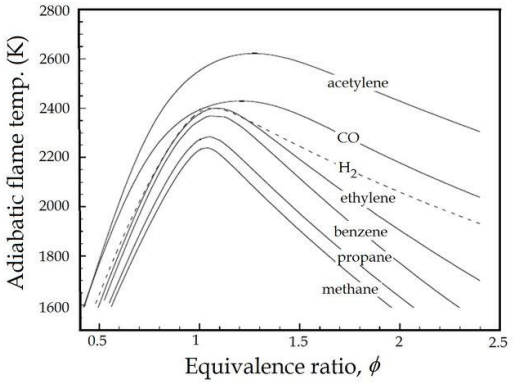

Figure 31: The adiabatic flame temperature as a function of the equivalence ratio for various fuel-air mixtures at standard temperature and pressure (STP) (Law, 2006).

Reduced Lifetime of Hot Gas Components

When compared to natural gas turbine operations, combustion of hydrogen results in greater moisture content in the exhaust gas and exposes the turbine components in the hot gas path to higher levels of heat transfer, as well as hot corrosion. Changes in cooling strategies and anti-corrosion methods will be required to switch from natural gas to hydrogen fuels in turbines.

Effects of the Wobbe Index

The Wobbe index for a fuel is a quantification of the heating value of a fuel arriving at the orifice of a burner from the fuel lines and is found by dividing the volumetric higher heating value of the gas by the square root of its specific gravity with respect to air. The greater the Wobbe index, the greater the heating value of the quantity of gas that will flow through a hole of a given size in a given amount of time (Emerson, 2007).

For a given combustor temperature and pressure and flow control valve position, two gases with different compositions but the same Wobbe index will give the same energy input to the system. However, fuel-flexible turbines that use pure natural gas, pure hydrogen, or mixtures of the two will require greater flexibility of the combustion systems and fuel controls because hydrogen has a much lower Wobbe index than natural gas, requiring nearly 3 times the volumetric fuel flow rate as natural gas (ETN Global, 2020).

In summary, when comparing a hydrogen fueled turbine to one that is fueled by natural gas, the risks for flashback, combustion instabilities, auto-ignition, thermal and corrosion-related issues to hot gas path components, and damage caused by oscillations in pressure are all inter-related and greatly enhanced. Each of these issues will require further research and development. Additionally, hydrogen gas turbines are also faced with component fatigue and potential leaks caused by hydrogen embrittlement of wetted surfaces, and the potential for hydrogen-based fires and explosions, as detailed in earlier sections of this report.

4.2 HYDROGEN SAFETY IN SOFC SYSTEMS

A SOFC is an energy conversion device that converts chemical energy into electrical energy with high-efficiency and low-pollutant emission. The SOFC utilizes hydrogen and oxygen as fuels on the anode and cathode respectively to generate electricity (Figure 32). The required hydrogen can be produced from natural gas by internal reforming within the fuel cell system, or be directly supplied to the fuel cell system through hydrogen pipelines.

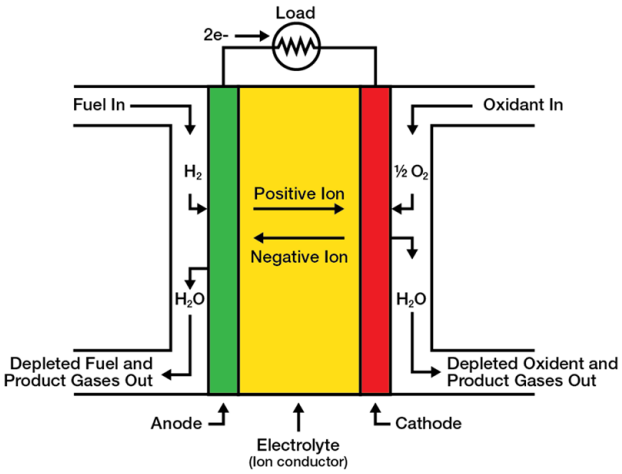

Figure 32: The schematic of a SOFC (NETL, 2022).

The principal safety hazards in the SOFCs are mostly associated with ignition and explosion from hydrogen leaks, as in other hydrogen-related systems. The secondary safety hazards are insulation fire, thermal injury, and electrical shock due to high voltage (200–400 V) generated in the SOFC stack (Calì et al., 2005). Hazards involved in high-pressure gas and asphyxiation can occur with a significant hydrogen leakage in the SOFC system.

The hydrogen leakage in the SOFC stacks can happen through the detachment of cell components and seal failure. These irreversible phenomena are mainly caused by the difference in the thermal-expansion coefficients of SOFC components due to temperature gradients and thermal cycles from ambient temperature to high operating temperature, and vice versa (Barelli et al., 2013). Rapid thermal cycling can lead to thermal and mechanical stress on the electrodes, electrolyte, and seals, followed by the degradation and detachment (Liu et al., 2010). Even abnormal behavior in a single cell can lead to subsequent catastrophic SOFC stack failure within minutes due to internal pressure buildup (Lim et al. 2008). The detachment and crack formation of cell materials including seals could ultimately result in fire and explosion in the presence of ignition sources such as sparks from welding or grinding, static electricity, electrical sparks, open flame, and hot surfaces.

One example of safety analysis on a SOFC system was conducted as EOS Project: SOFC Pilot Plant in Italy in 2005 (Calì et al., 2005). The maximum power produced by the SOFC unit (Figure 33) was 225 kWe and the thermal energy from the unit was utilized for heating and air conditioning of their office building. A hazard study on this system focused on identifying potential hardware failures and human errors that could lead to a potential injury and fatality, loss of performance, and equipment failure.

Figure 33: EOS project: SOFC Pilot Plant in Italy (Calì et al., 2005).

The identified safety and operability hazards from this study include fire, explosion, electrical shock, burn injury, and equipment damage. The recommended actions to be taken for mitigating the potential hazards were the installment of gas detectors, an alarm system, a ventilation system, excess flow check valves, pressure regulators, etc. Their SOFC unit actually carried seven combustible gas detectors, two smoke detectors, and one temperature detector. The gas detectors were connected to an automatic gas valve, so that the closure of the gas supply line would occur when high concentration of flammable gas was detected. The electrical equipment was located in an isolated cabinet to prevent any possible ignition. Two red emergency stop buttons were located on the front and back panels of the SOFC unit for the safety of personnel. The SOFC unit was placed on the ground level (concreate floor) and the testing room was equipped with two trailer-mounted powder extinguishers and a hydrant. This room had iron doors (fire resistance 30 min) and its wall was made of 25-cm thick clay bricks (fire resistance 120 min).

Haugom et al. (2007) conducted risk assessment studies for the planned hydrogen technology research center, Hytrec, in Norway. The planned hydrogen technology center included: a SOFC unit producing heat and electricity for the visitors center, a reformer using natural gas to produce H_2, an electrolyzer producing H_2 from water, LNG storage, vaporizers providing natural gas to the SOFC/reformer units, hydrogen pipelines, CO_2 capture and storage module, etc. The hydrogen suppled into the SOFC was to be produced both by natural gas reforming and by electrolysis of water.

They proposed the acceptance criteria for societal risk as a function of N curve (a frequency of N or more fatalities) in Figure 34. If the calculated risk is below the “Acceptable risk level”, there are no further actions needed to reduce the risk. In contrast, if the estimated risk is above the “Maximum risk level”, the potential risk must be reduced. If the function of N curve lies within the “As Low As Reasonable Practical (ALARP)” region, risk reducing measures should be implemented.

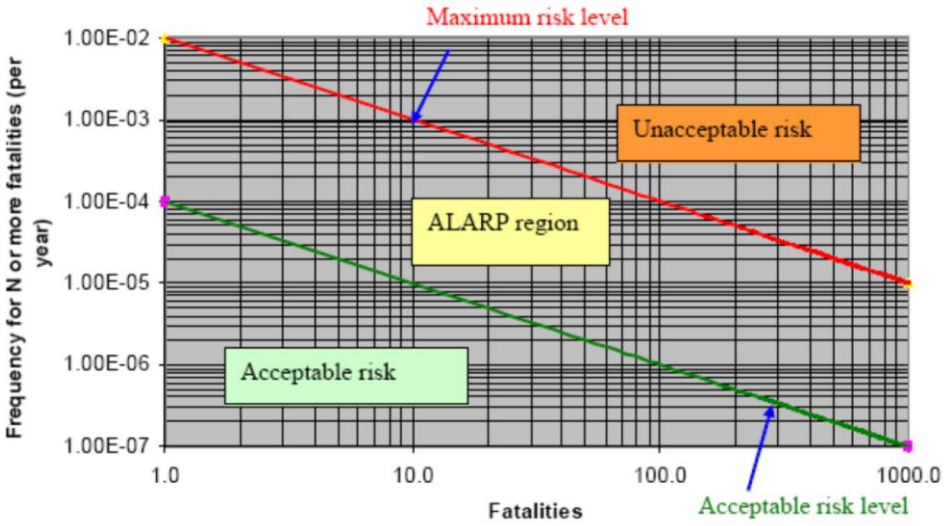

Figure 34: Risk acceptance criteria (Haugom et al., 2007).

Key safety assumptions to achieve the low risk of hydrogen explosion are placing the SOFC unit in a cabinet, isolation of valves and detectors, sufficient ventilation to handle small leaks in the cabinets, and shielding walls between the vaporizers and the storage tanks. The hydrogen leaks inside the electrolyzer and reformer cabinets should be detected within 5 s, followed by an automatic shutdown of the system.

According to the risk assessment results, the risk to the closest residents living within 150 m of Hytrec was 2.0E-7, which was assessed to be below the "Acceptable risk level". The risk contribution from accidents originating indoors was very low due to the ventilation system. However, large un-isolated releases from the electrolyzer and reformer unit was found to cause fatal impact with explosion overpressure. The recommended risk-reducing measures were reduction in the number of leak sources, control of ignition sources, optimization of detection and shutdown systems, utilization of ventilation and alarm systems, establishment of emergency preparedness and contingency plans, general routines and procedures for safe operation of the plant, etc.

From the safe SOFC operation point of view, Lv et al. (2016) studied the safe zone for a solid oxide fuel cell and gas turbine (GT) hybrid system fueled by biogas (4.53% CH_4, 23.64% H_2, 13.87% CO, 17.92% CO_2, and 40.04% N_2) with a mathematical model. Too high SOFC operational temperature and internal misdistribution of temperature can cause the performance degradation of SOFCs, materials deformation, and malfunction of the system, leading to gas leakage or serious accidents (Lv et al., 2015). Figure 35a shows the map of the safe operation zone for the compressor, which mainly suffers from surge and choke. Figure 35b shows the map of safe and unsafe zones for the hybrid system as a function of reduced air flow rate and relative fuel flow. In Figure 35b, the yellow zone on the bottom right shows the unbalanced energy zone where there are too much air flow and low fuel flow, which leads to thermodynamic failure of the overall system. The gray zone represents a regime where carbon is easily deposited in the reformer due to the low fuel flow rate, which causes the operational temperature of the reformer to decrease. The dark gray region presents the zone where the turbine inlet temperature (TIT) is too low, so that the operation of gas turbine is not recommended. The green zone is where the

safe operation of the hybrid system is possible. The operation with high and low efficiency can be achieved at low and high air flows, respectively. In the red zone, the SOFC and turbine are dramatically heated, and, in turn, thermal cracking and material deformation may occur on them. For safe operation the SOFC/GT hybrid systems, the operation in the red zone must be avoided to prevent any potential accident and injury due to the component damage. If the SOFC is fueled with pure hydrogen, then carbon deposition is not a concern.

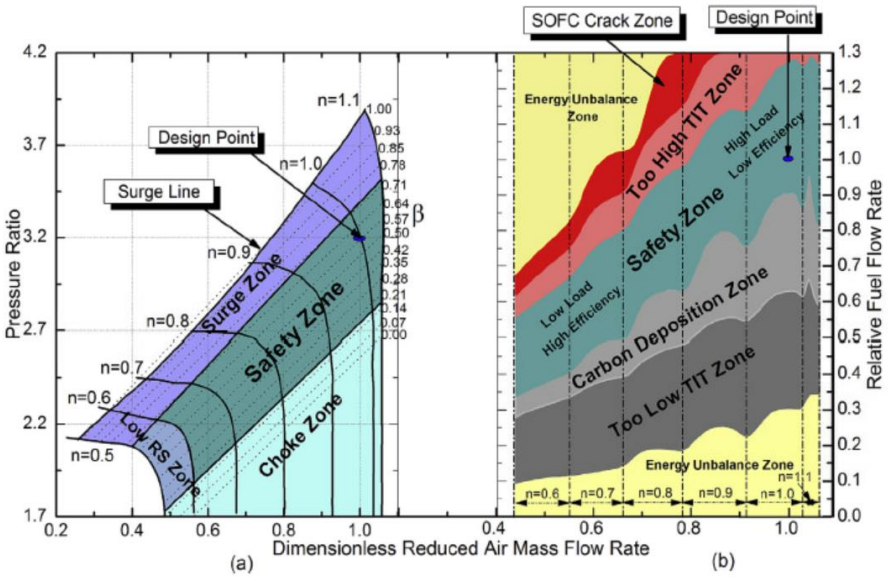

Figure 35: Map of the safe operation zone: (a) safe operation zone of compressor, (b) safe operation zone of SOFC/GT hybrid system (Lv et al., 2016).

Sharifzadeh et al. (2017) developed an optimization framework that ensures operational safety and enhances energy efficiency of the hybrid SOFC power plant incorporated with gas turbine, heat recovery, and steam generation. In this optimization program, the safety constraints to reduce risk of cell degradation or cracking, based on similar prior work on hybrid SOFC power systems were as follows:

- The temperature of the SOFC stacks must be maintained below 1,167 ℃ in order to avoid thermal degradation (Shirazi et al., 2012; Wu and Zhu, 2013).
- Turbine inlet temperature must be maintained below 1,277 ℃ to avoid thermal shock to process equipment (Shirazi et al., 2012; Wächter et al., 2010; Wu and Zhu, 2013).
- The steam to carbon ratio is maintained above 2 in order to avoid coke deposition (Wu et al., 2013).
- Too low fuel utilization leads to low steam content in the anode recycle and high turbine inlet temperature, increasing the risk of carbon deposition and compressor surge (Shirazi et al., 2012; Wu and Zhu, 2013).
- Too high fuel utilization leads to steep internal temperature gradients in the SOFC, promoting thermal cracking (Shirazi et al., 2012; Wu and Zhu, 2013).

- The fuel utilization must be maintained in the range of 75–90% (Shirazi et al., 2012; Wu and Zhu, 2013).
- The maximum cell current density to obtain a desired electrode reaction must be maintained below 5,000 A/m^2 (Shirazi et al., 2012).

The configuration of SOFC stacks is another safety aspect that needs to be carefully considered for practical applications. The SOFC stacks can be classified into two configurations: a) planar and (b) tubular designs, as shown in Figure 36. The planar cell design provides a short current path, resulting in higher power density and lower internal resistance, and also enables easier interconnect fabrication procedure than the tubular design. The advantages of the tubular design, on the other hand, are high thermal robustness, ease of sealing, and fast start up/shutdown (Golkhatmi et al., 2022). In order to avoid leakage and direct mixing of fuel and oxidant, air-tight sealing is necessary for the planar SOFCs. Sealant cracking can be caused by large local tensile stresses due to severe temperature gradients within the SOFC stacks. Figure 37 (a) shows a typical cracking structure of the electrolyte in the planar design cell after anodic reoxidation owing to tensile stresses and volume change by forming NiO. The degraded Ni-YSZ/YSZ/LSM anode-supported button cells after 120 h of operation in sour gas (H_2 + 50 ppm H_2S) are shown in Figure 37 (b). The delamination of the sealant (Schott 394) from a steel surface is shown in Figure 37 (c), which can be attributed to thermal stresses at the interface and contamination of the steel surface prior to sealant deposition (Zhigachev et al., 2022). It is critical to apply a sealant that has high thermal and chemical stability without generating crack growth, especially in the planar SOFC stacks to improve hydrogen safety.

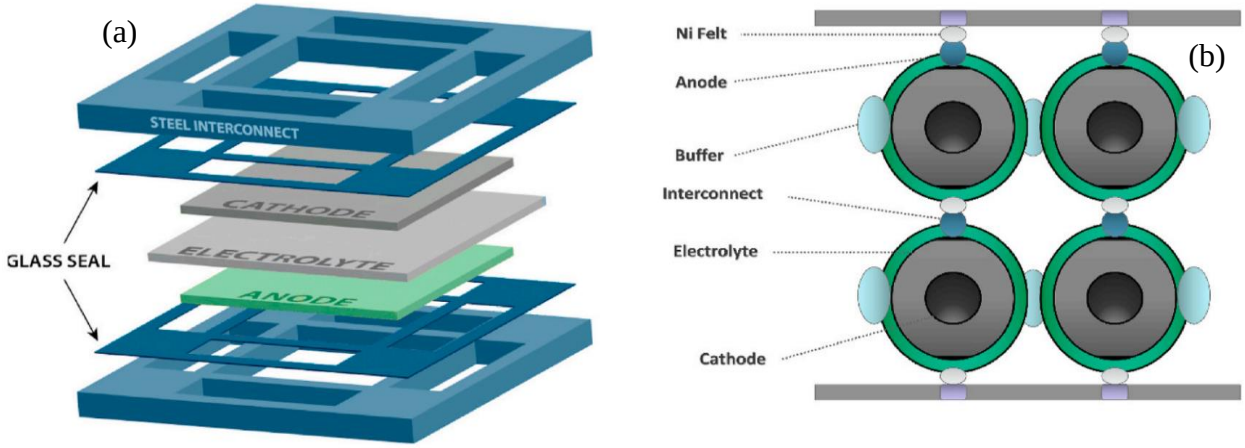

Figure 36: Illustrations of (a) planar and (b) tubular design of SOFC stacks (Golkhatmi et al., 2022).

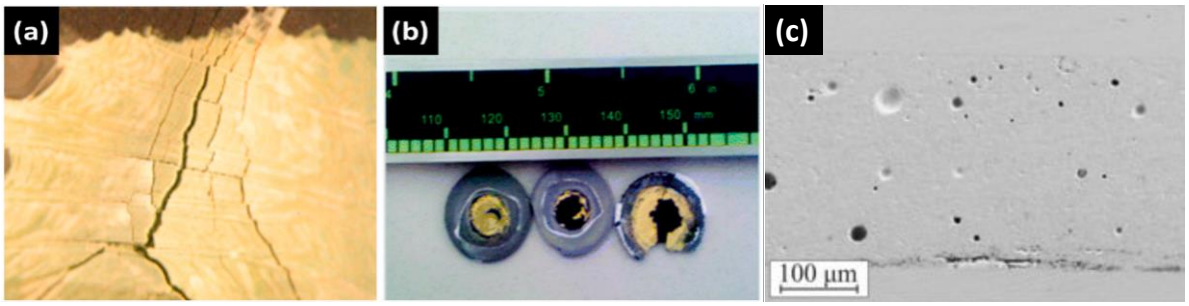

Figure 37: (a) A cracked electrolyte in the planar SOFC after anodic-reoxidation, (b) degraded SOFC button cells (Golkhatmi et al., 2022), and (c) SEM image of the cross-section of sealant (Schott 394)-steel assembly (Zhigachev et al., 2022).

Overall, the inherent hazards of the SOFC system are: 1) fire and explosion resulted from hydrogen leakage, and 2) electrical shocks due to high voltage output. When hydrogen is directly supplied into the SOFC system, the leaked hydrogen would quickly move upward due to its high buoyance and diffusivity. This property can help discharge hydrogen readily with appropriate ventilation. Natural gas is approximately 7 times heavier than hydrogen, so that when natural gas is fed instead of hydrogen the leaked gas in the SOFC system would diffuse upward much slower than hydrogen. If the leaked hydrogen or natural gas accumulates in an enclosed area, its concentration will build up in that space with the high risk of ignition and explosion. Therefore, the installation of ventilation systems is crucial and any source of ignition around the SOFC system must be eliminated to prevent detrimental consequence of gas leakage. In addition, sensitive and reliable gas sensors should be installed throughout the entire SOFC system to monitor any gas leakage. In case of emergency, the fuel valve needs to be automatically closed, and the SOFC stack also needs to take the automatic shut-down step upon leak detection with the gas sensors installed. Finally, the safe process operations should be carefully considered and applied into the initial SOFC design to improve the safety of SOFC processes.

4.3 HIGH-TEMPERATURE BULK HYDROGEN PRODUCTION

4.3.1 Solid Oxide Electrolyzer Cells (SOECs)

Solid oxide electrolyzer cells (SOECs) operate inversely to SOFCs by producing hydrogen from water in the form of steam by applying electricity (Figure 38). SOECs can be categorized into two different types based on a charge carrier in the electrolyte: 1) an oxygen ion-conducting SOECs (O-SOECs), and 2) a proton-conducting SOECs (H-SOECs). Compared to the O-SOECs, the H-SOECs require lower operation temperature due to high ionic conductivity, which leads to superior durability with less material degradation. Typical SOEC materials are similar to those used for SOFCs; however, SOEC degradation is approximately twice the rate as SOFCs (Mocoteguy and Brisse, 2013). The parameters affecting the SOEC degradation are operating temperature, current density, cell polarization, gas purity and type, and steam-to-hydrogen conversion rate.

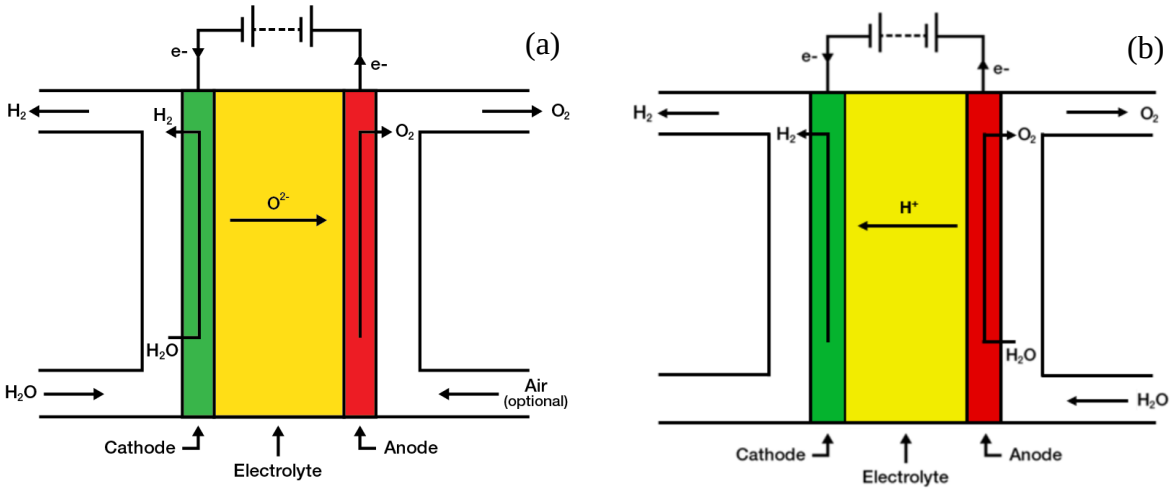

Figure 38: The schematic of solid oxide electrolyzer cells: (a) an oxide ion-conducting SOEC (NETL, 2022), and (b) a proton-conducting SOEC.

SOEC stack degradation is faster than single cell degradation due to the degradation on interconnect contact; contamination from tubing, interconnects and seals; and delamination or structural degradation around electrode/electrolyte interfaces. The structural degradation can be attributed to: 1) the formation of secondary phases originating from the diffusion of chromium contained in the interconnect materials of the oxygen electrode (Sohal et al., 2012), and 2) the formation of high internal oxygen pressure within the electrolyte (Jacobsen and Mogensen, 2008).

Degradation in the hydrogen/steam electrode were also reported which were caused by the re-localization of nickel at high current density under high humidity of the gas (Hauch et al., 2008). Electrolyte degradation can also take place in the SOECs due to: 1) surface grains structuration and void formation along grain boundaries, 2) formation of horizontally aligned pores, 3) formation of dense layers at the interface, and 4) destabilization of the interface (Schefold et al., 2012). In some cases, the voids formed along the grain boundaries generated cracks in the electrolyte (Jacobsen and Mogensen, 2008). From the SOEC safety point of view, degradation and detachment in the SOEC components can ultimately cause hydrogen to leak, resulting in the subsequent ignition and combustion around the SOEC stacks.

Therefore, it is critical to choose the degradation-resistant components for safe operation of SOECs. The requirements of the SOEC components for the safe and stable operation are as follows (Wendt, 1990; Ni et al., 2008):

- The thermal expansion coefficients of both anode and cathode electrodes should be as close as possible to that of electrolyte to prevent material failure of the electrolyte due to exceedingly high mechanical stress induced by thermal expansion mismatch.
- Electrodes and interconnect materials should be chemically and thermally stable in the highly reducing/oxidizing environments.
- The electrolyte should be chemically and thermally stable and be gastight to eliminate any possible recombination of hydrogen and oxygen.

Similar to the SOFC stacks, the configuration of SOEC stacks is also an important aspect when it comes to hydrogen safety. Figure 39 illustrates the schematics of (a) tubular and (b) planar SOECs. In the tubular cell, steam is supplied through the inside of the tube and the oxygen gas produced is extracted from the outer tube. The tubular SOEC presents higher mechanical strength and tighter sealing than the planar SOEC which has larger sealing area. Thus, the tubular configuration can be more suitable than the planar one for the safe operation of SOECs. However, the planar SOEC demonstrated much higher electrochemical performance due to the more uniform distribution of gas species and larger active area of the electrolyzer (Hino et al., 2004). In addition, the planar cells have better manufacturability, so that the planar SOECs may be a better option for the sake of the efficient operation of SOECs.

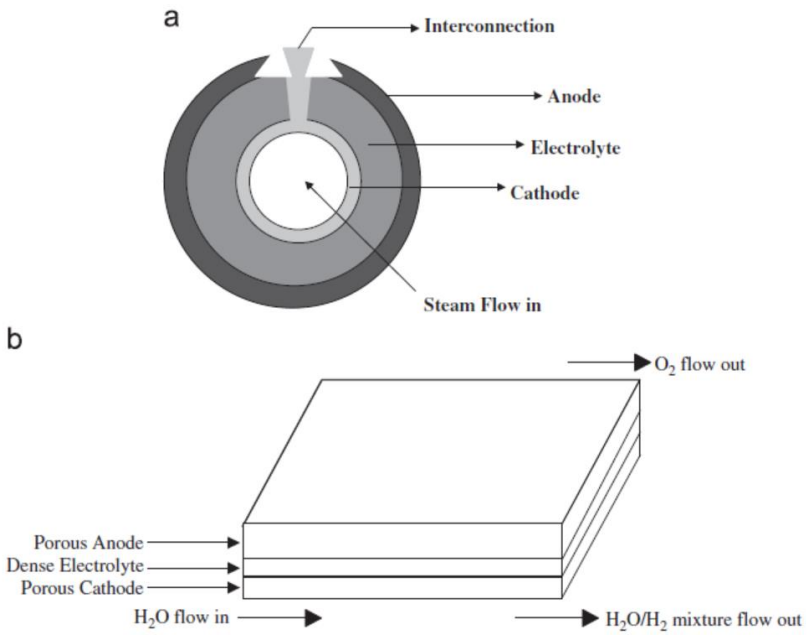

Figure 39: SOEC configurations: (a) tubular SOEC (end view) and (b) planar SOEC (Ni et al., 2008).

4.3.2 Steam Methane Reforming

4.3.2.1 Process Overview

The steam methane reforming (SMR) process is widely used in the hydrogen generation industry, making up approximately 99% of the hydrogen generated for industrial purposes (Chang et al., 2019; Mohammadfam and Zarei, 2015). In this process, natural gas pre-treated to remove moisture and sulfur is mixed with steam and is reacted with a nickel-based catalyst to convert the methane to hydrogen and carbon monoxide. A typical SMR process flow diagram is shown in Figure 40.

In this process, the natural gas feed is typically split into two streams. The first natural gas stream is used to fuel a burner that provides the heat required for the endothermic reforming reaction process in the reformer furnace unit (RFU, but mis-labeled as PFU in the figure). The

second natural gas stream contains the natural gas that will ultimately be used for hydrogen generation. This second gas stream is first compressed, dried, and pre-treated in a de-sulfurization unit (DSU) to remove any sulfur that might contaminant the catalyst materials located further downstream in the process. This desulfurized natural gas is then mixed with high-pressure, high-temperature steam and then introduced into a pre-reforming unit (PRU) to break the higher hydrocarbon compounds present in the natural gas down into methane and byproducts. It is then introduced into the reforming unit's reform tubes which contain the nickel-based catalyst which will "crack" the hydrocarbon chains, producing hydrogen gas, as well as CO and a small amount of residual CH_4. This reaction takes place at an approximate temperature of 800–920ºC and pressures up to 40 bar. As the unit operates with excess steam, the CO then reacts with the steam to form additional hydrogen and CO_2 (Chang et al., 2019).

The cracked gas leaves the RFU and is cooled to approximately 350 ºC and introduced into the first of two water-gas shift reactors (WGS) to further convert CO and steam into hydrogen and CO_2. After the first WGS reactor, commonly referred to as the high-temperature water-gas shift (or HT-WGS), the stream is further cooled to 200–300 ºC and introduced into a second, low-temperature water-gas shift reactor (LT-WGS) for further conversion. As in the RFU reformer tubes, these conversions are carried out in the presence of catalyst materials. (iron-chromium for the HT-WGS, and Cu-Zn for the LT-WGS.) (Chang et al., 2019). After the LT-WGS, the gas stream is then cooled via a chiller to condense out the steam, and the hydrogen gas is further purified via a pressure-swing adsorption process (PSA). The resulting gaseous hydrogen stream is roughly 99.99% pure and can be used onsite for power generation via gas turbines or solid oxide fuel cells or compressed and stored or transported for later use.

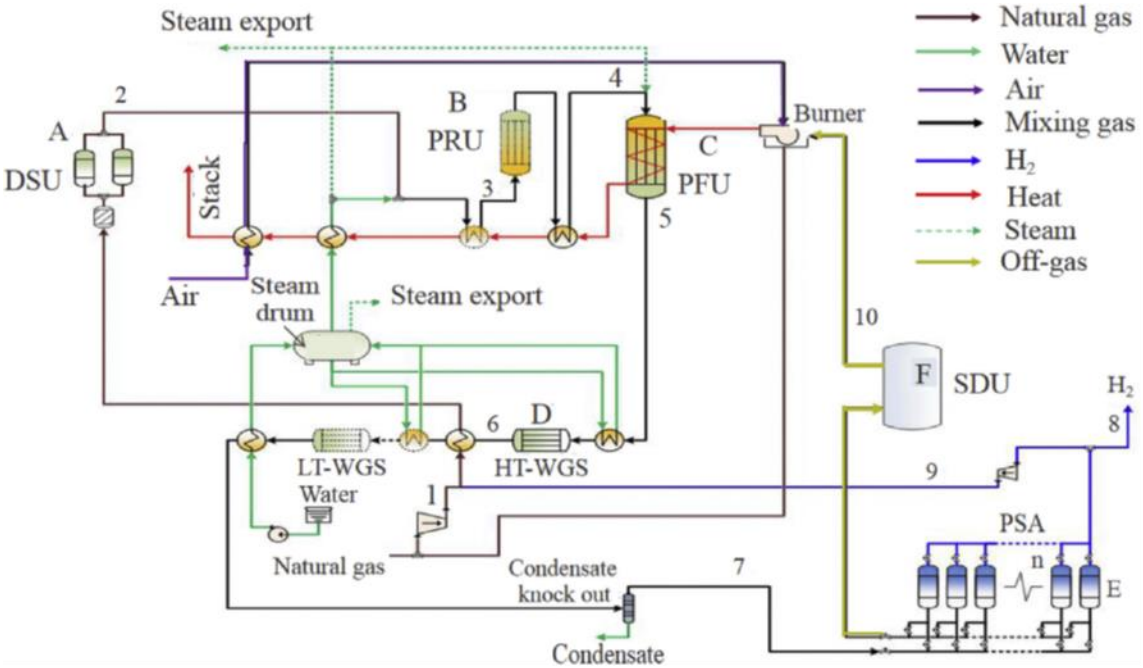

Figure 40: Process flow diagram of hydrogen generation via natural gas reforming (Chang et al., 2019).

4.3.2.2 Safety Considerations for Steam Methane Reforming

The primary safety-related concern for the SMR process is hydrogen leakage potentially leading to fires and/or explosions. There are four main sources for hydrogen leaks to occur in the SMR process: (1) mechanical leakage, (2) steam/carbon ratio and catalyst activity, (3) corrosion damage and hydrogen embrittlement, and (4) overpressure due to temperature and control system failures (Chang et al., 2019; Koc et al., 2011; Mohammadfam and Zarei, 2015; Saffers and Molkov, 2014).

Of the four leak sources listed in the previous paragraph, the primary risk is that of mechanical leakage (Chang et al., 2019). This can take the form of pipe leaks, equipment fatigue, unintentional damage by plant personnel, burn-through caused by localized over-heating, and weld and material defects under abnormal temperature changes. A low steam-to-carbon ratio can lead to carbon formation or deposition on internal surfaces inside the RFU reforming tubes and other reactor and piping components, which can lead to localized hot spots and burn-through, causing hydrogen leaks. Similarly, catalyst deactivation, normally the result of incomplete sulfur removal, can interrupt the hydrogen generation reaction, thereby aggravating carbon formation and deposition (Chang et al., 2019). Corrosion damage arising from the failure of corrosion protection coatings, etc., and hydrogen embrittlement can also lead to component failure and leaks. Finally, over pressurization of the hydrogen generation unit due to temperature and pressure instrumentation and control failures can lead to damaged or ruptured pipes and vessels, localized burn-though caused by hot spots; all of which can result in hydrogen leaks and subsequent risk for fires and explosions.

Many of these risk factors can be mitigated by use of corrosion and hydrogen-resistant materials, frequent inspection, and maintenance to detect early indicators of metal fatigue, corrosion, and localized thermal damage, frequent testing and calibration of instrumentation and control systems, and incorporation of active and passive deflagration and detonation mitigations measures.

4.3.3 Chemical Looping

4.3.3.1 Process Overview

A novel set of processes that have been studied for hydrogen production at NETL include chemical looping technologies. A chemical looping process uses a metal oxide powder as an "oxygen carrier," which can be used to oxidize or gasify fuels in lieu of air or pure oxygen. For hydrogen production, there are four chemical looping schemes designed to produce hydrogen as shown in Figure 41.

Process I consist of three reactors: fuel reactor, air reactor, and steam methane reformer. In the fuel reactor, the metal oxide fully oxidizes the fuel to produce carbon dioxide and steam. Using methane as an example:

$$MO_x + \frac{x-y}{4} CH_4 \rightarrow MO_y + \frac{x-y}{4} CO_2 + \frac{(x-y)}{2} H_2O \text{ where } x > y \qquad (4)$$

This reaction is either endothermic or exothermic depending on the metal oxide oxygen carrier chosen. In the air reactor, the reduced metal is reoxidized and recycled back to the fuel reactor to complete the cycle.

$$MO_y + \frac{x-y}{2} O_2 \rightarrow MO_x \text{ where } x > y \quad (5)$$

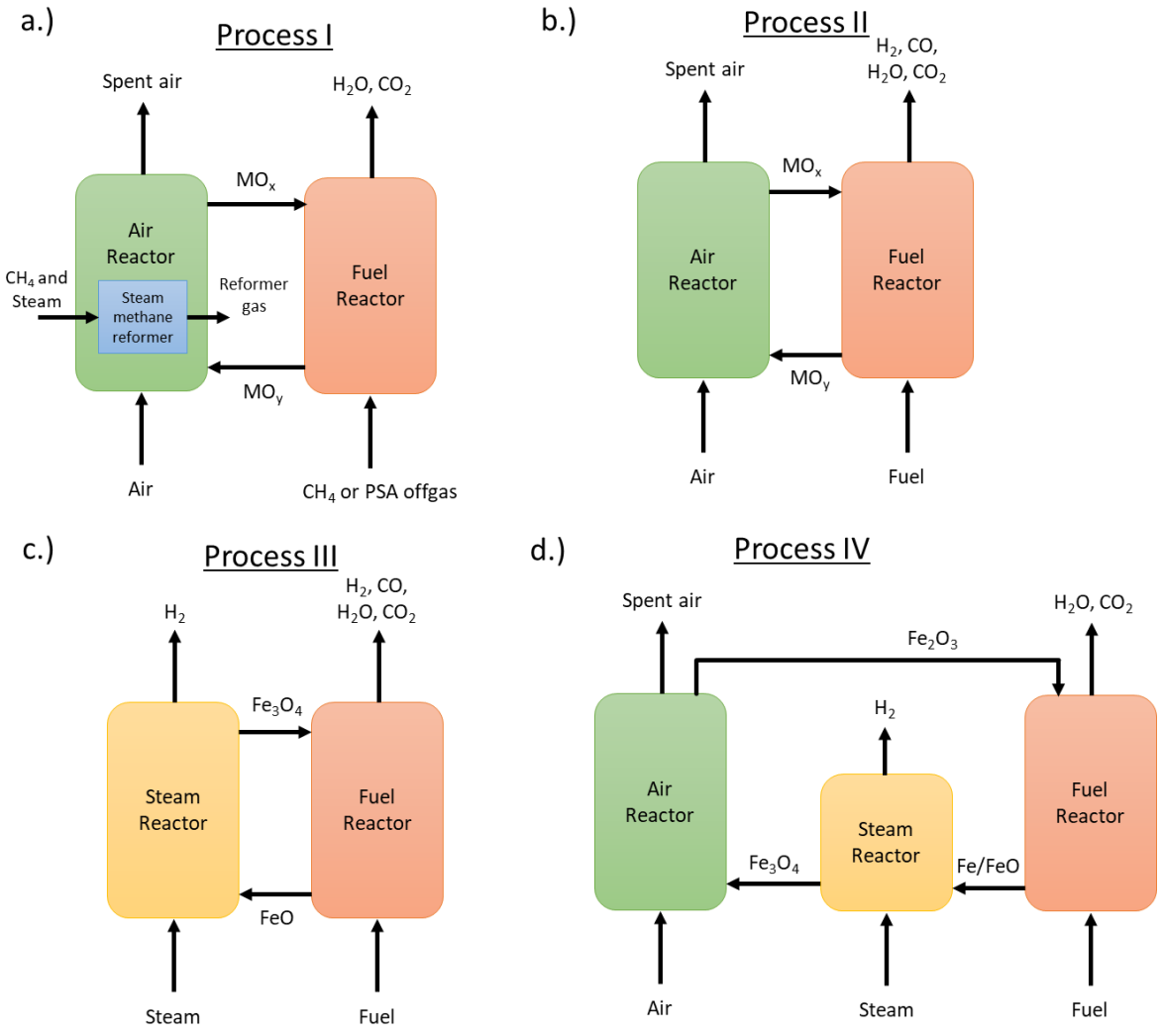

Figure 41: Chemical looping process configurations designed for hydrogen production.

The oxidation reaction for the oxygen carrier is exothermic. The energy from this reaction is transferred as sensible heat in the oxygen carrier to the fuel reactor to maintain temperature and, for the means of hydrogen production in this configuration, is used to provide heat to the endothermic steam reformer reactor. This configuration effectively acts to provide heat to the endothermic reforming reactions while simultaneously capturing carbon without a post-

combustion capture unit. Another advantage of this design is that the fluidized bed reactor transfers heat to the reformer tubes more efficiently than a natural gas fired furnace since the reactor tubes in the fluidized bed are immersed in hot moving solids (Ryden et al., 2008). The disadvantage of this process is that the resulting syngas still needs to be shifted and purified through water gas shift and pressure swing adsorption. Additionally, there is the potential for erosion of the reformer tubes in the fluidized bed.

Process II is a simpler process than Process I in that it only consists of a fuel reactor and air reactor. The reaction in the fuel reactor using methane as an example is:

$$MO_x + (x - y)\ CH_4 \rightarrow MO_y + (x - y)\ CO + 2(x - y)\ H_2 \text{ where } x > y \qquad (6)$$

producing syngas in addition to some carbon dioxide and steam. The reformate stream from the air reactor can be shifted and purified to produce hydrogen like steam methane reforming. The reaction in the air reactor is the same as in Process I. The advantage of this process is that it is simpler, requiring only two reactors instead of three.

Process III involves reduction of an oxygen carrier with fuel and reoxidation with steam, where iron oxide or another "water-splitting" material is used as the oxygen carrier. The reaction in the fuel reactor is

$$4\ Fe_3O_4 + CH_4 \rightarrow 12\ FeO + CO_2 + 2\ H_2O \qquad (7)$$

where the iron oxide in the form of magnetite (Fe_3O_4) is reduced to wuestite (FeO). Depending on the stoichiometry and fuel reactor design, CO and H_2 may exist in the product gas. The reduced iron oxide is sent to the steam reactor, where steam reacts with the iron oxide to produce hydrogen:

$$FeO + H_2O \rightarrow Fe_3O_4 + H_2 \qquad (8)$$

The iron oxide is reoxidized and sent back to the fuel reactor to be reduced again, completing the cycle.

Process IV consists of three reactors: a fuel reactor, steam reactor, and an air reactor. Like Process III, the oxygen carrier required for this process is iron oxide or a similar "water splitting" material. Fuel reacts in the fuel reactor according to Equation 7, and the wuestite reacts with steam to produce hydrogen in Equation 8 (Fan, 2010).

4.3.3.2 Safety Considerations for Chemical Looping Systems

In many aspects, chemical looping processes are inherently safer than direct-oxidation processes (e.g., partial oxidation or autothermal reforming of natural gas) as there is no direct mixing of fuel with gaseous oxidant, which could result in an explosion. However, the following is a list of process safety considerations.

For chemical looping processes that use a circulating fluidized bed or a circulating moving bed without the presence of valves in the solids flow, it is necessary to design means to ensure gases do not mix in the reaction vessel. Loop seals and seal pots are required in these systems. These devices work by injecting inert steam or carbon dioxide into strategic locations in the vessel, increasing the local pressure and forcing the inert gas to flow in both directions to prevent reducing and oxidizing gases from flowing past the injection point. If there is ever a point where reducing and oxidizing gases mix in a chemical looping reactor, the process operates above 800°C, which is above the autoignition temperature of hydrocarbon gases, preventing a buildup of flammable gases and subsequent explosion.

Compared to gasification and steam methane reforming, there are unique material considerations regarding piping material selection for chemical looping systems:

- For chemical looping processes that use a fixed bed configuration, whereby the gas flow in a reactor switches between oxidizing and reducing gases, there are material challenges to be able to withstand oxidizing and reducing environments.
- The product gases coming from the fuel reactors in Processes II and III will be similar in chemical composition to those found in steam methane reforming or solid-fuel gasification.
- If biomass is used as fuel in the fuel reactor in any process configuration listed, the syngas produced is less likely to contain tars because the oxygen carrier acts as a catalyst to break down tar compounds (Luo et al., 2013).
- Because of the oxygen carrier, sulfur products in the fuel reactor are usually in an oxidized form (e.g., SO_2 instead of H_2S). The state of the sulfur in the product gases will depend on the concentration of reduced sulfur species fed to the fuel reactor, but for the most part it will be in an oxidized form. Any metal sulfides that form in the fuel reactor will be burned in the air reactor to produce sulfur dioxide in the spent air stream. However, reactor operation and oxygen carriers are designed to minimize sulfide formation (Garcia-Labiano et al., 2009).
- Thermal nitrogen oxides (NO_x) are unable to form in the air reactor because of the lower operating temperature of chemical looping systems (~1000 °C instead of 1400 °C found in combustion turbines). High-temperature solids recovery is required for steam/hydrogen mixtures, since moisture can cause solids to cake on filters, causing drastically increased pressure drop.
- Silica refractories tend to dissociate and volatilize in high-temperature, hydrogen-rich environments (Whychell, 2022). In high carbon-content environments, silica becomes reduced to a volatile form of free/combined silica, leaving a granular residue of mullite or corundum (Wright and Wolff, 1948). The solubility of hydrogen in refractories consisting of molybdenum and tungsten is low, but columbium and tantalum-based refractories can become brittle in high hydrogen environments (Chandler and Walter, 1968).

4.3.4 Gasification

4.3.4.1 Process Overview

Solid fuel gasification is a fuel-versatile means of producing hydrogen. Gasification of solid fuels involves partially oxidizing carbonaceous fuels to produce a mixture of hydrogen, carbon monoxide, and potentially other combustible materials. The steps in a generic hydrogen production process through gasification are shown in Figure 42. The gasification process itself occurs in the "gasifier" unit. The overall gasification process consists of four key steps: (1) partial oxidation, (2) pyrolysis, (3) gasification, and (4) volatile cracking as well as several side-reactions. Partial oxidation is essentially a small amount of combustion that occurs in order to supply the heat necessary to complete the process, as gasification is endothermic. Pyrolysis is the process by which the solid fuel separates into its core components (volatiles, solid carbon, moisture, and ash) via the addition of thermal energy. The actual gasification reactions are where gases such as carbon dioxide and steam react with solid carbon to create lighter fuel gases (e.g., $C + CO_2 \rightarrow 2CO$ and $C + H_2O \rightarrow CO + H_2$). Finally, volatile cracking is a process where large hydrocarbons are broken down into smaller chains, eventually resulting in mostly CO and H_2 as products ("full" cracking, as opposed to "mild" cracking). Oxidants such as air or pure oxygen are injected into the vessel along with solid fuel to enable partial oxidation, while water or steam is supplied to enable the hydrogasification reaction.

There exists a variety of means of adding solid fuel to the system, including through the use of a lock hopper, an auger, and/or a water slurry. Solid fuels include coal, biomass, municipal solid waste, etc. The hydrogen content of the product syngas will vary depending on the hydrogen content of the solid fuel, the amount of steam used as oxidizer, the fuel/air feeding scheme, and gasifier geometry and operating conditions. Gasifiers can be designed as fixed bed, moving bed, fluidized (circulating or bubbling) bed, transport, or entrained flow, depending on the fuel feedstock required and quality of syngas required. For most hydrogen applications, an oxygen blown system is required since it is difficult and expensive to separate hydrogen from nitrogen. The gasifier vessel can either have a refractory brick-lined or water-cooled membrane wall. Ciferno and Marano (2002) provide representative syngas compositions for various gasifier designs and fuel feedstocks. This is important for selecting the right material for piping and downstream equipment. After the syngas is generated, it needs to be cooled. The syngas can be cooled by water quenching or using a syngas cooler or heat exchanger. The gasification process must be followed by a series of cleanup processes (as seen in Figure 42) to remove contaminants such as fly ash and chlorides. After the syngas is cooled and cleaned, the syngas undergoes a similar process scheme as in steam methane reforming, which includes water gas shift, acid gas (CO_2 and H_2S) removal, and pressure swing adsorption.

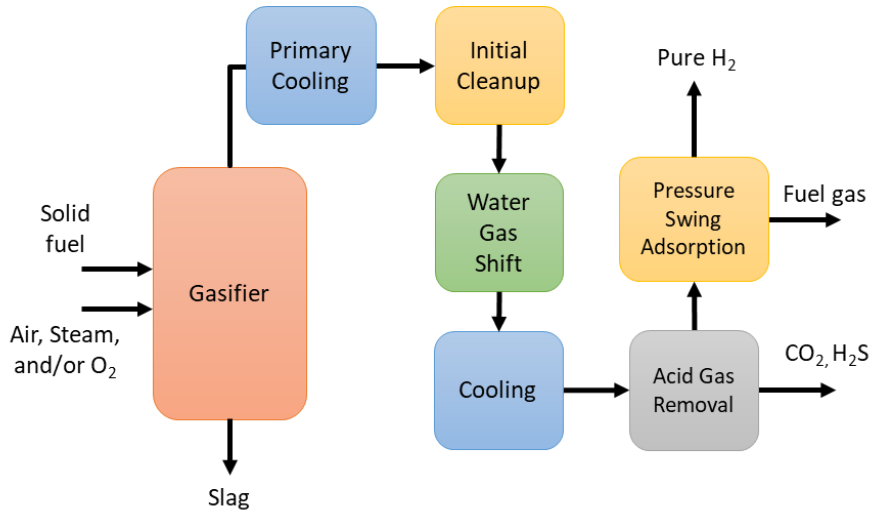

Figure 42: Simplified hydrogen production via gasification (including cleanup system).

4.3.4.2 Safety Considerations for Gasification

Many of the safety issues with steam methane reforming are also present for solid fuel gasification. However, unlike natural gas processes that produce hydrogen via gaseous streams, there are additional safety considerations for solid fuel gasification due to the challenge of solids handling. For one, the risk of explosion is greater with the presence of flammable gas as well as combustible dust (Perez et al., 2011). Ignition sources to consider besides those in SMR include buildup of combustible solids and hot solids discharged from vessels at high temperatures. To reduce the risk of flammable ignition due to electrical contact in coal or biomass feeding locations, equipment and instrumentation need to be designed for NFPA 70 Class II locations (combustible dust present) (Allen-Bradley, 2001).

The most error-prone area around the gasifier is the fuel and oxidant lines that feed the gasifier. Yun et al. (2016) describe several incidents and potential risks that involved in running their pilot-scale 3 ton/day and 20 ton/day coal gasifiers, and these incidents centered around the coal/oxygen feed system. The list of incidents in their two-stage gasifier include the following (Yun et al., 2016): In one incident, ferrules on a coal feeding tube became loose due to the impulse lines in the vicinity. As a result, the contents of the reactor at 1450 °C and 8 bar spewed out in a flame. A second incident involved a failed weld in the water-cooled coal feed tube as part of a top-fed, slagging gasifier. The syngas was able to backflow into the water system because the water pressure was less than the gasifier pressure. Syngas then leaked out of the vessel and resulted in an explosion. Other sources of accidents include blockage of valves due to slurry (Hayes, 2018) and cracking/collapse of the cold box in the air separation unit (Wang and Zhu, 2020). By its nature, it is more difficult to meter the flowrate of solids, and blockages are likely to occur.

In general, processes should be operated remotely without workers on the structure because of incidents such as these. This can be a challenge in developing countries where automation is limited. Because the area around the coal/oxygen feeding injection points are prone to failure, they should be monitored remotely with a closed circuit television or a webcam to ensure the safety of the operators in case of a rupture event. Process monitoring should also include

methods to measure the temperature of the shell in case of refractory failure (Higman and van der Burgt, 2008). Such methods include temperature-sensitive paint, fiber optic systems, etc.

It is recommended to use welded connections over Swagelok or threaded pipe for fuel/oxidant connections (Yun et al., 2012). Welded parts need to be subject to stringent QA/QC requirements, and they are often supplied by the manufacturer for this reason. However, the authors do not recommend using welded fittings that will contact syngas. Water cooling systems should pump water at a higher pressure than the operating pressure of the gasifier to prevent backflow of syngas through the system in case the metal or welds lose integrity. Other risks involved in operating a gasifier are due to the presence of carbon monoxide, chlorine, and sulfur compounds in the gas, which are toxic if inhaled.

5. AMMONIA SYSTEMS AND SAFETY

Ammonia is of considerable interest as a possible carbon-free alternative to hydrogen, or as a chemical form of hydrogen storage. Ammonia (NH_3), is more difficult to ignite than hydrogen, with higher auto-ignition temperature (650 °C), and it can condense into liquid under relatively modest conditions (under ~10 atm pressure at room temperature, or at -33 °C under ambient pressure) (MacFarlane et al., 2020), which makes its storage and transportation economically and operationally feasible. As a H_2 carrying agent, NH_3 also has a substantially higher volumetric atomic hydrogen density (0.11 kg_H/L_{NH3}) (Valera-Medina et al., 2018), which is much greater than other hydrogen carrying agents (such as hydrocarbons or simple alcohols) and even liquid H_2 (0.07 kg_{H2}/L_{H2}). More importantly, NH_3 can be suitable for all types of combustion engines, gas turbines, burners, and fuel cells, with appropriate design modifications. This makes NH_3 appealing for practical purposes and requires understanding of its properties and development of safe practices for its storage and handling.

Due to its widespread use in fertilizer, ammonia storage and transportation are well regulated by various federal, state, and local agencies. Pipeline transportation systems, tanker trucks, and tank cars are the most common methods to transport a pressurized liquefied ammonia from points of production to sites where it will be permanently stored or used for industrial purposes (Lan et al., 2012). Currently there are approximately 3,300 miles (~5,311 kilometer) of 6–8 inches (152–203 mm) diameter carbon steel pipelines in the U.S., which transport approximately 2 million tons of ammonia per year (PHMSA, 2015). Ammonia pipelines normally operate at 250 psi (1,723 kPa) pressure.

Ammonia is highly soluble in water, which is beneficial for some industrial, agricultural, and consumer uses. As an energy storage media, it will have the highest energy density and most likely perform best without any water in it, which is described as anhydrous.

5.1 ANHYDROUS AMMONIA PROPERTIES

Some physical properties of anhydrous ammonia are summarized in Table 14. It boils at -33.3 °C at 1 atm pressure, making it commonly a vapor but possible to transport as a refrigerated liquid. At temperatures above its critical temperature of 133 °C, it is a vapor irrespective of the pressure applied. When liquid anhydrous NH_3 is stored in an appropriate container at a temperature between the boiling and critical point, anhydrous liquid NH_3 remains in equilibrium with NH_3 vapor, and the vapor pressure of liquid NH_3 increases with rising temperature (see Figure 43 for reference)(Tanner Industries. Inc., 1998).

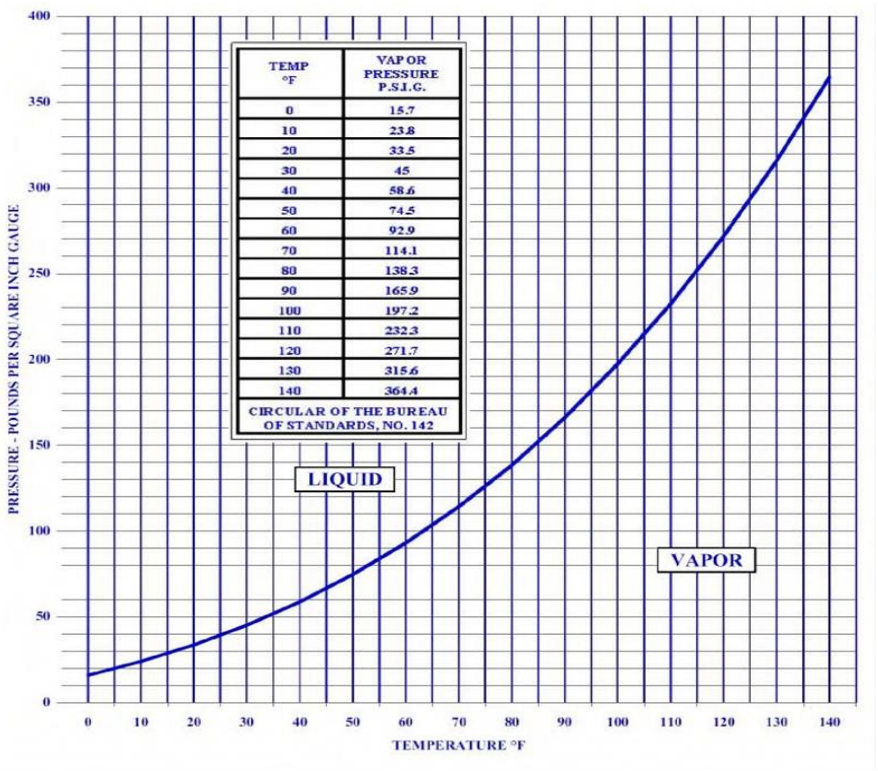

Figure 43: Vapor pressure-temperature relationship between liquid and anhydrous ammonia.

Table 14: Some Physical Constants of Ammonia (OSHA, 2022b; Haynes, 2011; Compressed Gas Association, 1990)

Physical Constants	
Molecular symbol	NH_3
Molecular weight	17.031
Boiling point at 1 atm	-33.3 °C (-28 °F)
Freezing point at 1 atm	-77.7 °C (-108 °F)
Critical temperature	133.0 °C (271.4 °F)
Critical pressure	11425 kPa (1657 psia)
Vapor density at 25 °C, 1 atm	0.696 g/L
Heat of Combustion (at 25 °C, 1 atm)	382.8 kJ/mol

5.2 TOXICITY OF ANHYDROUS AMMONIA

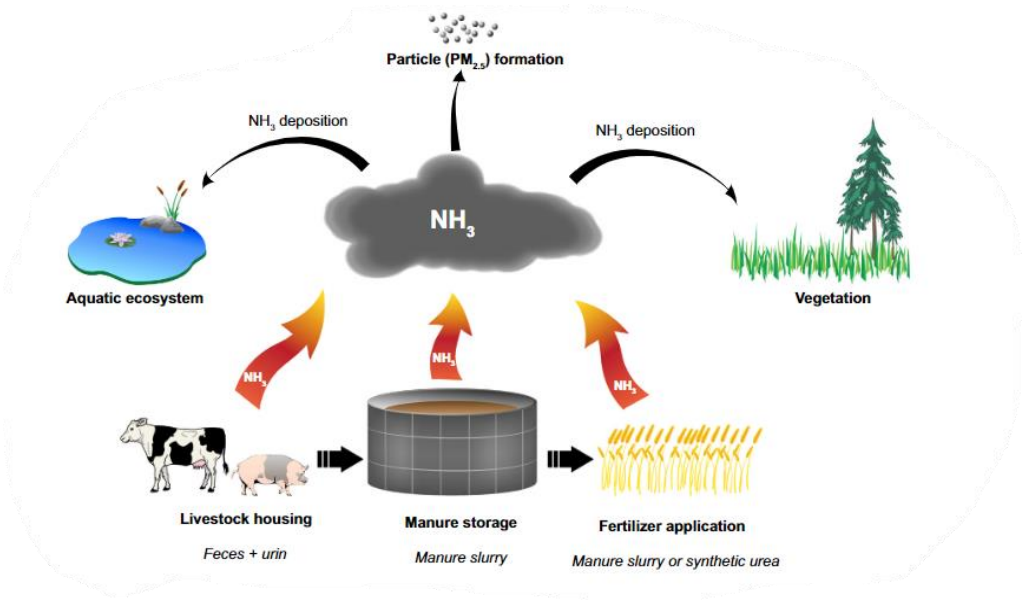

Figure 44: Environmental consequences of NH_3 emission from agriculture and livestock (Sigurdarson et al., 2018).

As shown in Figure 44, nitrogen needed for all living organisms comes from non-toxic concentrations of NH_3 produced by bacteria in water and soil (Sigurdarson et al., 2018). However, if present in excess, NH_3 can harm all living organisms in the soil, water, and air. In water, the pH and temperature play a crucial role in deciding its structure and toxicity but regardless of these factors a large amount of NH_3 in contact with surface water can severely impact aquatic life (even at a concentration of 0.02 mg/L). Hence, water contaminated with fertilizer ammonia should not be dumped in/exposed to any storm drains, rivers, drainage ditches, wetlands, or lakes. Similarly, specific procedures must be followed to prevent adverse environmental effects if NH_3 contaminates the soil.

Ammonia poses known health affect dangers to humans. Levels of exposure have been studied for safety (NIOSH, 2019; OSHA, 2022b). High levels of ammonia can irritate and burn the skin, mouth, throat, lungs, and eyes. Very high levels of ammonia can damage the lunges or cause death. Workers may be harmed from exposure to ammonia. The level of exposure depends upon dose, duration, and work being done. As a result of prior research, OSHA permissible exposure limit (PEL) for anhydrous NH_3 is 50 parts per million (ppm) (based on a full shift, 8-hour time weighted average (TWA) exposure) (USDA, 2022). Anhydrous NH_3 also has a short-term exposure limit (STEL) of 35 ppm, an immediately dangerous to life or health value (IDLH) of 300 ppm (OSHA, 2022b), and a human smell threshold of 5 ppm (NJ Health, 2016).

5.3 AMMONIA STORAGE EQUIPMENT AND LEAKS

5.3.1 Ammonia Storage Tanks

To minimize leaks and other safety issues from stationary anhydrous liquid NH_3 storage tanks, tanks are designed and built following OSHA (U.S. Department of Labor)-*29 CFR 1910.111-*

Storage and Handling of Anhydrous NH_3 (OSHA, 2022a), ASME Boiler and Pressure Vessel Code (ASME, 2022), and CGA (Compressed Gas Association) G-2.1–2014 (ANSI, 2022), as appropriate to the local legal requirements, to at least a minimum rating of 250 PSIG.

Moreover, anhydrous liquid NH_3 storage tanks should be in a place that is away from main doors, overhead doors, and high foot traffic areas where they will not be subjected to damage by vehicles or corrosive materials, or falling objects but should remain accessible for maintenance and re-filling purposes. The location should be clear of combustible materials, away from external heat sources and severe summer sun conditions to avoid any possibility of internal pressure development; but to ensure the safety of the nearby residents, if any such mishap happens, the tank should be located away from building air intakes, open windows or anywhere that the odor of NH_3 could cause problems (Tanner Industries, Inc., 2018).

To stabilize the anhydrous liquid NH_3 storage tanks, they are also preferred to be mounted on concrete, masonry, or structural steel supports and firm concrete or masonry foundations (Tanner Industries, Inc., 2018), but the piping connections to the tank should allow for tank movement due to settling, expansion or contraction. And arrangements should be made to protect the piping against the effects of jarring, striking, vibration, settling, and external corrosion (Tanner Industries, Inc., 2018).

5.3.2 Storage and Piping Materials for Anhydrous Ammonia

Anhydrous liquid NH_3 does not corrode iron/steel, and common metals but will react rapidly with copper, brass, zinc, and many alloys, especially those containing copper. Therefore, only steel or ductile iron should be used for anhydrous liquid NH_3 containers, piping, and valves. All fittings should be forged steel and non-malleable metals must not be used. Unions with brass seats must not be used (Minnesota Department of Agriculture, 2022). The primary safety standards for ammonia safety are guided by ASME B31.3. and OSHA 1910.111. Because of ammonia's widespread use in agriculture as a fertilizer, simplified recommendations have been developed by other organizations, such as Minnesota Department of Agriculture.

The normal operating pressure for anhydrous liquid NH_3 is 30–150 psi and the containers made of carbon steel (a type of mild steel) are good for storage as they can sustain pressure up to 250 psi. However, it is suggested to use stainless steel of types 304, 310, and 321 for NH_3 storage which can sustain even higher pressures (transportable tanks typically fail at a pressure of ~1,400–1,500 psi and are tested every 5 years to a pressure of 375 psi) (Committee of Stainless Steel Producers, 1978).

Piping and transfer lines should be also made of NH_3 safe materials and monitored regularly. Steel/malleable iron pipes (Minnesota Department of Agriculture, 2022) are acceptable, but galvanized or brass or rubber pipes or fittings should not be used. Other fittings such as valves, pressure relief valves, and back checks should also be ammonia safe.

All piping, pipe joints, tanks, and tank fittings should be tested for signs of corrosion, damage, wear, and leaks initially after assembling the set-up, and every three months thereafter. To identify leaks, the NH_3 detection method described below should be followed.

Liquid ammonia is non-corrosive and hence internal corrosion is not an issue. However, the presence of impurities such as water and oxygen in a pressurized liquefied ammonia can promote SCC (Teel, 1980). SCC depends on the materials (composition of alloys, metallurgical structure, heat treatment, and welding) and the environmental factors such as: temperature and presence of

impurities (Pratt, 1976). Fine-grain steel appears to offer an advantage over coarse-grain steels in resisting to SCC in air-contaminated ammonia. It has been shown that the susceptibility of steel alloys to SCC is proportional to their yield strength (Pratt, 1976). For this reason, pipelines or storage tanks should be made from materials that can resist SCC. NH_3 is corrosive to copper, brass, and zinc alloys (Valera-Medina et al., 2018). Galvanic coupling of titanium, stainless alloy or copper-nickel with steel may accelerate the SCC of steel in ammonia even in the presence of 0.2% (wt) water and 1–2 ppm oxygen (Teel, 1980). Table 15 summarizes the list of materials that can be used to transport anhydrous liquid ammonia.

Table 15: Chemical Compatibility of Materials with Liquid and Gaseous Ammonia (PHMSA, 2015)

Materials	Liquid Anhydrous Ammonia
Nickel	U
Aluminum	U
Bronze	U
Carbon Steel	B
304 Stainless Steel	B
316 Stainless Steel	A
Hastelloy	A
Titanium	B

A = Excellent, materials show little or no effect after exposure to ammonia.

B = Fair, may be affected after exposure to ammonia. Corrosion and loss of physical properties is possible.

U = Unsatisfactory, is unsuitable when the materials exposed to ammonia.

Material selection is still a challenge in ammonia power plants, due to the temperatures and the media involved. Ammonia power plants face different types of high-temperature material degradation such as hydrogen attack, creep, metal nitriding, metal dusting, and embrittlement (Korkhaus and Feser, 2007). At temperatures above 150 °C (300 °F) ammonia will decompose forming hydrogen and nitrogen. Under these conditions there is the possibility of HTHA, which may lead to embrittlement. At high temperature, hydrogen diffuses into the metal and reacts to form an embrittling hydride phase. Metal dusting is a form of corrosion of steel alloys which occurs when susceptible materials are exposed to environments with high carbon activities (Table 15). A metastable metal carbide (M_3C) species forms and migrates away from the surface. The corrosion manifests itself as a break-up of bulk metal to metal powder. In long-term service and temperatures around 520 ^oC, nitrogen diffuses into the surface of the steel alloys used for ammonia reactors and creates a case-hardened surface of a ferrous alloy (metal nitriding), which changes the mechanical proprieties of the materials and leads to the rupture of the material (Korkhaus and Feser, 2007). Currently, materials selection for high-temperature ammonia

processes is a challenge because of the difficulty of prediction of metal dusting, which is a time-dependent degradation mechanism. Challenges include estimating the service life of the materials and developing repair procedures in cases involving metal dusting, hydrogen attack, and metal nitriding.

5.3.3 Anhydrous Ammonia Leak Detection and Maintenance

This section summarizes anhydrous NH_3 leak detection and maintenance responsibilities recommended by Tanner Industries Inc. (1998), a major commercial supplier of anhydrous ammonia and equipment. These are recommendations to industrial and agriculture customers. If there is a leak in an NH_3 tank, that can be easily detected by the sharp, pungent odor of the vapor and should be approached with caution. To identify the leak location and its size and nature sulfur sticks or moist litmus test papers or NH_3 gas detectors should be used. Sulfur sticks are used so that when the smoke from a lighted sulfur stick comes in contact with the leaking area, a cloud of white smoke will be produced. A moistened litmus paper, when used, turns into a dark purple/pink-colored paper when in contact with NH_3.

There are more advanced and safer methods of leak detection using electronic ammonia detectors. The most advanced and safest method is to use NH_3 detectors, which can be either fixed or portable to avoid any unsafe exposure to gases or chemicals.

In case of small leaks, NH_3 can be temporarily contained by covering the area with water-soaked towels (which will have to be replaced when saturated); but if there is a large leak, eliminate the NH_3 source, if possible, by closing off the valves and call 911 for immediate assistance. When dealing with anhydrous NH_3, gloves and other appropriate PPEs must be worn.

If corrosion is detected, that should be cleaned, primed, and coated with a white gloss epoxy paint. Non-insulated containers should have a reflective surface. All valves should be painted but the valve stems, should not be painted as it can get in the stem packing and cause leaks. Vent valves or the safety relief valves should not be painted either as it can clog the valve.

Many small leaks in storage tanks are caused by seasonal temperature fluctuations. This occurs when different materials are used to prepare those NH_3 storage tanks. Since different materials have different expansion and contractions rates, different parts of NH_3 storage tanks expand and contract differently and cause leaks when in contact with each other (Raghava Chari, 2022; Minnesota Department of Transportation, 2022; NDSU, 2022).

Another major cause of leakage is due to improper cleaning of these tanks. Severe damage can occur if storage tanks are not properly emptied before cleaning with water. Since water dissolves NH_3 very well, any NH_3 present in the form of vapor and/or liquid gets dissolved in water creating a vacuum in the tank (when closed). This may cause the tank to implode. Therefore, the following steps must be followed when cleaning a tank:

- Vent properly
- Do not wash tanks with H_2O and find an alternative solution that cannot solubilize NH_3 well
- Follow specific procedure (purge with N_2, then fill with air, and maintain 1 atm pressure in the container)

6. POTENTIAL TOPICS FOR SAFETY TECHNOLOGY DEVELOPMENT TO SUPPORT HYDROGEN USE

During the course of this review, several areas of opportunity for technology development were identified to improve the safety of systems for hydrogen production, storage, and conversion to electricity. The opportunities include improvements to detection of hydrogen leaks, prevention of material failures, and reduction of costs for safety assurance. While these technology areas have been identified primarily to support hydrogen turbines and SOFCs, and hydrogen production by fuel reforming or gasification with carbon capture, they are expected to be beneficial to other hydrogen systems as well, including pipelines and vehicle fueling stations, and hydrogen fueled industrial processes.

The identified opportunity areas for hydrogen safety technology research and development are summarized:

- Identification and testing of additional metal alloys which resist hydrogen embrittlement and hot hydrogen attack.
- Development of automated inspection technologies to ensure quality of construction, particularly for welds and key components.
- Combustion systems for hydrogen turbines which resist flashback while producing low levels of NOx.
- High-temperature hydrogen sensors for monitoring pre-ignition purge cycles in combustion turbines, which pose additional concern due to the buoyant nature of hydrogen.
- Low-cost, wide-area hydrogen leak detection technologies, to effectively provide leak detection throughout a large facility.
- Hydrogen concentration sensing in blend fuels for hydrogen turbines, SOFCs, and industrial equipment.
- Techno-economic analysis of the addition of odorants to hydrogen.

In addition, there are special concerns for liquid hydrogen and other hydrogen storage means, such as ammonia.

6.1 DISCUSSION OF POTENTIAL TOPIC AREAS

This section discusses potential technology research and development areas which would enhance safety for widespread hydrogen production, storage, and conversion to electricity, which were identified during the course of this review.

6.1.1 Materials and Fabrication

Hydrogen embrittlement and HTHA were reviewed in Section 2.2. While some engineering materials have been studied for these phenomena, testing of additional alloys would identify additional materials which could be used with hydrogen under various load and pressure conditions. Additional useable material options would be expected to reduce the cost of hydrogen systems.

Along with the base materials, welding materials and weld inspection are areas which would benefit from additional technology development. As noted in Appendix B, the ASME B31.12 Hydrogen Piping code has increased inspection requirements in comparison to B31.3. Improvements to automated weld inspection of hydrogen systems would improve safety assurance and reduce costs. Artificial intelligence may provide a powerful tool in improving inspections.

6.1.2 Combustion Systems

Hydrogen combustion hazards, particularly for gas turbines, were reviewed in prior sections. The most mature approach to maintaining stable combustion with hydrogen is through diffusion flame combustion. However, this generally results in much higher NOx production than the modern low-NOx combustion systems for natural gas, based on lean-premixed technology. Lean premixed technology is much more susceptible to flashback and other combustion instabilities, making their transition to operation on high hydrogen fuels a significant challenge. Artificial intelligence may be a beneficial tool in the design of improved combustion systems for hydrogen.

In addition, the ignition sequence for gas turbines and other gas fueled combustion equipment typically begins with a purge cycle, where the entire combustion system is flushed with air, before the controlled injection of fuel begins. This prevents the occurrence of a large, uncontrolled combustion event during ignition. Due to its buoyancy, however, hydrogen tends to accumulate in unique ways and is more difficult to purge. As a result, additional hydrogen sensors which can survive the high-temperature conditions of normal operation would support safety through assurance of the successful completion of a purge cycle.

Hydrogen blends are proposed as a possible approach to reducing carbon content, relative to natural gas. However, hydrogen blends with natural gas are likely to vary in composition, which will result in variations in flame speed, heating value, and other combustion properties. For both safety and optimal system operation, online monitoring of fuel composition would be beneficial.

6.1.3 Developing Solid Sorbents for Ammonia

The changing supply and demand of NH_3 necessitate an effective adoption of a technology which can effectively and economically store NH_3. Storing and transporting liquified NH_3 have various safety concerns (as stated in the earlier sections), however, most of the issues related to bulk storage and transportation of liquified NH_3 can be managed. Storing and using NH_3 in vehicles and other domestic end user applications presents additional safety issues due to the reduced technical knowledge of the public. However, there are still major issues for other ammonia-based applications, as they not only involve effective storing capabilities, but also efficient release procedures when needed. For vehicle applications these NH_3 storage capabilities need to meet stringent targets, such as those developed by U.S. DRIVE (a government-industry partnership between the U.S. DOE, U.S. automobile manufacturers, and energy and utility companies) to be able to compete with existing systems (Van Hassel et al., 2015). There are additional concerns about capturing residual ammonia from hydrogen that may be produced from stored ammonia.

To overcome these issues, various sorbent systems have been developed in recent decades which can help safely store and transport NH_3 and release it when needed in a controlled manner. However, each of the existing systems has its limitations. Typically, these sorbents are made of

metal halides which bind the ammonia to form corresponding metal amine complexes, such as $Mg(NH_3)_6Cl_2$ and $Ca(NH_3)_8Cl_2$. Other sorbent systems exist including metal boranes (Bluhm et al., 2006), metal-organic frameworks (MOF) (Ramlogan et al., 2020), and activated carbon (Van Hassel et al., 2015). While these sorbent systems are efficient and economically viable to prepare, metal boranes and activated carbons suffer from ammonia adsorption limitations; while the MOF-based systems are difficult to reuse practically after a couple of cycles due to their slow structural degradation at temperatures above 75 ºC (Nguyen et al., 2020). An opportunity exists for research on safer small storage and ammonia cleanup applications.

6.1.4 Low-Cost, Wide-Area Hydrogen Leak Detection Technology

Blending hydrogen in natural gas pipelines is a proposed method for delivering hydrogen to markets, providing a more cost-effective and sustainable supply of hydrogen. This approach requires continuous pipeline monitoring and maintenance to ensure the safe and reliable delivery of hydrogen to the point of end-use. For this approach, therefore it is critical to improve the integrity of natural gas pipelines with the aid of H_2 leak detection devices along the widely distributed pipeline network.

While there are a large number of point sensors for hydrogen commercially available, optical fiber-based sensor technology provides the advantage of lower cost for distributed real-time monitoring over long distances. There is an opportunity to develop an optical fiber sensor which is capable of detecting hydrogen and methane simultaneously and selectively to monitor for gas leaks from pipelines. Developing the optical fiber sensor for the leak detection of both H_2 and CH_4 would enable safer hydrogen transport through existing natural gas pipelines with remote real-time hydrogen monitoring capabilities. In addition, the optical fiber sensor capable of sensing both H_2 and CH_4 could be deployable to SOFCs, turbines, and combustion systems to optimize fuel efficiency and to enhance operational safety.

6.1.5 High-Temperature Hydrogen Sensors

Hydrogen-fueled high-temperature equipment such as turbines, SOFCs, and combustion systems require monitoring of purge cycles due to the high buoyancy of hydrogen which can cause it to be more easily trapped within equipment. To improve safety, this purge cycle monitoring requires thermally stable hydrogen sensors which can endure the high-temperature operations of these systems.

One possible approach is a sapphire-based fiber sensor, which has high melting point (2054 ºC). This sensor would be an ideal platform for hydrogen sensing at high temperatures (>800 ºC). This type of optical fiber has resistance to hydrogen damage, preventing hydrogen-induced optical property changes. Applying a hydrogen-selective sensing layer along with a protective layer to the sapphire optical fiber may enable monitoring of hydrogen concentration in the high-temperature systems.

6.1.6 Hydrogen Odorants

Natural gas has added odorants (normally sulfur compounds) making a leak easily detectable by smell to improve the safety of the pipeline and distribution systems. In most natural gas applications, the odorants have no significant impact on the use of the natural gas. Hydrogen has no intrinsic odor, so the vision of widespread distribution of hydrogen leads to the question of the need for addition of an odorant. Unlike natural gas, hydrogen may be used directly in a fuel

cell for electrical production, without a fuel reformer. However, fuel cells are poisoned by sulfur compounds, so use of an odorant will likely require preprocessing of hydrogen to remove the odorant prior to a fuel cell. Widespread distribution of pure hydrogen may necessitate a new, dedicated distribution system, because reuse of the natural gas system may not be safe. These issues, and others, make the consideration of the addition of an odorant to hydrogen a complex question. Further analysis of the techno-economic impact of various scenarios would be beneficial to policy decisions.

7. REFERENCES

Allen-Bradley. Class/Division Hazardous Location. Publication 800-WP003A-EN-P - October 2001. https://literature.rockwellautomation.com/idc/groups/literature/documents/wp/800-wp003_-en-p.pdf (accessed Feb 17, 2022).

ANSI/CGA G-2.1-2014 - Requirements for the Storage and Handling of Anhydrous Ammonia. https://webstore.ansi.org/Standards/CGA/ANSICGA2014 (accessed May 22, 2022).

API. 8. E. API recommended practice 941, "Steels for Hydrogen Service at Elevated Temperatures and Pressures in Petroleum Refineries and Petrochemical Plants," American Petroleum Institute, 2016.

Appl, M. *Ammonia: Principles and Industrial Practice*; Wiley-VCH, 1999.

ASME. BPVC Boilers and Pressure Vessels. BPVC Boilers and Pressure Vessels - ASME (accessed May 22, 2022).

Astbury, G. R.; Hawksworth, S. J. Spontaneous ignition of hydrogen leaks: A review of postulated mechanisms. *International Journal of Hydrogen Energy* **2007,** *32*, 2178–2185.

Aziz, M.; TriWijayanta, A.; Nandiyanto, A. B. D. Ammonia as effective hydrogen storage: A review on production, storage and utilization. *Energies.* **2020,** *13*, 1–25.

Baranzahi, A.; Spetz, A.L.; Andersson, B.; Lundstrom, I. Gas sensitive field-effect devices for high temperatures. *Sensors and Actuators B* **1995,** *26*, 165–169.

Baranzahi, A.; Spetz, A.L.; Glavmo, M.; Carlsson, C.; Nytomt, J.; Salomonsson, P.; Jobson, E.; Haggendal, B.; Martensson, Lundstrom, I.P.M. Response of metal oxide-silicon carbide sensors to simulated and real exhaust gases. *Sensors and Actuators B* **1997,** *43*, 52–59.

Barelli, L.; Barluzzi, E.; Bidini, G. Diagnosis methodology and technique for solid oxide fuel cells: a review. *Int. J. Hydrogen Energy* **2013,** *38*, 5060–5074.

Barrera, O.; Tarleton, E.; Tang, H.; Cocks, A. Modelling the Coupling Between Hydrogen Diffusion and the Mechanical Behaviour of Metals. *Computational Materials Science* **2016,** *122*, 219–228.

Barrett, P. R.; Ahmed, R.; Menon, M.; Hassan, T. Isothermal low-cycle fatigue and fatigue-creep of Haynes 230. *International Journal of Solids and Structures* **2016,** *88–89*, 146–164.

Becker, H.; Hinds, G. Preliminary screening of candidate odorants for the hydrogen gas grid: impact on fuel cell performance; NPL Report (RES) 004; July 2019.

Berdiyeva, P.; Karabanova, A.; Grinderslev, J. B.; Johnsen, R. E.; Blanchard, D.; Hauback, B. C. Synthesis, structure and NH3 sorption properties of mixed Mg1-xMnx(NH3)6Cl2 ammines. *Energies* **2020,** *13*.

Bluhm, M. E.; Bradley, M. G.; Butterick, R.; Kusari, U.; Sneddon, L. G. Amineborane-based chemical hydrogen storage: Enhanced ammonia borane dehydrogenation in ionic liquids. *J Am Chem Soc.* **2006**, *128*, 7748–9.

Boon-Brett, L.; Bousek, J.; Black, G.; Moretto, P.; Castello, P.; Hübert, T.; Banach, U. Identifying performance gaps in hydrogen safety sensor technology for automotive and stationary applications. *Int. J. Hydrogen Energy* **2010,** *35*, 373–384.

Bouam, A.; Aissani, S.; Kadi, R. Gas turbine performances improvement using steam injection in the combustion chamber under Sahara conditions. *Oil & Gas Science and Technology – Rev. IFP* **2008,** *63*, 251–261. DOI: 10.2516/ogst:2007076.

Braun, N.; Eilers, J.; Müller, D. Odorant for Hydrogen Based on Acrylate and Acetophenone. U.S. Patent, US 8,545,724 B2, 2013.

Buttner, W. J.; Burgess, R.; Schmidt, K.; Wright, H.; Rivkin, C.; Weidner, E.; Oritiz-Cebolla, R.; Bonato, C.; Moretto, P.; Hill, L.; James, C. W. Hydrogen safety sensor performance and use cap analysis. Conference paper; 7th International Conference on Hydrogen Safety, Hamburg, Germany, 2017.

Calì, M.; Fontana, E.; Giaretto, V.; Orsello, G.; Santarelli, M. The EOS Project: A SOFC Pilot Plant in Italy Safety Aspects. International Conference on Hydrogen Safety, Pisa, Italy, 2005.

Cappelletti, A.; Martelli, F. Investigation of a pure hydrogen fueled gas turbine burner. *International Journal of Hydrogen Energy* **2017,** *42*, 10513–10523.

Chandler, W. T.; Walter, R. J. Hydrogen Effects in Refractory Metals. In *Refractory Metal Alloys Metallurgy and Technology*; Machlin, I., Begley, R. T., Weisert, E. D., Eds.; Springer: Boston, MA, 1968. DOI: 10.1007/978-1-4684-9120-3_6

Chang, Y.; Zhang, C.; Shi. J.; Li, J.; Zhang, S.; Chen, G. Dynamic Bayesian network based approach for risk analysis of hydrogen generation unit leakage. *International Journal of Hydrogen Energy* **2019,** *44*, 26665–26678.

Chauhan, P. S.; Bhattacharya, S. Hydrogen gas sensing methods, materials, and approach to achieve parts per billion level detection: A review. *Int. J. Hydrogen Energy* **2019,** *44*, 26076–26099.

Cheng, X.; Shi, Z.; Glass, N.; Zhang, L. Zhang, J. Song, D. Liu, Z.; Wang, H.; Shen, J. A Review of PEM Hydrogen Fuel Cell Contamination: Impacts, Mechanisms, and Mitigation. *J. Power Sources* **2007,** *165*, 739–756.

Chorpening, B. T.; Straub, D. L.; Huckaby, E. D.; Benson, K. J. *Detection of Lean Blowout and Combustion Dynamics Using Flame Ionization*; ASME Paper GT2005-68612, 2005.

Christensen, C. H.; Sørensen, R. Z.; Johannessen, T.; Quaade, U. J.; Honkala, K.; Elmøe, T. D. Metal ammine complexes for hydrogen storage. *J Mater Chem* **2005,** *15*, 4106–8. https://pubs.rsc.org/en/content/articlehtml/2005/jm/b511589b

Ciferno, J.; Marano, J. *Benchmarking Biomass Gasification Technologies for Fuels, Chemicals and Hydrogen Production*; U.S. Department of Energy, National Energy Technology Laboratory, 2002.

Committee of Stainless Steel Producers. *Stainless Steels in Ammonia Production*; American Iron and Steel Institute Washington, DC, 1978.

Compressed Gas Association, *Handbook of Compressed Gases*, 3rd Ed., Van Nostrand Reinhold, New York, 1990.Cui, L.; Chen, Y.; Zhang, G. An optical fiber hydrogen sensor with Pd/Ag film. *Optoelectron. Lett*. **2009,** *5*, 220–223.

Derwent, R. G.; Stevenson, D. S.; Utembe, S. R.; Jenkin, M. E.; Khan, A. H.; Shallcross, D. E. Global Modelling Studies of Hydrogen and Its Isotopomers using STOCHEM-CRI: Likely Radiative Forcing Consequences of a Future Hydrogen Economy. *Int. J. Hydrogen Energy* **2020,** *45*, 9211–9221.

Derwent, R.; Simmonds, P.; O'Doherty, S.; Manning, A.; Collins, W.; Stevenson, D. Global Environmental Impacts of the Hydrogen Economy. *Int. J. Nuclear Hydrogen Production and Application* **2006,** *1*, 57–67.

DNV GL. Hydrogren Purity – Final Report; HY4HEAT (WP2) Hydrogen Purity & Colourant; DNV GL – Report No. 10123173-FINAL PURITY, 2019.

DOE. *Hydrogen Production: Natural Gas Reforming, Hydrogen and Fuel Cell Technologies Office*; U.S. Department of Energy, 2022a. www.energy.gov.

DOE. *Strategic Vision*; U.S. Department of Energy, Office of Fossil Energy and Carbon Management (FECM), 2022b

EIA. U.S. Energy Information Administration. Electric Power Monthly, February 2022, Preliminary Data. https://www.eia.gov/energyexplained/electricity/electricity-in-the-us-generation-capacity-and-sales.php

EIA. U.S. Energy Information Administration. Natural Gas Annual, September 2021b. https://www.eia.gov/energyexplained/natural-gas/use-of-natural-gas.php

Emerson. The Wobbe Index and Natural Gas Interchangeability; Emerson application data document, 2007. www.emerson.com/documents/automation/white-paper-wobbe-index-natural-gas-interchangeability-ras-en-133638.pdf (accessed Feb 10, 2022).

ETN Global. European Turbine Network. *Hydrogen Gas Turbines:The Path Towards A Zero-Carbon Gas Turbine*; 2020. www.etn.global/wp-content/uploads/2020/02/ETN-Hydrogen-Gas-Turbines-report.pdf (accessed Feb. 10, 2022).

Fan, L.-S. *Chemical Looping Systems for Fossil Energy Conversions*; John Wiley and Sons, 2010.

Flynn, P.; Sprague, M. Hydrogen Odorants and Odorant Selection Method. U.S. Patent 8,394,553 B2, 2013.

Folga, S. M. *Natural Gas Pipeline Technology Overview*; ANL/EVS/TM/08-5; Environmental Science Division, Argone National Laboratory: Lemont, IL, 2007.

Furtado, A. M. B.; Wang, Y.; Glover, T. G.; Levan, M. D. MCM-41 impregnated with active metal sites: Synthesis, characterization, and ammonia adsorption. *Microporous Mesoporous Mater.* **2011,** *142*, 730–9.

Garcia-Labiano, F.; de Diego, L.F.; Gayan, P.; Adanez, J.; Abad, A. Dueso, C. Effect of Fuel Gas Composition in Chemical-Looping Combustion with Ni-Based Oxygen Carriers. 1. Fate of Sulfur. *Ind. Eng. Chem. Res.* **2009,** *48*, 2499–2508.

Ghosh, R. N.; Tobias, P.; Golding, B. Influence of interface states on high temperature SiC sensors and electronics. *Material Research Symposium* **2003,** *742*, 363.

Ghosh, R.N.; Tobias, P. SiC field-effect devices operating at high temperature. *J. Electronic Materials* **2005,** *34*, 345–350.

Gillette, J. L.; Kolpa, R. L. *Overview of Interstate Hydrogen Pipeline Systems*; ANL/EVS/TM/08-2; Environmental Science Division, Argone National Laboratory: Lemont, IL, 2007.

Golkhatmi, S. Z.; Asghar, M. I.; Lund, P. D. A review on solid oxide fuel cell durability: Latest progress, mechanisms, and study tools. *Renewable and Sustainable Energy Reviews* **2022,** *161*, 112339.

Griebel, P. Gas turbines and hydrogen. In *Hydrogen science and engineering: materials, processes, systems and technology*; John Wiley, 2016; pp. 1011–1032.

Hall, J. E.; Hooker, P.; Willoughby, D. Ignited releases of liquid hydrogen: safety considerations of thermal and overpressure effects. *International Journal of Hydrogen Energy* **2014,** *39*, 20547–20553.

Hauch, A.; Ebbesen, S. D.; Jensen, S. H.; Mogensen, M. Solid oxide electrolysis cells; microstructure and degradation of the Ni/Yttria-stabilized zirconia electrode. *J. Electrochem. Soc*. **2008**, *155*, B1184–1193

Haugom, G. P.; Holmefjord, K. O.; Skogseth, L. O. Assessment and Evaluation of 3rd Party Risk For Planned Hydrogen Demonstration Facility. Int. Conf. on Hydrogen Safety, S. Sebastian, Spain, 2007.

Hayakawa, A.; Goto, T.; Mimoto, R.; Arakawa, Y; Kudo, T.; Kobayashi, H. Laminar burning velocity and Markstein length of ammonia/air premixed flames at various pressures. *Fuel* **2015,** *159*, 98–106.

Hayes, H. State discloses likely cause of Eastman explosion. TimesNews: Kingsport, TN, April 11, 2018. https://www.timesnews.net/news/business/state-discloses-likely-cause-of-eastman-explosion/article_212e42e5-3663-5678-acf0-ffb60c2de6c0.html

Haynes, W. M., and Lide, D. R., eds. *CRC Handbook of Chemistry and Physics*, 92 Ed., CRC Press, Boca Raton, 2011.

Heidari, A.; Wen, J. X. Flame acceleration and transition from deflagration to detonation in hydrogen explosions. *International Journal of Hydrogen Energy* **2014,** *39*, 6184–6200.

Henriquez, D. D. O.; Cho, I.; Yang, H.; Choi, J.; Kang, M.; Chang, K. S.; Jeong, C. B.; Han, S. W.; Park, I. Pt nanostructures fabricated by local hydrothermal synthesis for low-power catalytic-combustion hydrogen sensors. *ACS Appl. Nano Mater*. **2021,** *4*, 7–12.

Herring, D. *Hydrogen Embrittlement*; Wire Forming Technology International, Initial Publications Inc.; 2010.

Heyen, G.; Kalitventzeff, B. A comparison of advanced thermal cycles suitable for upgrading existing power plant. *Applied Thermal Engineering* **1999,** *19*, 227–237.

Hibino, K.; Takahashi, T. Yagami, Y.; Wada, M.; Ochi, T.; Kaijo, K. Inagaki, T.; Asai, Y.; Zeng, Y.; Suzuki, T.; Niimi, H. Fuel Gas for a Fuel Cell. U.S. Patent Application 2003/0126796 A1, 2003.

Higman, C.; van der Burgt, M. *Gasification*, 2nd Ed. Gulf Professional Publishing, 2008.

Hino, R.; Haga, K.; Aita, H.; Sekita, K. R&D on hydrogen production by high-temperature electrolysis of steam. *Nucl. Eng. Des*. **2004,** *233*, 365–375.

Hong, J.; Lee, S.; Seo, J.; Pyo, S.; Kim, J.; Lee, T. A highly sensitive hydrogen sensor with gas selectivity using a PMMA membrane-coated Pd nanoparticle/single-layer graphene hybrid. *ACS Appl. Mater. Interfaces* **2015,** *7*, 3554–3561.

Hu, J.; Sun, Y.; Xue, Y.; Zhang, M.; Li, P.; Lian, K.; Zhuiykov, S.; Zhang, W.; Chen, Y. Highly sensitive and ultra-fast gas sensor based on CeO_2-loaded In_2O_3 hollow spheres for ppb-level hydrogen detection. *Sensors and Actuators B* **2018,** *257*, 124–135.

Hübert, T.; Boon-Brett, L.; Black, G.; Banach, U. Hydrogen sensors – A review. *Sensors and Actuators B* **2011,** *157*, 329–352.

Hughes, R. C.; Schubert, W. K. Thin films of Pd/Ni alloys for detection of high hydrogen concentrations. *J. Appl. Phys*. **1992,** *71*, 542–544.

Hughes, R. C.; Schubert, W. K.; Buss, R. J. Solid-state hydrogen sensors using palladium-nickel alloys: effect of alloy composition on sensor response. *J. Electrochem. Soc.* **1995,** *142*, 249–254.

Hunter, G. W.; Neudeck, P. G.; Gray, M.; Androjna, D.; Chen, L. Y.; Hoffman Jr., R. W.; Liu, C. C., Wu, Q. H. SiC-based gas sensor development. *Materials Science Forum* **2000,** *338–342*, 1439–1442.

Hunter, G. W.; Neudeck, P. G.; Xu, J.; Lukcol, D.; Trunek, A.; Artale, M.; Lampard, P.; Androjna, D.; Makel, D.; Ward, B.; Liu, C. C. Development of Si-based gas sensors for aerospace applications. *Materials Research Society Symposium Proceedings, Silicon Carbide 2004 – Materials, Processing, and Devices*, 2004; pp. 287–297.

HySafe. Biennial Report on Hydrogen Safety (Version 1.2), Chapter III; 2007. http://www.hysafe.org/BRHS

Industrial Health and Safety Review (website). Fire and Explosion Hazards, www.isrmag.com/fire-and-explosion (accessed Feb 07, 2022).

Inyawilert, K.; Wisitsoraat, A.; Liewhiran, C.; Tuantranont, A.; Phanichphant, S. H_2 gas sensor based on PdO_x-doped In_2O_3 nanoparticles synthesized by flame spray pyrolysis. *Appl. Surf. Sci.* **2019,** *475*, 191–203.

Jacobsen, T.; Mogensen, M. The course of oxygen partial pressure and electric potentials across an oxide electrolyte cell. *ECS Trans*. **2008,** *13*, 259–273.

Jiang, H.; Yang, R.; Tang, X.; Burnett, A.; Lan, X.; Xiao, H.; Dong, J. Multilayer fiber optic sensors for in situ gas monitoring in harsh environments. *Sensors and Actuators B* **2013,** *177*, 205–212.

Kalamaras, A. M. E. C. M. Hydrogen Production Technologies: Current State and Future Developments. In Conference Papers in Energy, 2013.

Kandasamy, S.; Trinchi, A.; Wlodarski, W.; Commi, E.; Sberveglieri, G. Hydrogen and hydrocarbon gas sensing performance of Pt/WO3/SiC MROSiC devices. *Sensors and Actuators B* **2005,** *111–112*, 111–116.

Kaniyoor, A.; Imran Jafri, R.; Arockiadoss, T.; Ramaprabhu, S. Nanostructured Pt decorated graphene and multi walled carbon nanotube based room temperature hydrogen gas sensor. *Nanoscale* **2009,** *1*, 382–386.

Khoshnaw, F.; Gubner, R. *Corrosion Atlas Case Studies*; Elsevier Inc, 2021.

Kim, H.; Pak, Y.; Jeong, Y.; Kim. W.; Kim, J.; Jung, G. Y. Amorphous Pd-assisted H_2 detection of ZnO nanorod gas sensor with enhanced sensitivity and stability. *Sens. Actuators B: Chem.* **2018,** *262*, 460–468.

Klarstrom, D. *Aerospace and Hight Temperaure Performace Alloys Database* ; CINDAS, LLC, West Lafayette, IN, 2009.

Koc, R.; Kazantis, N.K.; Ma, Y.H. Process safety aspects in water-gas-shift (WGS) membrane reactors used for put hydrogen production. *Journal of Loss Prevention in the Process Industries* **2011,** *24*, 852–869.

Kondalkar, V. V.; Park, J.; Lee, K. MEMS hydrogen gas sensor for in-situ monitoring of hydrogen gas in transformer oil. *Sensors & Actuators: B. Chemical* **2021,** *326*, 128989.

Kopasz, J. P. Fuel Cells and Odorants for Hydrogen. *Int. J. Hydrogen Energy* **2007,** *32*, 2527–2531.

Korkhaus, J.; Feser, J. Failure Mechanisms and Material Degradations at High Temperatures in Ammonia Plants; *Ammonia Technical Manual*, 2007.

Korotcenkov, G.; Han, S. D.; Stetter, J. R. Review of electrochemical hydrogen sensors. *Chem. Rev.* **2009,** *109*, 1402–1433.

Kushi, T. Effects of sulfur poisoning on degradation phenomena in oxygen electrodes of solid oxide electrolysis cells and solid oxide fuel cells. *Int. J. Hydrogen Energy* **2017,** *42*, 9396–9405.

Lan, R.; Irvine, J. T.; Tao, S. Ammonia and Related Chemicals as Potential Indirect Hydrogen Storage Materials. *International Journal of Hydrogen Energy* **2012,** *37*, 1482–1494.

Law, C. K. *Combustion physics*; Cambridge University Press: Cambridge, UK, 2006.

Leighton, P. A. *Photochemistry of Air Pollution*; Academic Press: New York, 1961.

Lim, H.-T.; Virkar, A. V. A study of solid oxide fuel cell stack failure by inducing abnormal behavior in a single cell test. *J. Power Sources* **2008,** *185*, 790–800.

Liu, L.; Kim, G.-Y.; Chandra, A. Modeling of thermal stresses and lifetime prediction of planar solid oxide fuel cell under thermal cycling conditions. *J. Power Sources* **2010,** *195*, 2310–2318.

Liu, Y.; Li, Y. Signal analysis and processing method of transmission optical fiber hydrogen sensors with multi-layer Pd-Y alloy films. *Int. J. Hydrogen Energy* **2019,** *44*, 27151–27158.

Liu, Y.; Liu, Z.; Wei, J.; Lan, Y.; Yang, S.; Jin, T. Evaluation and prediction of the safe distance in liquid hydrogen spill accident. *Process Safety and Environmental Protection* **2021,** *146*, 1–8.

Lowesmith, B. J.; Hankinson, G.; Chynowyth, S. Safety issues of the liquefaction, storage and transportation of liquid hydrogen: An analysis of incidents and HAZIDS. *International Journal of Hydrogen Energy* **2014,** 39, 20516–20521.

Luna-Moreno, D.; Monzón-Hernάndez, D.; Villatoro, J.; Badenes, G. Optical fiber hydrogen sensor based on core diameter mismatch and annealed Pd-Au thin films. *Sens. Actuators B: Chem*. **2007,** *125*, 66–71.

Lundstrom, I.; Sundgren, H.; Winquist, F.; Erikson, M.; Rulcker, C. K.; Spetz, A. L. Twenty-five years of field effect gas sensor research in Linkoping. *Sensors and Actuators B* **2007,** *121*, 247–262.

Luo, S.; Majumder, A.; Chung, E.; Xu, D.; Bayham, S.; Sun, Z.; Zeng, L.; Fan, L.-S. Conversion of Woody Biomass Materials by Chemical Looping Process—Kinetics, Light Tar Cracking, and Moving Bed Reactor Behavior. *Ind. Eng. Chem. Res.* **2013,** *52*, 14116–14124. DOI: 10.1021/ie4020952

Lv, X.; Liu, X.; Gu, C.; Weng, Y. Determination of safe operation zone for an intermediate temperature solid oxide fuel cell and gas turbine hybrid system. *Energy* **2016,** *99*, 91–102.

Lv, X.; Weng, Y.; Effect of operating parameters on a hybrid system of intermediate-temperature solid oxide fuel cell and gas turbine. *Energy* **2015,** *91*, 10–19.

Lynch, S. P. Hydrogen Embrittlement (HE) Phenomena and Mechanism. In *Stress Corrosion Cracking, Theory and Practice*;Woodhead Publishing Limited: Oxford; 2011; pp. 90–30.

MacFarlane, D. R.; Cherepanov, P. V.; Choi, J.; Suryanto, B. H. R.; Hodgetts, R. Y.; Bakker, J. M.; Ferrero Vallana, F. M.; Simonov, A. N. A Roadmap to the Ammonia Economy. *Joule* **2020,** *4*, 1186–1205. https://doi.org/10.1016/j.joule.2020.04.004.

Malmali, M.; Le, G.; Hendrickson, J.; Prince, J.; McCormick, A. V.; Cussler, E. L. Better Absorbents for Ammonia Separation. *ACS Sustain Chem Eng.* **2018,** *6*, 6536–46.

Malmali, M.; Reese, M.; Mccormick, A. V.; Cussler, E. L. Converting Wind Energy to Ammonia at Lower Pressure; 2017. https://pubs.acs.org/sharingguidelines

Marchi, C. S. Hydrogen Compatibility of Materials; In DOE EERE Fuel Cell Technologies Office Webinar, 2013.

Mihailov, S. J. Fiber Bragg grating sensors for harsh environments. *Sensors* **2012,** *12*, 1898–1918.

Milani, D.; Kiani, A.; McNaughton, R. Renewable-powered hydrogen economy from Australia's perspective. *International Journal of Hydrogen Energy* **2021,** *45*, 24125–24145.

Minnesota Department of Agriculture. Anhydrous Ammonia System Piping Requirements. https://www.mda.state.mn.us/sites/default/files/2019-11/nh3pipingreqs.pdf (accessed May 24, 2022).

Minnesota Department of Transportation. Anhydrous Ammonia in Propane Cylinders Safety Considerations for Mitigation. New (mn.gov) (accessed Aug. 12, 2022).

Mocoteguy, P.; Brisse, A. A review and comprehensive analysis of degradation mechanisms of solid oxide electrolysis cells. *Int. J. Hydrogen Energy* **2013**, *38*, 15887–15902.

Mohammadfam, I.; Zarei, E. Safety risk modeling and major accidents analysis of hydrogen and natural gas releases: A comprehensive risk analysis framework. *International Journal of Hydrogen Energy* **2015,** *40*, 13653–13663.

Molkov, V. Hydrogen Safety Engineering and Standards, Comprehensive Renewable Energy, 2nd ed.; Elsevier Inc., 2020. https://doi.org/10.1016/B978-0-12-819727-1.00023-6.

Molkov, V.; Saffers, J-B. The correlation for non-premixed hydrogen jet flame length in still air. *Proceedings of the 10th International Symposium on Fire Safety Science*, June 2011, University of Maryland, USA. (in print).

Motaung, D. E.; Mhlongo, G. H.; Makgwane, P. R. Dhonge, B. P.; Cummings, F. R.; Swart, H. C.; Ray, S. S. Ultra-high sensitive and selective H_2 gas sensor manifested by interface of n-n heterostructure of CeO_2-SnO_2 nanoparticles. *Sens. Actuators B: Chem*. **2018,** *254*, 984–995.

Nam, J.; Lee, Y.; Joo, S.; Yoon, Y.; Yoh, J.L. Numerical analysis of the effect of the hydrogen composition on a partially premixed gas turbine combustor. *International Journal of Hydrogen Energy* **2019,** *44*, 6278–6286.

Nanninga, N.; Slifka, A.; Levy, Y.; White, C. A Review of Fatigue Crack Growth for Pipeline Steels Exposed to Hydrogen. *Journal of Research of the National Institute of Standards and Technology* **2010,** *115*, 137–452.

NDSU. *Anhydrous Ammonia: Managing The Risks*; AE1149; NDSU Agriculture and Extension; September 2021.

Nesser, I. Liquid Hydrogen Bulk Storage Introduction. 2022 Liquid Hydrogen Technologies Workshop, Hydrogen and Fuel Cell Technologies Office, U.S. Department of Energy, virtual workshop, Feb 22–23, 2022. https://www.energy.gov/eere/fuelcells/liquid-hydrogen-technologies-workshop

NJ Health. Ammonia, Hazard Substance Fact Sheet. New Jersey Department of Health, Feb 2016. 0084.pdf (nj.gov) (accessed Sept. 16, 2022).

NETL. SOFC operating principle. U.S. Department of Energy, National Energy Technology Laboratory, 2022. https://netl.doe.gov/coal/sofc/operating-principle

NFPA. NFPA 58: Liquefied Petroleum Gas Code; National Fire Protection Association, 2020.

NFPA. NFPA 67: Guide on Explosion Protection for Gaseous Mixtures in Pipe Systems; National Fire Protection Association, 2019.

NFPA. NFPA 68: Standard on Explosion Protection by Deflagration Venting; National Fire Protection Association, 2018.

NFPA. NFPA 69: Standard on Explosion Prevention Systems; National Fire Protection Association, 2019.

Nguyen, T. N.; Harreschou, I. M.; Lee, J. H.; Stylianou, K. C.; Stephan, D. W. A recyclable metal–organic framework for ammonia vapour adsorption. *Chem Commun.* **2020,** *56*, 9600–3. https://pubs.rsc.org/en/content/articlehtml/2020/cc/d0cc00741b

Ni, M.; Leung, M. K. H.; Leung, D. Y. C. Technological development of hydrogen production by solid oxide electrolyzer cell (SOEC). *Int. J. Hydrogen Energy* **2008,** *33*, 2337–2354.

Noble, D.; Wu, D.; Emerson, B.; Sheppard, S.; Lieuwen, T.; Angello, L. Assessment of Current Capabilities and Near-Term Availability of Hydrogen-Fired Gas Turbines Considering a Low-Carbon Future. *Journal of Engineering for Gas Turbines and Power* **2021,** *143*, 1–10.

NIOSH. Ammonia; Workplace Safety and Health Topics National Institute for Occupational Safety and Health, 2019. Ammonia | NIOSH | CDC

Novelli, P. C.; Lang, P. M.; Masarie, K. A.; Hurst, D. F.; Myers, R.; Elkins, J. W. Molecular Hydrogen in the Troposphere: Global Distribution and Budget. *J. Geophysical Research*, **1999,** *104*, 30427–30444.

Nowotny. J.; Veziroglu. T. N. Impact of Hydrogen on the Environment. *Int. J. Hydrogen Energy* **2011,** *36*, 13218–13224.

Oberg, S.; Odenberger, M.; Johnsson, F. Exploring the competitiveness of hydrogen-fueled gas turbines in future energy systems. *International Journal of Hydrogen Energy* **2020,** *47*, 624–644.

Ocko, I.; Hamburg, S. P. Climate consequences of hydrogen leakage. *Atmospheric Chemistry and Physics* **2022**; Preprint.

Ogata, T. Hydrogen Embrittlement Evaluation in Tensile Properties of Stainless Steels at Cryogenic Temperatures. AIP Conference Proceedings; 2008; 986, 124.

Oran, E. S.; Chamberlain, G.; Peklaski, A. mechanisms and occurrence of detonations in vapor cloud explosions. *Progress in Energyand Combustion Science* **2020,** *77*, 1008004.

OSHA. Occupational Safety and Health Administration. United States Department of Labor. https://www.osha.gov/laws-regs/regulations/standardnumber/1910/1910.111 (accessed May 18, 2022a).

OSHA. Occupational Safety and Health Administration. United States Department of Labor. AMMONIA | Occupational Safety and Health Administration (osha.gov) (accessed Sept. 16, 2022b).

Oskarsson, H. Material Challenges in Industrial Gas Turbine. In Proceedings of Sino-Swedish Structural Materials Symposium, 2007.

Palacios, A.; Bradley, D. Conversion of natural gas jet flame burners to hydrogen. *International Journal of Hydrogen Energy* **2021,** *46*, 17051–17059

Park, N.-H.; Akamatsu, T.; Itoh, T.; Izu, N.; Shin, W. Calorimetric thermoelectric gas sensor for the detection of hydrogen, methane and mixed gases. *Sensors* **2014,** *14*, 8350–8362.

Pérez, S.; Belsue, M.; González, O.; Unzurrunzaga, A.; Azkarate, I. Safety aspects in the production and separation of hydrogen from biomass. Proceedings from the International Conference of Hydrogen Safety, San Francisco, CA, 2011.

PHMSA. *Study of Nonpetroleum Hazardous Liquids Transported by Pipeline*; U.S. Department of Transportation (DOT); Administration, Pipeline and Hazardous Materials Safety, 2015.

Pratt, D. R. *Compatibility of Ammonia with Candidate Dry Cooling System Materials*; BNWL-1992-UC-38; Pacific Northwest Laboratory: Richland, WA; 1976.

Quarton, C. J.; Samsatli, S. Power-to-gas for injection into the gas grid: What can we learn from real-life projects, economic assessments and systems modelling? *Renewable and Sustainable Energy Reviews* **2018,** *98*, 302–316.

Raghava Chari, S. NH3 Storage Tanks Ammonia Gas Venting Issue – Root Cause Analysis; Instrumentation Tools. https://instrumentationtools.com/nh3-storage-tanks-ammonia-gas-venting-issue-root-cause-analysis/ (accessed May 24, 2022)

Ramlogan, M. V.; Rabinovich, A.; Rouff, A. A. Thermochemical Analysis of Ammonia Gas Sorption by Struvite from Livestock Wastes and Comparison with Biochar and Metal-Organic Framework Sorbents. *Environmental Science and Technology* **2020,** *54*, 13264–73.

Reardon, H.; Hanlon, J. M.; Grant, M.; Fullbrook, I.; Gregory, D. H. Ammonia uptake and release in the MnX2-NH3 (X = Cl, Br) systems and structure of the Mn(NH3)nX2 (n = 6, 2) ammines. *Crystals* **2012,** *2*, 193–212.

Rydén, M.; Lyngfelt, A.; Mattisson, T. Chemical-Looping Combustion and Chemical-Looping Reforming in a Circulating Fluidized-Bed Reactor Using Ni-Based Oxygen Carriers. *Energy Fuels* **2008,** *22*, 2585–2597. DOI: 10.1021/ef800065m

Saffers, J.-B.; Molkov, V. V. Hydrogen safety engineering framework and elementary design safety tools. *International Journal of Hydrogen Energy* **2014,** 6268–6285.

Saffers, J.-B.; Molkov, V. V. Towards hydrogen safety engineering for reacting and non-reacting hydrogen releases. *Journal of Loss Prevention in the Process Industries* **2013,** *26*, 344–350.

Sahoo, T.; Kale, P. Work function-based metal–oxide–semiconductor hydrogen sensor and its functionality: a review. *Adv. Mater. Interfaces* **2021,** *8*, 2100649.

Sanger, A.; Kumar, A.; Chauhan, S.; Gautam, Y. K.; Chandra, R. Fast and reversible hydrogen sensing properties of Pd/Mg thin film modified by hydrophobic porous silicon substrate, *Sens. Actuators B: Chem*. **2015,** *213*, 252–260.

Schefold, J.; Brisse, A.; Tietz, F. Nine thousand hours of operation of a solid oxide cell in steam electrolysis mode. *J. Electrochem. Soc*. **2012,** *159*, A137–134.

Schultz, M. G.; Diehl, T.; Brasseur, G. P.; Zittel, W. Air Pollution and Climate-Forcing Impacts of a Global Hydrogen Economy. *Science* **2003,** *302*, 624–627.

Shafiei, M.; Kalantar-zadeh, K.; Wlodarski, W.; Comini, E.; Ferroni, M.; Sberveglieri, G.; Kaciulis, S.; Pandolfi, L. Hydrogen gas sensing performance of Pt/SnO2 nanowires/SiC MOS devices. *Int. J. Smart Sensing and Intelligent Systems* **2008,** *1*, 771–783.

Shafiei, M.; Yu, J.; Arsat, R.; Kalantar-zadeh, K.; Comini, E.; Ferroni, M.; Sberveglieri, G.; Wlodarski, W. Reversed bias Pt/nanostructured ZnO Schottky diode with enhanced electric field for hydrogen sensing. *Sensors and Actuators B* **2010,** *146*, 507–512.

Shaikh, A. S. Development of a γ’ Precipitation Hardening Ni-Base Superalloy for Additive Manufacturing. Master Thesis in Materials Engineering. Chalmers University of Technology, Gothenburg, Sweden, 2018.

Sharifzadeh, M.; Meghdari, M.; Rashtchian, D. Multi-objective design and operation of solid oxide fuel cell (SOFC) triple combined-cycle power generation system: Integrating energy efficiency and operational safety. *Applied Energy* **2017,** *185*, 345–361.

Sharma, H. J.; Sslorkar, M. A.; Kondawar, S. B. H_2 and CO gas sensor from SiO_2/polyaniline composite nanofibers fabricated by electrospinning. *Adv. Mater. Proc.* **2017,** *2*, 61–66.

Shevyakov, G. G.; Tomilin, V. P.; Kondrashkov, Y. A. Deposit with VINITI, N3671-80 (in Russian). *Engineering Physical Journal*. (Reproduced in: Schevyakov GG and Savelieva NI (2004) Dispersion and combustion of hydrogen jet in the open atmosphere. *International Scientific Journal for Alternative Energy and Ecology 1* **1980,** *9.*

Shirazi, A.; Aminyavari, M.; Najafi, B.; Rinaldi, F.; Razaghi, M.; Thermal economic-environmental analysis and mutl-objective optimization of an internal-reforming solid oxide fuel cell gas turbine hybrid system. *Int. J. Hydrogen Energy* **2012,** *37*, 19111–19124.

Sigurdarson, J. J.; Svane, S.; Karring, H. The Molecular Processes of Urea Hydrolysis in Relation to Ammonia Emissions from Agriculture. *Reviews in Environmental Science and Biotechnology*; Springer; April 17, 2018; pp 241–258. https://doi.org/10.1007/s11157-018-9466-1

Silva, S. F.; Coelho, L.; Frazao, O.; Santos, J. L.; Malcata, F. X. A review of palladium-based fiber-optic sensors for molecular hydrogen detection. *IEEE Sensors J.* **2012**, *12*, 93–103.

Smith, R. A. *Hydrogen Purity Standard*; Compressed Gas Association, 2004.

Sohal, M. S.; O'brien, J. E.; Stoots, C. M.; Sharma, V. I.; Yildiz, B.; Virkar, A. Degradation issues in solid oxide cells during high temperature electrolysis. *J. Fuel Cell Sci. Technol*. **2012,** *9*, 11017–11026.

Solomon, S.; Qin, D.; Manning, M.; Chen, Z.; Marquis, M.; Averyt, K. B.; Tignor, M.; Miller, H. L. AR4 Climate Change 2007: The Physical Science Basis. *Contribution of Working Group I to the Forth Assessment Report of the Intergovernmental Panel on Climate Change*; Cambridge University Press: Cambridge; 2007.

Soo, M. T.; Cheong, K. Y.; Noor, A. F. M. Advances of SiC-based MOS capacitor hydrogen sensors for harsh environment applications. *Sensors and Actuators B* **2010,** *151*, 39–55.

Spetz, A.; Arbab, A.; Lundstrom, I. Gas sensors for high-temperature operation based on metal oxide silicon carbide (MOSiC) devices. *Sensors and Actuators B* **1993,** *15*, 19–23.

Stiller, C.; Thorud, B.; Bolland, O.; Kandepu, R.; Imsland, L. Control strategy for a solid oxide fuel cell and gas turbine hybrid system. *J. Power Sources* **2006,** *158*, 303–315.

Sun, H.; Geng, J.; Wang, c.; Rong, G.; Gao, X.; xu, J.; Yang, d. Optimization of a hydrogen liquefaction process utilizing mixed refrigeration considering stages of ortho-para hydrogen conversion. *International Journal of Hydrogen Energy* **2022,** in press. https://doi.org/10.1016/j.ijhydene.2022.03.215

Sundriyal, P.; Bhattacharya, S. Polyaniline silver nanoparticle coffee waste extracted porous graphene oxide nanocomposite structures as novel electrode material for rechargeable batteries. *Mater. Res. Express* **2017,** *4*, 0355012017.

Tang, X.; Pu, L.; Shao, X,; Lei, G.; Li, Y.; Wang, X. Dispersion Behavior and safety study of liquid hydrogen leaks under different application situations. *International Journal of Hydrogen Energy* **2020,** *45*, 31278–31288.

Tang, X.; Remmei, K.; Lang, X.; Deng, J.; Xiao, H.; Dong, J. Perovskite-type oxide thin film integrated fiber optic sensor for high-temperature hydrogen measurement. *Analytical Chemistry* **2009,** *81*, 7844–7848.

Tanner Industries, Inc. Storage & Handling – Anhydrous Ammonia Table of Contents Anhydrous Ammonia Safety Anhydrous Ammonia Properties Physical Constants of Anhydrous Ammonia Properties of Liquid Anhydrous Ammonia At Various Temperatures Anhydrous Ammonia Storage Tank Location A.; Tanner Industries, Inc. (1998) https://www.tannerind.com/PDF/Storage_%20Handling_NH_3_Rev_version_8.31.20.pdf

Tashie-Lewis, B. C.; Nnabuife, S. G. Hydrogen Production, Distribution, Storage and Power Conversion in a Hydrogen Economy - A Technology Review. *Chemical Engineering Journal* Advances **2021,** *8*, 100172.

Teel, R. B. *The Stress Corrosion Cracking of Steels in Ammonia- A Survey -With Consideration Given to OTEC Design*; ANL/OTEC-BCM-008; Argonne National Laboratory: Illinois; 1980 .

Thornton, J. D.; Chorpening, B. T.; Sidwell, T. T.; Strakey, P.; Huckaby, E. D. *Flashback Detection Sensor for Hydrogen Augmented Natural Gas Combustion*; ASME Paper GT2007-27865; 2007.

Thornton, J. D.; Straub, D. L.; Chorpening, B. T.; Huckaby, E. D.; Richards, G. A.; Benson, K. *A Combustion Control and Diagnostics Sensor for Gas Turbines*; ASME Paper GT2004-53392; 2004.

Trinchi, A.; Wlodarski, W.; Li, Y. X. Hydrogen sensitive Ga_2O_3 Schottky diode sensors based on SiC. *Sensors and Actuators B* **2004,** *100*, 94–98.

U.K. Health and Safety Executive (website), Offshore guidance on jet fires, hse.gov.uk/offshore/strategy/jet.htm. (accessed Feb 07, 2022).

U.S. Chemical Saferty and Hazard Investigation Board . N. 2005-04-B, "Positive Materials Verification: Prevent error During Alloys Steel Systems Maintenance," U.S. Chemical Saferty and Hazard Investigation Board, 2006.

USDA. Health Hazard Information Sheet Ammonia Refrigerant. Food Safety and Inspection Service, U.S. Department of Agriculture. (Ammonia (usda.gov) (accessed Sept. 16, 2022).

Uribe, F. A.; Gottesfeld, S.; Zawodzinski Jr. T. A. Effect of Ammonia as Potential Fuel Impurity on Proton Exchange Membrane Fuel Cell Performance. *J. Electrochem. Soc*. **2002,** *149*, 293–296.

Ustolin, F.; Paltrinieri, N. Hydrogen Fireball Consequence Analysis. *Chemical Engineering Transactions* **2020,** *82*, 211–216.

Valera-Medina, A.; Xiao, H.; Owen-Jones, M.; David, W.; Bowen, P. Ammonia for power. *Progress in Energy and Combustion Science* **2018,** *69*, 63–102.

Van Hassel, B. A.; Karra, J. R.; Santana, J.; Saita, S.; Murray, A.; Goberman, D. Ammonia sorbent development for on-board H2 purification. *Sep Purif Technol* **2015,** *142*, 215–26. http://dx.doi.org/10.1016/j.seppur.2014.12.009

Verkamp, F. J.; Hardin, M.; Williams, J. R. Ammonia combustion properties and performance in gas turbine burners. *International Symposium of Combustion* **1967,** *11*, 985–992.

Wächter, C.; Lunderstädt, R.; Joos, F. Using linear control theory for parameterization of a controller for a SOFC/GT hybrid power plant. *J. Fuel Cell Sci. Technol*. **2010,** *7*, 31003–31012.

Wang, B.; Zhu, Z. A brief report and analysis on the July 19, 2019, explosion in the Yima gasification plant in Sanmenxia, China. *Process Safety Progress* **2020,** *39*, 12095.

Wang, F.; Kishimoto, H.; Ishiyama, T.; Develos-Bagarinao, K.; Yamaji, K.; Horita, T.; Yokokawa, H. A review of sulfur poisoning of solid oxide fuel cell cathode materials for solid oxide fuel cells. *J. Power Sources* **2020,** *478*, 228763.

Wang, L.-Q.; Ma, H.-H.; Shen, Z.-W.; Chen, D/-G. Experimental study of DDT in hydrogen-methane-air mixtures in a tube filled with square orifice place. *Process Safety and Environmental Protection* **2018,** *116*, 228–234.

Wang, Z.; Wang, Y.; Afshan, J. H. S. A review of mettalic tanks for H_2 storage with a view to application in future green shipping. *International Journal of Hydrogen Energy* **2021,** *46*, 6151–6179.

Watson, R. T.; Core Writing Team, Climate Change 2001: Synthesis Report, *Contribution of Working Groups I, II, and III to the Third Assessment Report of the Intergovernmental Panel on Climate Change*; Cambridge University Press: Cambridge; 2001.

Weiner, S. C. Advancing the hydrogen safety knowledge base. *International Journal of Hydrogen Energy* **2014,** *39*, 20357–20361.

Weiner, S. C.; Fassbender, L. L. Lessons learned from safety events. *International Journal of Hydrogen Energy* **2012,** *37*, 17358–17363.

Wendt, H. Electrochemical hydrogen technologies: electrochemical production and combustion of hydrogen. Elsevier Science Publishers: New York; 1990.

Whychell, D. T. Effects of Hydrogen Gas at 1450°C on Select Fibrous Alumina Insulation Products. https://www.zircarceramics.com/wp-content/uploads/2017/02/Effects-of-Hydrogen-Gas-at-1450%C2%B0C-on-Select-Fibrous-Alumina-Insulation-Products.pdf (accessed Feb 4, 2022).

Wright, I.; Gibbons, T. Recent Developments in Gas Turbine Materials and Technology and Their Implications for Syngas Firing. *International Journal of Hydrogen Energy* **2007,** *32*, 3610–3621.

Wright, R. E.; Wolff, H. I. Refractory problems in production of hydrogen by pyrolysis of natural gas. *J. American Ceramic Society* **1948,** *31*, 31–38.

Wu, X. J.; Zhu, X. J. Optimization of a solid oxide fuel cell and micro gas turbine hybrid system, *Int. J. Energy Res*. **2013,** *37*, 242–249.

Xiao, H.; Oran, E. S. Flame acceleration and deflagration-to-detonation transition in hydrogen-air mixture in a channel with an array of obstacles of different shapes. *Combustion and Flame* **2020,** *220*, 378–393.

Yan, A. Fiber optic sensors for energy applications under harsh environemtal conditions, Ph.D. Thesis, University of Pittsburgh, 2017.

Yan, K.; Toku, Y.; Morita, Y.; Ju, Y. Fabrication of multiwall carbon nanotube sheet based hydrogen sensor on a stacking multi-layer structure. *Nanotechnology* **2018,** *29*, 375503–375515.

Yang, F.; Wang, T.; Deng, X.; Dang, J.; Huang, Z.; Hu, S.; Li, Y.; Ouyang, M. Review on hydrogen safety issues: Incident statistics, hydrogen diffusion, and detonation process. *International Journal of Hydrogen Energy* **2021,** *46*, 31467–31488.

Yeom, C.; Kim, Y. Adsorption of ammonia using mesoporous alumina prepared by a templating method. *Environ Eng Res.* **2017,** *22*, 401–6.

Yun, Y.; Gu, J.H.; Chung, S.W. Accident Cases and Safety Issues in Gasification Plants." "Waste Management and Resource Efficiency. *Proceedings of 6th IconSWM 2016*. Sadhan Kumar Ghosh, Ed.; Springer; 2016.

Yun, Y.; Lee, S. J.; Chung, S. W. Considerations for the Design and Operation of Pilot-Scale Coal Gasifiers. In *Gasification for Practical Applications*. IntechOpen, Ed., 2012. DOI: 10.5772/49951.

Zamel, N.; Li, X. Effect of Contaminants on Polymer Electrolyte Membrane Fuel Cells, *Progress in Energy and Combustion Science* **2011,** *37*, 292–329.

Zhang, S.; Chi, J.; Xiao, Y. Performance analysis of a partial oxidation steam injected gas turbine cycle. *Applied Thermal Engineering* **2015,** *91*, 622–629.

Zhao, Z.; Sevryugina, Y.; Carpenter, M. A.; Xia, H.; Welch, D. All-optical hydrogen sensor based on a high alloy content palladium thin film. *Sens. Actuators B: Chem*. **2006,** *113*, 532–538.

Zhigachev, A. O.; Agarkova, E. A.; Matveev, D. V.; Bredikhin, S. I. $CaO\text{-}SiO_2\text{-}B_2O_3$ Glass as a Sealant for Solid Oxide Fuel Cells. *Ceramics* **2022,** *5*, 642–654.

APPENDIX A - HAZARD ANALYSIS FOR FECM HYDROGEN SYSTEMS

A general hazard analysis was conducted for hydrogen use and storage in several applications of greatest interest to FECM. Applications analyzed were solid oxide fuel cells (SOFC), gas turbines using hydrogen blends, gas turbines using pure hydrogen, steam methane reformers, and gasification.

The hazard analysis team consisted of researcher engineers and scientists, a Professional Engineer, and a Certified Safety Professional (CSP). Team member experience included design, construction, and operation of the high-pressure hydrogen system at NETL used to supply hydrogen to the high-pressure combustion facility, including the SIMVAL 3 MW pressurized combustor with optical access, as well and several smaller laboratory hydrogen systems used for combustion, fuel cell, and sensors research. SIMVAL was used to study the combustion behavior of hydrogen and hydrogen-natural gas blends under conditions and scale relevant to industrial gas turbines.

In the analysis, each application was divided into systems and subsystems. Potential hazards associated with each subsystem were identified. Recognized hazard mitigations were identified for each listed hazard. Mitigations were taken from many sources including widely recognized consensus standards from the American Society of Mechanical Engineers (ASME), the National Fire Protection Association (NFPA), the American National Standards Institute (ANSI), the Compressed Gas Association (CGA), as well as the U.S. Department of Labor, Occupational Safety and Health Administration (OSHA), and U.S. Department of Energy (DOE) standards and regulations.

In addition to this analysis, the team also attempted to identify hazard or mitigation differences between hydrogen and natural gas.

The hazard analysis is summarized in the following tables.

GENERAL SYSTEMS

SUBSYSTEM	HAZARD	MITIGATIONS/CODE	DIFFERENCE(S) FROM NATURAL GAS
Gas Cylinders	Fire/explosion from hydrogen leak	Proper storage according to NFPA 2, NFPA 55	None; high-pressure steel cylinders for both gases
		Use refillable stationary storage	
		Outdoor storage (segregation from the SOFC stack)	
		Interconnected hydrogen system shall be grounded per NFPA 2, Chapter 7 and CGA 5.4. Ducting carrying hydrogen should be grounded per NFPA 2 L.3.4.5 (Best Management Practice).	
		Area gas monitors, requirements in NFPA 2 – 6.13	
		Segregate fuel gas cylinders from oxidizers (20 ft or a wall with a 0.5 hr fire rating, no line of sight between the gases), and keep them away from ignition sources NFPA 2, NFPA 55	
		Wear antistatic clothing and footwear	
		Ventilation for indoor storage	
	Asphyxiation	Modeling can be done to determine if an asphyxiation hazard exists. Mitigations could include a restrictive flow orifice 29 CFR 1910.134, OSHA Respiratory Protection Standard	

SUBSYSTEM	HAZARD	MITIGATIONS/CODE	DIFFERENCE(S) FROM NATURAL GAS
Process Piping	Fire/explosion from hydrogen leak	Design piping according to ASME B31.3 and B31.12; NFPA 67, 68, 69	H_2 designed to B31.12. Design pressure limitations based on materials. Materials limited by embrittlement. Maintaining energy flow rate requires larger piping, and higher pressures. High-temperature hydrogen attack
		Brazed or welded joints for leak-free connection are required for severe cyclic service as determined by the owner/designer, and underground (B31.12; B31.3)	
	Contamination in line (particulate, burrs, etc.)	Chemical/mechanical cleaning process described in NFPA 2, NFPA 55, CGA 5.4.	
	Hydrogen embrittlement	Careful alloy selection (use aluminum as structural material due to its low susceptibility to hydrogen, not using cast iron and hydride-forming metals and alloys), B31.12	
	Corrosion due to impurities (H_2S, CO_2, O_2, other acids; water also needed but does not corrode by itself)	Material selection; minimizing moisture and impurities in the system. Water removal system.	
		Surface films to reduce hydrogen absorption (copper, gold)	
	High-temperature hydrogen attack (if applicable, e.g., for steel alloys above 250 °C)	Alloy selection Coatings will mitigate high-temperature oxidation and reduce permeation and diffusion of hydrogen to the bulk material	
Pressure Relief Devices	Fire/explosion due to auto ignition due to reverse Joule-Thompson effect or expansion	CGA 5-5, NFPA 68	Reverse Joule-Thompson does not apply to natural gas. Hydrogen changes flow rate at critical flow conditions (sonic). Greater likelihood of auto ignition when venting.

SUBSYSTEM	HAZARD	MITIGATIONS/CODE	DIFFERENCE(S) FROM NATURAL GAS
Relief Vent	Fire/explosion due to auto ignition due to reverse Joule-Thompson effect or expansion, potential detonation (DDT)	Proper sizing of the relief vent to decrease potential for acceleration (deflagration instead of detonation), CGA 5-5, NFPA 68	Deflagration venting requirements differ Total flow likely higher to meet same power requirement, will impact relief vent
Reformer	Leak and fire	Proper mechanical design including alloy selection	
	Hydrogen embrittlement	Alloy selection	
	High-temperature hydrogen attack (if applicable, e.g., for steel alloys above 250 °C)	Alloy selection	
	Carbon deposition from poor operation	Appropriate sensors, control systems and maintenance/inspection	
	Overpressurization and rupture	Appropriate sensors, control systems and maintenance/inspection	
Hydrogen Separation Unit	Ignition/explosion while performing installation and replacement of the unit	Minimize equipment and labors, enabling short turndowns	N/A
	H_2 leaks through the membranes (metallic membranes: embrittlement, poisoning with H_2S, CO)	Select robust and contaminant-resistant separation units that require very little operator attention or maintenance	
	Carbon and ceramic membranes: brittle, stability issue in water vapor	Add hydrogen sensors	
	Polymer membrane (swelling, compaction)	Segregation	
	Asphyxiation	Ventilation	

SUBSYSTEM	HAZARD	MITIGATIONS/CODE	DIFFERENCE(S) FROM NATURAL GAS
Refractory-Lined Hydrogen Combustor	Hydrogen may react with the refractory material which may change its property High-temperature corrosion and wear	Selection via the refractory material	Burning hydrogen will produce more water, which is the cause of corrosion Modification of liner or refractory material is needed to switch from natural gas to hydrogen
Sensors (Effect of H_2)	Sensor failure	Develop explosion/ignition proof sensors Performance-based standards: UL 2075, CSA C22.2 No. 152-M1984, FM 6310, FM 6320, ISO 26142 Safety and shock standards: UL 61010-1, UL 60079, IEC 60079, CSA C22.2 No. 152-M1984, FM 3600, FM 3615, FM 3810 Interface standards: UL 864, UL 2017, FM 3010	Ignition is easier with hydrogen
	Hydrogen darkening of optic fiber; hydrogen diffusion into glass changes properties so it does not transmit light as well over time	Careful selection of fiber for use of crystalline optical fiber	Hydrogen darkening does not occur in natural gas

SOFC SYSTEMS

SUBSYSTEM	HAZARD	MITIGATIONS/CODE	DIFFERENCE(S) FROM NATURAL GAS
SOFC Stack	Fire/explosion from leak (seal degrading)	Avoid sources of ignition, electrical spark, static electric friction, etc. Wear antistatic clothing and footwear. ANSI/CSA-FC-1, NFPA 853	**H_2:** No fuel reformer for H_2. Greater hazard of fire or explosion (H_2 has approximately 4 times higher permeation than methane; greater likelihood of leak) Seals have greater likelihood of leakage Possible H_2 embrittlement in the interconnect **Natural gas:** If carbon deposition occurs from coking then it can block the fuel supply manifold, causing pressure build-up in the fuel supply system, potentially causing leakage. A hydrogen fuel supply prevents carbon deposition. Sulfur compounds in natural gas odorants, if they pass into the SOFC stack, cause irreversible sulfidation which deteriorates the electrodes resulting in delamination between electrode and electrolyte, and possible gas leakage.
	Ignition within stack	Install alarm/shutdown systems to prevent damage beyond the stack. Protective enclosure	
	Leak (mechanical failure)	Locate the electrical/electronic components below any possible sources of leakage due to hydrogen buoyancy. Ventilation Gas detectors	
	Temperature injury	Wear appropriate PPE Thermal insulation Protective housing Containment Segregation	
	Sudden failure and risk from thermal stress, carbon formation, and catalyst poisoning	Emergency procedures	
	Electrical shock caused by high-voltage output (200-400 V) from the stack	Grounded enclosure	
	Short circuit across the output busbars	Proper separation of busbars, NFPA70	

SUBSYSTEM	HAZARD	MITIGATIONS/CODE	DIFFERENCE(S) FROM NATURAL GAS
Afterburner	Structural damage due to high operating temperature. Gas leakage	Control the internal temperature distribution of afterburner below the stability temperature limit of steel (1500 °C) Manage temperature by adjusting the flow rates of the inlet air and fuel gases, and by adjustable by-passes and splitters	
	Explosion	During the ignition/warm-up phase, the afterburner must be supplied with natural gas rather than hydrogen-rich anode off-gas During the fuel transition stage, in which the methane gas is progressively replaced by the anode off-gas and cathode off-gas, the flame barrier temperature needs to be maintained at around 600–650 °C	The afterburner inlet gas temperature should not exceed the self-ignition point of the residual gas (610 °C for CH_4, 560 °C for H_2). This is to prevent flashback to the fuel cell
	Thermal injury	Place in an insulated box	
Reformer	See General above	See General above	NOTE: There is no reformer with pure H_2 fuel

SOEC SYSTEMS

SUBSYSTEM	HAZARD	MITIGATIONS/CODE	DIFFERENCE(S) FROM NATURAL GAS
SOEC Stack	Fire/explosion from leak (seal degrading)	Avoid sources of ignition, electrical spark, static electric friction, etc. Wear antistatic clothing and footwear. IEC 62282-8-101:2020	N/A
	Ignition within stack	Install alarm/shutdown systems to prevent damage beyond the stack. Protective enclosure	
	Leak (mechanical failure)	Locate the electrical/electronic components below any possible sources of leakage due to hydrogen buoyancy. Ventilation Gas detectors	
	Temperature injury	Wear appropriate PPE Thermal insulation Protective housing Containment Segregation	
	Sudden failure and risk from thermal stress	Emergency procedures	
	Short circuit across the input busbars	Proper separation of busbars, NFPA70 Grounded enclosure	

GAS TURBINES SYSTEMS - HYDROGEN BLENDS

SUBSYSTEM	HAZARD	MITIGATIONS/CODE	DIFFERENCE(S) FROM NATURAL GAS
Process Piping	See General above	See General above	Similar to SOFC Piping will be larger for turbine (than SOFC) Higher pressure and volumes
Combustion System	Flashback and blowout; purging before ignition sequence High-temperature hydrogen attack Hydrogen embrittlement	Longer purge; diffusion flame combustion system to mitigate flashback and blowout; specialized combustor design; optimized air speeds/flow velocities Material selection for hydrogen exposure	Due to higher flame speed of H_2 than NG, purging is more difficult due to hydrogen buoyancy, tending to collect in high spaces
Turboexpander	H_2 embrittlement of turbine blades; high-temperature hydrogen attack	Material selection is critical	Thermal barrier coatings for natural gas turbines do not provide corrosion protection vs. high-temperature corrosion. Alloys for natural gas are limited vs. high-temperature hydrogen attack
Casing (Pressure Vessel)	Hydrogen embrittlement High-temperature hydrogen attack	Materials selected to avoid hydrogen embrittlement and high-temperature hydrogen attack	Does not fall under the Pressure Vessel Code
Sensors (Effect of H_2)	Flame sensor failure to detect pure hydrogen flame	Obtain a flame sensor that is listed and approved for the application, NFPA 85, Section 5.1.3.	Natural gas has an easily visible blue flame; hydrogen flame is nearly invisible but does have ultraviolet emission
Effects of Fuel Changes	Increased fuel and oxidizer flow rates	Appropriate design and control systems	Due to the lower energy density of hydrogen compared to natural gas, fuel flow rates will increase as hydrogen concentration increases

GAS TURBINES SYSTEMS – PURE H_2

SUBSYSTEM	HAZARD	MITIGATIONS/CODE	DIFFERENCE(S) FROM NATURAL GAS
Process Piping	See General above	See General above	Similar to SOFC
Combustion System	Flashback and blowout; purging before ignition sequence	Longer purge; diffusion flame combustion system; specialized combustor design; optimized air speeds/flow velocities for premix combustion; steam addition/dilution to reduce flame speed	Greater issue with flashback for pure H_2
Turboexpander	Hydrogen embrittlement of turbine blades; high-temperature hydrogen attack	Material selection is critical	Greater issue for pure H_2 than blend (will depend on the % of H_2 in the blend)
Casing (Pressure Vessel)	Hydrogen embrittlement; high-temperature hydrogen attack	Materials selected to avoid hydrogen embrittlement and high-temperature hydrogen attack	Does not fall under the Pressure Vessel Code
Sensors (Effect of H_2)	Flame sensor failure to detect pure hydrogen flame	Obtain a flame sensor that is listed and approved for the application, NFPA 85, Section 5.1.3.	Natural gas has an easily visible blue flame; hydrogen flame is nearly invisible but does have ultraviolet emission

GASIFICATION SYSTEMS

SUBSYSTEM	HAZARD	MITIGATIONS/CODE	DIFFERENCE(S) FROM NATURAL GAS
Process Piping	See General above	See General above	
Gasifier	Uncontrolled ignition (ignition sequence problem)	Start off on natural gas and monitoring the ignition process when solids are added, NFPA 850, Chapter 16.5.2	
Solid Feed	Blockage causing overpressurization/ backflow leading to explosion	NEC Class II, Div 2 for environments pertaining to combustible dust Proper piping design to move solids	Combustible solid present in addition to flammable gas
Cylinder/Storage	See General above	See General above	
Hydrogen Separation Unit	See General above	See General above	
Pressure Relief	See General above	See General above	See General above
Natural Gas Reformer	See General above	See General above	See General above
Relief Vent	See General above	See General above	See General above

STEAM METHANE REFORMING (SMR) SYSTEMS

SUBSYSTEM	HAZARD	MITIGATIONS/CODE	DIFFERENCE(S) FROM NATURAL GAS
Process Piping	See General above	See General above	See General above
Cylinder/Storage	See General above	See General above	See General above
Hydrogen Separation Unit	See General above	See General above	See General above
Pressure Relief	See General above	See General above	See General above
Natural Gas Reformer	See General above	See General above	See General above

APPENDIX B - SUMMARY OF RELEVANT SAFETY CODES

ASME B31.12

1. Title, Organization, and Standard Number

Hydrogen Piping and Pipelines, ASME B31.12

2. Scope of Standard

Based on studies conducted by the ASME, it was determined that gaps existed between the current piping codes and standards, and hydrogen infrastructure applications. ASME formed a team to develop a new code for hydrogen piping and pipelines. This new code would address design, construction, operation, and maintenance of the hydrogen systems. The code is intended to account for the adverse effects of hydrogen on carbon and low alloy steel pipe operating in the hydrogen embrittlement range.

This code is applicable to piping in gaseous and liquid hydrogen service and to pipelines in gaseous hydrogen service, and includes the joint connecting to vessels and equipment, but not the equipment themselves. It includes the location and type of support elements, but not the structure to which the support elements attach.

The scope of the code is divided into two areas: industrial piping and pipelines. In addition to their own specific details, they also reference the general requirements section.

General Requirements contains definitions and requirements for items including: materials, welding, brazing, heat treating, forming, testing, inspection, examination, operation, and maintenance. In addition, it contains QA/QC topics common to the two areas.

Industrial Piping includes requirements for components, design, fabrication, assembly, erection, inspection, examination, and testing of piping. This includes for hydrogen service included in petroleum refineries, refueling stations, chemical plants, power generation plants, semiconductor plants, cryogenic plants, hydrogen fuel appliances, and related facilities.

Excluded from the scope of industrial piping:

- Internal components of fired heaters, vessels, heat exchangers, pumps, compressors and other fluid handling or processing equipment
- Elevated temperature fluid service as defined by ASME B31.3
- High pressure fluid service as defined by ASME B31.3

Pipelines sets forth requirements for components, design, installation, and testing of hydrogen pipelines. This includes transmission pipelines, and service lines used for transporting hydrogen from a production facility to the point of use.

Excluded from the scope of pipelines:

- Design and manufacture of pressure vessels
- Pipeline systems with temperatures above 450 °F and below -80 °F
- Pipeline systems above 3,000 psig

- Pipeline systems with a moisture content greater than 200 ppm
- Pipeline systems with less than 10% hydrogen by volume

3. Short Summary of the Topic of the Standard

The intent of the code is to set forth engineering requirements deemed necessary for safe design, construction, installation, inspection, testing, operation, maintenance, and quality system program of piping and pipeline systems in hydrogen service.

4. Relevance to H_2 Safety

This standard is relevant to hydrogen safety in nearly all industrial, commercial, and R&D applications.

5. Sections Relevant to H_2 Safety (if it is a minor topic of the standard)

All sections of this standard are relevant to hydrogen use and safety.

6. Comparison to Standard Requirements/Outcomes (ASME B31.12 vs. B31.3)?

The ASME B31.12 standard is more stringent than ASME B31.3 in some areas. These include:

- Higher degrees of required non-destructive evaluation (NDE), especially radiographic testing (RT) on medium (design pressure 150–600 psig) and high-pressure systems (greater than 600 psig)
- Materials Performance Factor and requirement for the number of full displacement cycles during service life to be increased by a factor of ten under certain conditions that can result in greater minimum wall thicknesses
- Welding preheat of base metals of all thicknesses including under 1”
- Restrictions on materials used
- Additional essential variables for welding procedures, creating a need to qualify new welding procedures

7. Specific Examples of Different Outcomes

Additional cost and extended schedules would result from a system designed to B31.12. For example, a hydrogen containing pipeline with a design pressure of 2,500 psig.

Designed to ASME B31.3 it would require 5% of all circumferential groove welds be RT, while ASME B31.12 would 100% of the welds have RT. In addition, the acceptance criteria are more stringent for B31.12, resulting in the likelihood of additional rejected welds, required weld repairs, and extended schedules. This is potentially compounded by the requirement that post weld heat treatment (PWHT), if applicable, must be completed before RT. In the case of rejected welds, PWHT would be performed again after the weld repair and before the RT of the repair.

For the calculation of minimum required pipe thickness, B31.12 has an additional Materials Performance Factor (Mf), resulting in increased wall thickness (depending on material and design pressure). Take the example of the 2,500 psig system and apply it to 18 in. ASTM

A106 carbon steel pipe. With the addition of the Mf in the calculation, the required wall thickness increases approximately 10%.

B31.12 specifically requires preheat to 175 °F for all carbon steel pipe regardless of thickness. B31.3 only recommends it for pipe greater than 1-in. thick. Depending on the thickness and diameter of the pipe, this could have significant impact on schedule and cost.

B31.12 for pipelines has a more restricted list of accepted materials. For most pipelines only conveying hydrogen from the point of production to the point of use, there should be little to no impact.

Welding Procedure Specifications (WPS) that are qualified to ASME B31.12 have additional essential variables that will require many fabricators to create new WPS to comply with B31.12 and require their welders and/or welding operators to qualify to these new WPS.

8. Impact on Costs

Impacts to the cost for designing, fabricating, testing, operating, and maintaining a system designed to B31.12 vs. B31.3 could be very large depending on the scale and the service of the hydrogen system. The increase cost would be primarily due to the additional NDE and materials.

The cost associated with the 100% RT could be significant. Assuming the 18 in. schedule 140 pipe from the point of production to the point distribution is 1 mi., the pipe sections are 20-ft long, and the cost to RT a weld is $900. B31.12 would require that all 264 welds have full RT at a cost of $237,000. B31.3 would only require that 5% of the welds have full RT at a cost of $11,880. The difference being $225,120 for only one mile. The cost difference is likely to be much higher as the inspection process for 100% of the welds may interfere with production.

The additional requirement of preheat for all welds, would likely require that one or more additional technicians be hired solely for the purpose of preheating pipe.

The qualification of new WPS and qualification of welder and/or welding operators will be an additional upfront cost.

9. Other Notes of Potential Interest

None

CGA G-5 - Hydrogen

1. Title, Organization, and Standard Number

Compressed Gas Association, CGA G-5 Hydrogen

2. Scope of Standard

This standard contains an overview of hydrogen and associated hazards.

3. Short Summary of the Topic of the Standard

This standard provides general physical and general information about hydrogen and some basic descriptions of safe use practices and hazard mitigations.

4. Relevance to H_2 Safety

This standard describes the physical properties of hydrogen and some basic descriptions of hazard controls/safe use practices of the gas. The standard covers hydrogen containers, including cylinders and tanks, gaseous and liquid hydrogen systems, and general precautions and handling guidelines.

5. Sections Relevant to H_2 Safety (if it is a minor topic of the standard)

All sections of this standard are relevant to hydrogen use and safety.

6. Comparison to Standard Requirements/Outcomes (H_2 from natural gas)

This standard applies specifically to hydrogen operations.

7. Specific Examples of Different Outcomes

Similar to NFPA 2, many aspects of this standard could result in catastrophic situations if not followed. Examples may be failure to monitor for potential explosive hydrogen gas release into an area, failure to provide adequate ventilation to a project area, or provide required explosion venting.

8. Impact on Costs

Impacts to the cost for using hydrogen could range from little cost to thousands of dollars. For example, this standard may require the installation of a sophisticated ventilation system or gas monitoring system to safely use hydrogen in a particular area. There are numerous requirements throughout the standard that can result in costly mitigations.

9. Other Notes of Potential Interest

None

CGA G-5.5 – Hydrogen Vent Systems

1. Title, Organization, and Standard Number

Compressed Gas Association, CGA G-5.5 – Hydrogen Vent Systems

2. Scope of Standard

This standard contains design guidelines for hydrogen vent systems used in gaseous and liquid hydrogen systems and provides recommendations for safe operations of these vent systems.

3. Short Summary of the Topic of the Standard

This CGA standard provides an overview of the properties of hydrogen, including its flammability, temperature impact, diffusion and leakage characteristics, asphyxiation hazard, characteristics of liquid hydrogen, and hydrogen embrittlement. System considerations for the design and operation of a hydrogen vent system are included.

4. Relevance to H_2 safety

This standard provides a detailed overview of hydrogen and its hazards in the Code in Section 4.

The following System Considerations are discussed with guidelines in the Code in Section 5:

- Hydrogen discharges shall be discharged using an engineered vent system. Typical discharges include purging of piping or components, manual vent valves, pressure control devices, or pressure relief device activation.
- Mechanical considerations are discussed (ability of the structure to withstand ice, wind, and seismic loading).
- Vent stack support detail considerations, including the ability to withstand the extreme temperatures of liquid discharges. Brackets to support the vent stack are required to be constructed of stainless steel or other noncorrosive and minimally conductive materials.

5. Sections Relevant to H_2 Safety (if it is a minor topic of the standard)

All sections of this standard are relevant to hydrogen use and safety.

6. Comparison to Standard Requirements/Outcomes (H_2 from natural gas)

This standard applies specifically to hydrogen operations.

7. Specific Examples of Different Outcomes

None

8. Impact on Costs

Impacts to the cost for using hydrogen could range from little cost to thousands of dollars. For example, this standard may require the installation of a sophisticated ventilation system or gas monitoring system to safely use hydrogen in a particular area. There are numerous requirements throughout the standard that can result in costly mitigations.

9. Other Notes of Potential Interest

None

NFPA 2

1. Title, Organization, and Standard Number

Hydrogen Technologies Code National Fire Protection Agency (NFPA) 2

2. Scope of Standard

This code provides safeguards for the generation, installation, storage, piping, use and handling of hydrogen in compressed gas (GH_2) or cryogenic liquid (LH_2) form. The goal of the standard is to provide a reasonable level of safety, property preservation, and public welfare from the hazards created by fire, explosion and hazardous conditions associated with gaseous and liquified hydrogen.

3. Short Summary of the Topic of the Standard

This standard addresses the items in item #2 in detail. It covers a variety of items including fire prevention control area, occupancy, piping systems (grounding, construction/materials/pressure relief), ventilation, electrical equipment, fire alarms,

explosion control, fire protection, gas detection, gas cabinets, cleaning/purging of gas lines, etc.). Installation, location, storage and use of hydrogen are covered in detail.

4. Relevance to H_2 Safety

This standard is relevant to hydrogen safety in nearly all industrial, commercial, and R&D applications. The purpose of this standard is to allow work with hydrogen and to reduce or eliminate the possibilities of fire or explosion.

The standard addresses:

- General fire safety requirements associated with hydrogen
- Performance-based design methodologies
- Detailed hydrogen use/storage requirements.
- General requirements for gaseous hydrogen systems.
- General requirements for use and storage of liquified hydrogen.
- Gaseous hydrogen fueling facilities.
- Liquified hydrogen fueling facilities.
- Hydrogen fuel cell power systems.
- Hydrogen generation systems.
- Combustion applications
- Equipment that uses hydrogen as an atmosphere for use in furnaces regulated by NFPA 86
- Laboratory uses of hydrogen
- Parking garages and repair garages.

5. Sections Relevant to H_2 Safety (if it is a minor topic of the standard)

All sections of this standard are relevant to hydrogen use and safety.

6. Comparison to Standard Requirements/Outcomes (H_2 from natural gas)

This standard is designed for hydrogen use. When other gases are involved (including natural gas), references are made to NFPA 55. That standard more specifically addresses the differences.

7. Specific Examples of Different Outcomes

Many aspects of this standard could result in catastrophic situations if not followed. Examples may be failure to monitor for potential explosive hydrogen gas release into an area, failure to provide adequate ventilation to a project area, or using a non-spark resistant impeller in a ventilation system to vent hydrogen.

8. Impact on Costs

Impacts to the cost for using hydrogen could range from little cost to thousands of dollars. For example, this standard may require the installation of an enhanced ventilation system or gas monitoring system to safely use hydrogen in a particular area. Other costly upgrades may include, construction materials (prevention of hydrogen embrittlement), fire detection equipment, pressure relief equipment, and numerous other potential upgrades. There are numerous requirements throughout the standard that can result in costly mitigations.

9. Other Notes of Potential Interest

The use of gaseous system with over 5,000 standard feet of gas is referred to as a "Bulk System" and carries additional requirements above those of "Non-Bulk Systems".

NFPA 55

1. Title, Organization, and Standard Number

Compressed Gases and Cryogenic Fluids Code, National Fire Protections Association 55

2. Scope of Standard

This standard applies to the installation, storage, use and handling of all compressed gases and cryogenic fluids in industrial, commercial, and R&D settings.

3. Short Summary of the Topic of the Standard

This code applies to the installation, storage, use and handling of compressed gases and cryogenic fluids in portable and stationary cylinders, containers, equipment, and tanks in all occupancies. It should be noted that this standard applies to all gases, not just hydrogen. Chapter 10, "Gas Hydrogen Systems" and Chapter 11, "Bulk Liquified Hydrogen Systems" specifically cover hydrogen. Methane is not covered by these chapters. NFPA 2 has incorporated nearly all of the requirements from these chapters.

4. Relevance to H_2 Safety

As mentioned above, this standard is applicable to all gases and cryogens, including hydrogen. Chapter 10 and 11 are specific to hydrogen.

The standard addresses:

- Hazardous Materials Classification, including the breakdown of gases into classes (e.g. – flammable gas, pyrophoric gas, corrosive gas, toxic gas, etc.).
- Building related controls for all gases and cryogens
- General guidelines for compressed gas, including system design, containers, labeling, storage, and handling.
- Flammable Gases
- Cryogenic gases.
- Bulk oxygen systems.
- Gaseous hydrogen systems
- Liquified hydrogen systems
- Medical gases
- Corrosive gases.
- Oxidizing gases.
- Pyrophoric gases.
- Toxic and highly toxic gases
- Design of bulk liquified hydrogen systems.
- Gas generation systems.

- Carbon dioxide systems.
- Ethylene oxide system requirements.
- Acetylene cylinder charging plants.
- Liquid nitrous oxide systems.
- Cryogenic fluids central supply systems.

ANNEX C of NFPA 55 discusses physical properties of hydrogen gas. It is provided as an information source on the gas.

ANNEX G of NFPA 55 discussed the OSHA Hydrogen Standard 29 1910.103 and its requirements. OSHA 1910.103 establishes requirements for hydrogen systems.

5. Sections Relevant to H_2 Safety (if it is a minor topic of the standard)

All sections of this standard are relevant to hydrogen use and safety.

6. Comparison to Standard Requirements/Outcomes (H_2 from natural gas)

Natural gas and hydrogen are both covered under the provisions of this standard, including Chapter 7, "Flammable Gases". Chapters 10 and 11 differentiate different requirements for hydrogen.

7. Specific Examples of Different Outcomes

As in NFPA 2, many aspects of this standard could result in catastrophic situations if not followed. Examples may be failure to monitor for potential explosive hydrogen gas release into an area, failure to provide adequate ventilation to a project area, or using a non-spark resistant impeller in a ventilation system to vent hydrogen.

8. Impact on Costs

As was the case in NFPA 2, Impacts to the cost of business for using hydrogen could range from little cost to thousands of dollars. For example, this standard may require the installation of a sophisticated ventilation system or gas monitoring system to safely use hydrogen in a particular area. There are numerous requirements throughout the standard that can result in costly mitigations.

9. Other Notes of Potential Interest

NFPA 2 incorporated the applicable parts of this standard into its latest revision.

OSHA 29 CFR 1910.103

1. Title, Organization, and Standard Number

Hydrogen, OSHA 29 CFR 1910.103

2. Scope of Standard

This standard applies to gaseous and liquified hydrogen systems in general industry.

3. Short Summary of the Topic of the Standard

This code is a legally enforceable OSHA standard. It covers much of the same ground as NFPA 2, although in much less detail. It covers stationary or moveable hydrogen containers,

pressure regulators, safety relief devices, manifolds, and piping. There are references to ASME and DOT requirements, although some of the references are decades old.

4. Relevance to H_2 Safety

This standard is relevant to hydrogen safety in nearly all industrial, commercial, and R&D applications subject to OSHA regulation.

OSHA 1910.103 establishes requirements for hydrogen systems. The distance tables in the standard are based on the 1969 version of NFPA 50A. This standard (50A) no longer exists and was incorporated into NFPA 55 in 2003 to standardize hydrogen requirements. Some highlights of the standard are:

- Hydrogen systems shall be designed in accordance with AME Boiler and Pressure Code, Section 8 (1968 version of the code). Piping shall be designed and constructed in accordance with ASME B31.1-1967. Current practice dictates that ASME B31.3 be used.
- Equipment shall be suitable for hydrogen service.
- Guidance is provided for pressure relief design and discharge location.
- Hydrogen containers must be bonded to the system.
- Location requirements are specified in the standard.
- Location requirements are specified in Table H-1 and Table H-2.
- Construction requirements are provided, including ventilation, fire resistant building materials, explosion venting, electrical equipment, heating (steam, hot water, or indirect means if possible), and pressure relief devices.
- Liquified gases are also addressed with respect to the same items as gaseous hydrogen systems.
- Tables H-3 and H-4 address locations and separation distances for liquified systems.

5. Sections Relevant to H_2 Safety (if it is a minor topic of the standard)

All sections of this standard are relevant to hydrogen use and safety.

6. Comparison to Standard Requirements/Outcomes (H_2 from natural gas)

This standard applies specifically to hydrogen operations.

7. Specific Examples of Different Outcomes

Similar to NFPA 2, many aspects of this standard could result in catastrophic situations if not followed. Examples may be failure to monitor for potential explosive hydrogen gas release into an area, failure to provide adequate ventilation to a project area, or provide required explosion venting.

8. Impact on Costs

Impacts to the cost for using hydrogen could range from little cost to thousands of dollars. For example, this standard may require the installation of a sophisticated ventilation system or gas monitoring system to safely use hydrogen in a particular area. There are numerous requirements throughout the standard that can result in costly mitigations.

9. Other Notes of Potential Interest

This standard is legally enforceable. It is an old standard which may have some outdated references.

OSHA 29 CFR 1910.111

1. Title, Organization, and Standard Number

Storage and Handling of Anhydrous Ammonia, 1910.111

2. Scope of Standard

This standard applies to anhydrous ammonia systems in general industry.

3. Short Summary of the Topic of the Standard

This code is a legally enforceable OSHA standard. It covers the design, construction, location, installation, and operation of anhydrous ammonia systems.

4. Relevance to H_2 Safety

This standard is relevant to anhydrous ammonia safety in nearly all industrial, commercial, and R&D applications subject to OSHA regulation. It is relevant if anhydrous ammonia is being used to store hydrogen.

OSHA 1910.111 establishes requirements for anhydrous ammonia systems. The following items are among the topics specified in the standard.

- Anhydrous ammonia systems shall be designed, installed, and inspected in accordance with ANSI K61.1, "Safety Requirements for the Storage and Handling of Anhydrous Ammonia"
- Hydrogen containers must be bonded to the system.
- Location requirements are specified in the standard.
- Labeling/marking requirements for containers are detailed.
- Pipes/tubing/fittings requirements are listed.
- Hose specifications are provided.
- Safety relief device requirements are specified.
- Respiratory protection must be kept in a suitable location near the tank.
- Liquid transfer requirements.
- Liquid level gaging device requirements.
- Requirements for systems utilizing stationary, nonrefrigerated storage containers.
- Refrigerated storage system requirements.
- Tank motor vehicles for the transportation of ammonia requirements.
- Requirements for systems mounted on farm vehicles.

5. Sections Relevant to H_2 Safety (if it is a minor topic of the standard)

This section would apply to all systems using ammonia to store and transport hydrogen.

6. Comparison to Standard Requirements/Outcomes (H_2 from natural gas)

This standard does not apply to natural gas.

7. Specific Examples of Different Outcomes

Failure to follow this standard could result in vessel failure and/or leakage of corrosive ammonia gas. Failure impacts could be injuries/fatalities and/or significant equipment damage.

8. Impact on Costs

Impacts to the cost for using ammonia could range from little cost to thousands of dollars.

9. Other Notes of Potential Interest

This standard is legally enforceable.

CGA G-2

1. Title, Organization, and Standard Number

Anhydrous Ammonia, Compressed Gas Association, CGA G-2

2. Scope of Standard

This code provides introductory information about anhydrous ammonia to various parties such as shippers, carriers, distributors, safety administrators, etc.

3. Short Summary of the Topic of the Standard

This standard addresses several anhydrous ammonia issues. Chapters of G-2 cover the following information:

- Composition and synthesis of ammonia (Haber-Bosch Process).
- An extensive summary of the physical properties of ammonia.
- An extensive summary of commercial uses of ammonia. No mention is made of hydrogen storage.
- A summary of regulatory codes for ammonia, including DOT, OSHA, EPA, DHS.
- Health effects/hazards and first aid guidelines for ammonia exposures.
- Guidelines for controlling leaks, fire prevention, and emergency response actions.
- Safety and security guidelines, including training requirements, personal protective equipment, and other hazard mitigations.
- Extensive guidelines for anhydrous ammonia tank cars and associated operations.
- Cargo tank motor vehicle operations and design/safety requirements.
- Portable tank design and use guidelines.
- Compressed gas cylinder specifications and use guidelines.
- Barges and ship requirements for anhydrous ammonia transport and usage.
- Anhydrous ammonia pipeline specifications and guidelines.

- Stationary container guidelines.
- Piping and equipment material specifications and design.

4. Relevance to H_2 Safety

This standard is specifically for anhydrous ammonia. It would be relevant for operations involving hydrogen storage in anhydrous ammonia, such as: Construction Site; Fuels, Common Equipment, and Protection; and Turbines, Generators, and Internal Combustion Engines.

5. Sections Relevant to H_2 Safety (if it is a minor topic of the standard)

Please see answer above.

6. Comparison to Standard Requirements/Outcomes (H_2 from natural gas)

None

7. Specific Examples of Different Outcomes

None

8. Impact on Costs

N/A

9. Other Notes of Potential Interest

None

Brian J. Anderson
Director
National Energy Technology Laboratory
U.S. Department of Energy

David Miller
Chief Research Officer
Science & Technology Strategic Plans
& Programs
National Energy Technology Laboratory
U.S. Department of Energy

Bryan Morreale
Associate Laboratory Director for
Research & Innovation
Research & Innovation Center
National Energy Technology Laboratory
U.S. Department of Energy

NETL Technical Report Series